National Library
of Canada

Acquisitions and
Bibliographic Services Branch

395 Wellington Street
Ottawa, Ontario
K1A 0N4

Bibliothèque nationale
du Canada

Direction des acquisitions et
des services bibliographiques

395, rue Wellington
Ottawa (Ontario)
K1A 0N4

Your file Votre référence

Our file Notre référence

NOTICE

The quality of this microform is heavily dependent upon the quality of the original thesis submitted for microfilming. Every effort has been made to ensure the highest quality of reproduction possible.

If pages are missing, contact the university which granted the degree.

Some pages may have indistinct print especially if the original pages were typed with a poor typewriter ribbon or if the university sent us an inferior photocopy.

Reproduction in full or in part of this microform is governed by the Canadian Copyright Act, R.S.C. 1970, c. C-30, and subsequent amendments.

AVIS

La qualité de cette microforme dépend grandement de la qualité de la thèse soumise au microfilmage. Nous avons tout fait pour assurer une qualité supérieure de reproduction.

S'il manque des pages, veuillez communiquer avec l'université qui a conféré le grade.

La qualité d'impression de certaines pages peut laisser à désirer, surtout si les pages originales ont été dactylographiées à l'aide d'un ruban usé ou si l'université nous a fait parvenir une photocopie de qualité inférieure.

La reproduction, même partielle, de cette microforme est soumise à la Loi canadienne sur le droit d'auteur, SRC 1970, c. C-30, et ses amendements subséquents.

Canada

UNIVERSITY OF ALBERTA

STUDIES ON THE MECHANISMS OF BIODISPOSITION OF DIRECTLY-LABELED ^{99m}Tc-ANTIBODIES

BY

LANNY YANJUN XUE ©

A THESIS

SUBMITTED TO THE FACULTY OF GRADUATE STUDIES AND RESEARCH IN PARTIAL FULFILLMENT OF THE REQUIREMENTS FOR THE DEGREE OF

DOCTOR OF PHILOSOPHY

IN

PHARMACEUTICAL SCIENCES

FACULTY OF PHARMACY AND PHARMACEUTICAL SCIENCES

EDMONTON, ALBERTA

FALL, 1994

ISBN 0-315-95293-8

Canada

Name Xue, Lanny Yanjun

Dissertation Abstracts International is arranged by broad, general subject categories. Please select the one subject which most nearly describes the content of your dissertation. Enter the corresponding four-digit code in the spaces provided.

Pharmacy
SUBJECT TERM

0572
SUBJECT CODE

U·M·I

Subject Categories

THE HUMANITIES AND SOCIAL SCIENCES

COMMUNICATIONS AND THE ARTS
Architecture 0729
Art History 0377
Cinema 0900
Dance 0378
Fine Arts 0357
Information Science 0723
Journalism 0391
Library Science 0399
Mass Communications 0708
Music 0413
Speech Communication 0459
Theater 0465

EDUCATION
General 0515
Administration 0514
Adult and Continuing 0516
Agricultural 0517
Art 0273
Bilingual and Multicultural 0282
Business 0688
Community College 0275
Curriculum and Instruction 0727
Early Childhood 0518
Elementary 0524
Finance 0277
Guidance and Counseling 0519
Health 0680
Higher 0745
History of 0520
Home Economics 0278
Industrial 0521
Language and Literature 0279
Mathematics 0280
Music 0522
Philosophy of 0998
Physical 0523
Psychology 0525
Reading 0535
Religious 0527
Sciences 0714
Secondary 0533
Social Sciences 0534
Sociology of 0340
Special 0529
Teacher Training 0530
Technology 0710
Tests and Measurements 0288
Vocational 0747

LANGUAGE, LITERATURE AND LINGUISTICS
Language
- General 0679
- Ancient 0289
- Linguistics 0290
- Modern 0291

Literature
- General 0401
- Classical 0294
- Comparative 0295
- Medieval 0297
- Modern 0298
- African 0316
- American 0591
- Asian 0305
- Canadian (English) 0352
- Canadian (French) 0355
- English 0593
- Germanic 0311
- Latin American 0312
- Middle Eastern 0315
- Romance 0313
- Slavic and East European 0314

PHILOSOPHY, RELIGION AND THEOLOGY
Philosophy 0422
Religion
- General 0318
- Biblical Studies 0321
- Clergy 0319
- History of 0320
- Philosophy of 0322

Theology 0469

SOCIAL SCIENCES
American Studies 0323
Anthropology
- Archaeology 0324
- Cultural 0326
- Physical 0327

Business Administration
- General 0310
- Accounting 0272
- Banking 0770
- Management 0454
- Marketing 0338

Canadian Studies 0385
Economics
- General 0501
- Agricultural 0503
- Commerce-Business 0505
- Finance 0508
- History 0509
- Labor 0510
- Theory 0511

Folklore 0358
Geography 0366
Gerontology 0351
History
- General 0578
- Ancient 0579
- Medieval 0581
- Modern 0582
- Black 0328
- African 0331
- Asia, Australia and Oceania 0332
- Canadian 0334
- European 0335
- Latin American 0336
- Middle Eastern 0333
- United States 0337

History of Science 0585
Law 0398
Political Science
- General 0615
- International Law and Relations 0616
- Public Administration 0617

Recreation 0814
Social Work 0452
Sociology
- General 0626
- Criminology and Penology 0627
- Demography 0938
- Ethnic and Racial Studies 0631
- Individual and Family Studies 0628
- Industrial and Labor Relations 0629
- Public and Social Welfare 0630
- Social Structure and Development 0700
- Theory and Methods 0344

Transportation 0709
Urban and Regional Planning 0999
Women's Studies 0453

THE SCIENCES AND ENGINEERING

BIOLOGICAL SCIENCES
Agriculture
- General 0473
- Agronomy 0285
- Animal Culture and Nutrition 0475
- Animal Pathology 0476
- Food Science and Technology 0359
- Forestry and Wildlife 0478
- Plant Culture 0479
- Plant Pathology 0480
- Plant Physiology 0817
- Range Management 0777
- Wood Technology 0746

Biology
- General 0306
- Anatomy 0287
- Biostatistics 0308
- Botany 0309
- Cell 0379
- Ecology 0329
- Entomology 0353
- Genetics 0369
- Limnology 0793
- Microbiology 0410
- Molecular 0307
- Neuroscience 0317
- Oceanography 0416
- Physiology 0433
- Radiation 0821
- Veterinary Science 0778
- Zoology 0472

Biophysics
- General 0786
- Medical 0760

EARTH SCIENCES
Biogeochemistry 0425
Geochemistry 0996
Geodesy 0370
Geology 0372
Geophysics 0373
Hydrology 0388
Mineralogy 0411
Paleobotany 0345
Paleoecology 0426
Paleontology 0418
Paleozoology 0985
Palynology 0427
Physical Geography 0368
Physical Oceanography 0415

HEALTH AND ENVIRONMENTAL SCIENCES
Environmental Sciences 0768
Health Sciences
- General 0566
- Audiology 0300
- Chemotherapy 0992
- Dentistry 0567
- Education 0350
- Hospital Management 0769
- Human Development 0758
- Immunology 0982
- Medicine and Surgery 0564
- Mental Health 0347
- Nursing 0569
- Nutrition 0570
- Obstetrics and Gynecology 0380
- Occupational Health and Therapy 0354
- Ophthalmology 0381
- Pathology 0571
- Pharmacology 0419
- Pharmacy 0572
- Physical Therapy 0382
- Public Health 0573
- Radiology 0574
- Recreation 0575
- Speech Pathology 0460
- Toxicology 0383

Home Economics 0386

PHYSICAL SCIENCES
Pure Sciences
Chemistry
- General 0485
- Agricultural 0749
- Analytical 0486
- Biochemistry 0487
- Inorganic 0488
- Nuclear 0738
- Organic 0490
- Pharmaceutical 0491
- Physical 0494
- Polymer 0495
- Radiation 0754

Mathematics 0405
Physics
- General 0605
- Acoustics 0986
- Astronomy and Astrophysics 0606
- Atmospheric Science 0608
- Atomic 0748
- Electronics and Electricity 0607
- Elementary Particles and High Energy 0798
- Fluid and Plasma 0759
- Molecular 0609
- Nuclear 0610
- Optics 0752
- Radiation 0756
- Solid State 0611

Statistics 0463

Applied Sciences
Applied Mechanics 0346
Computer Science 0984
Engineering
- General 0537
- Aerospace 0538
- Agricultural 0539
- Automotive 0540
- Biomedical 0541
- Chemical 0542
- Civil 0543
- Electronics and Electrical 0544
- Heat and Thermodynamics 0348
- Hydraulic 0545
- Industrial 0546
- Marine 0547
- Materials Science 0794
- Mechanical 0548
- Metallurgy 0743
- Mining 0551
- Nuclear 0552
- Packaging 0549
- Petroleum 0765
- Sanitary and Municipal 0554
- System Science 0790

Geotechnology 0428
Operations Research 0796
Plastics Technology 0795
Textile Technology 0994

PSYCHOLOGY
General 0621
Behavioral 0384
Clinical 0622
Developmental 0620
Experimental 0623
Industrial 0624
Personality 0625
Physiological 0989
Psychobiology 0349
Psychometrics 0632
Social 0451

UNIVERSITY OF ALBERTA

RELEASE FORM

NAME OF AUTHOR Lanny Yanjun Xue

TITLE OF THESIS Studies on the Mechanisms of Biodisposition of Directly-Labeled ^{99m}Tc-Antibodies

DEGREE Doctor of Philosophy

YEAR THIS DEGREE GRANTED Fall, 1994

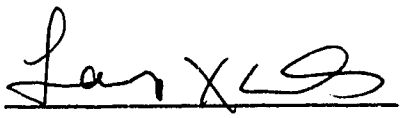

330 N
Michener Park
Edmonton, AB
Canada T6H 4M5

DATED Oct. 3, 1994

UNIVERSITY OF ALBERTA

FACULTY OF GRADUATE STUDIES AND RESEARCH

The undersigned certify that they have read, and recommend to the Faculty of Graduate Studies and Research for acceptance, a thesis entitled STUDIES ON THE MECHANISMS OF BIODISPOSITION OF DIRECTLY-LABELED ^{99m}Tc-ANTIBODIES submitted by LANNY YANJUN XUE in partial fulfillment of the requirements for the degree of DOCTOR OF PHILOSOPHY in PHARMACEUTICAL SCIENCES (Biotechnology and Radiopharmacy).

Dr. A.A. Noujaim (Supervisor)

Dr. T.R. Sykes (Co-supervisor)

Dr. L.I. Wiebe

Dr. M.R. Suresh

Dr. A.J. McEwan

Dr. P.L. Mann (External Examiner)

Date: Oct. 3 , 1994

DEDICATED

to

my wife Julie Zhang and our daughter Kristine

for their unlimited tolerance, understanding and love

ABSTRACT

This work was primarily devoted to studies on the mechanisms of biodisposition of directly-labeled ^{99m}Tc-antibodies. High background radioactivity in normal tissues such as liver and kidney is a major detriment to the use of radiolabeled antibodies (MAbs) for diagnosis and therapy. An understanding of the mechanisms involved in the uptake and metabolism of radiolabeled MAbs by tissues, the major concern of this work, may provide insights and approaches that would reduce the undesirable deposition of the labeled antibody in normal tissues.

The studies on the metabolism and *in vivo* fate of ^{99m}Tc-MAb were conducted using various chromatographic techniques for the analysis of the radiolabeled species in serum, urine, bile and homogenates of liver and kidneys obtained at various time intervals after the administration of ^{99m}Tc-MAb to mice. Virtually all (99-100%) of the radioactivity in serum was associated with the intact antibody. The radioactivity in the liver homogenates was strictly protein-bound to either intact MAb or low molecular weight species. In kidney extracts, the majority of the radioactivity was protein-bound ^{99m}Tc, with less than 8% of the activity being non-protein-bound. Multiple ^{99m}Tc-containing species were found in urine and bile. Evidence supporting the presence of ^{99m}Tc-cysteine and ^{99m}Tc-glutathione in bile, kidney and urine was also obtained.

A systematic investigation of the roles of the radionuclide (^{99m}Tc) and the protein moiety, and the nature of tissues was performed *in vivo* and *in vitro* to elucidate the mechanisms of uptake. The role of thiol transchelation with ^{99m}Tc in tissues was established by studying the effects of sulfhydryl modulation on ^{99m}Tc-antibody behavior *in vivo* and the influence of *in vitro* challenge with thiol-containing compounds on the association of ^{99m}Tc with the antibody. *In vitro* and *in vivo* studies indicated that both Fab and Fc portions on the antibody molecule as well as the intact antibody played important roles in the uptake of the radiolabel by normal tissues. The liver blood-pool was found to contribute about two-thirds of the *in vivo* liver radioactivity. These observations should be of value for the proper design of labeled antibodies and interpretation of tissue distribution studies. Appropriate choice of nuclides and the assessment of approaches for radiolabel attachment may optimize the biodistribution pattern of the radiolabeled MAb. This evaluation of directly-labeled ^{99m}Tc-antibodies serves to establish the basic pattern of radiolabel biodisposition and metabolism, the underlying mechanism for this pattern and various features which may assist in the further development of these agents for radioimmunoscintigraphy.

ACKNOWLEDGEMENT

I would like to express my sincere appreciation to Dr. A. A. Noujaim and Dr. T. R. Sykes for their guidance and friendship during the course of this research.

My sincere thanks are extended to the following people who contributed to the successful completion of this research: Drs. Ze Peng, Y. K. Tam, X. B. Wang and Fassil Hailu; Mr. Thomas Woo and Chris Ediss; and Ms. Cindy Erickson, Penney Bandura and Diane Jette.

The support and friendship from the staff and students of the Faculty of Pharmacy and Pharmaceutical Sciences, University of Alberta, are greatly appreciated.

I would also like to thank my MOM and DAD for their continuous support, encouragement and loving guidance through the years.

The financial supports of Biomira Inc. and Biomira Research Inc., Edmonton, Canada, are gratefully acknowledged.

TABLE OF CONTENTS

LIST OF TABLES

LIST OF FIGURES

LIST OF ABBREVIATIONS

AA	ascorbic acid
ADCC	antibody-dependent cell cytotoxicity
ASC system	cellular transport system for alanine, serine, cysteine and their homologs
ATP	adenosine triphosphate
BATO	boronic acid adducts of Tc-oximes
BFC	bifunctional chelate
BSA	bovine serum albumin
BSO	DL-buthionine-[S,R]-sulfoximine
C3	third complement component
carbogen	95/5% O_2/CO_2
CDR	complementarity determining region
CEA	carcincembryonic antigen
CPM	counts per minute
cGy	centiGray
CSAp	colon-specific antigen-p
DADT	diaminodithiol
ddH_2O	double distilled, deionized water
DPM	disintegrations per minute
DTE	dithioerythritol
DTPA	diethylenetriaminepentaacetic acid
DTS	bis-N-methylthiol semicarbazone
DTT	dithiothreitol
EC	electron capture

ECIA	extracorporeal immunoadsorption
EDTA	ethylenediaminetetraacetic acid
EGTA	ethylene glycol-bis-(β-aminoethyl) N,N'-tetra-acetic acid
ELISA	enzyme-linked immunosorbent assay
$F(ab')_2$	antigen-binding fragment, generated by digestion of IgG with pepsin
Fab	antigen-binding fragment, generated by digestion of IgG with papain
FBS	fetal bovine serum
Fc	fragment, crystallizable
FPLC	fast protein liquid chromatography
GSH	glutathione
GSSG	glutathione disulfide
h	hour
HAHA	human anti-human antibody
HAMA	human anti-mouse antibody
HAT	hypoxanthine-aminopterin-thymidine selective medium
HBSS	Hanks' balanced salt solution
HEPES	N-2-hydroxyethylpiperazine-N-2-ethane sulfonic acid
HIgG	human immunoglobulin G
HPLC	high performance liquid chromatography
HV	hypervariable region
%ID	percent injected dose
Ig	immunoglobulin
IL-2	interleukin-2

i.p.	intraperitoneal
IT	isomeric transition
ITLC	instant thin layer chromatography
i.v.	intravenous
kBq	kilobecquerel
keV	kilo-electron volt
L15 medium	Leibovitz medium
LMW	low molecular weight
MAbs	monoclonal antibodies
MAG_3	mercaptoacetyltriglycine
mBq	megabecquerel
µCi	microcurie
MDP	methylene diphosphonate
2-ME	2-mercaptomethanol
MeOH	methanol
min	minute
MT	metallothionein
MW	molecular weight
NS	normal saline
OTC	(-)-2-oxothiazolidine-4-carboxylate
p	probability
PBS	phosphate buffered saline
pFc'	Fc pieces
p.i.	post-injection
r	Pearson product-moment correlation coefficient
RES	reticuloendothelial system
rHu-IFN	recombinant human interferon
rpm	revolution per minute

R-Tc	"reduced and hydrolyzed" ^{99m}Tc
SD	standard deviation
SDS-PAGE	sodium dodecile sulfate - polyacrylamide gel electrophoresis
T1/2	half-life
TCA	trichloroacetic acid
TF-antigen	Thomsen-Friedenreich antigen
UV	ultraviolet
Ve	elution volume
Vo	void volume

INTRODUCTION

Subsequent to the introduction of the hybridoma technology by Kohler and Milstein in 1975 which enabled the production of monoclonal antibodies in almost unlimited quantities (1), there was a rapid increase and diversification of clinical applications of radiolabeled antibodies. Radioimmunoscintigraphy, one of these applications, has been performed in thousands of patients and its clinical value has been demonstrated in oncological diagnosis, detection of infection and inflammation, and cardiovascular applications such as the detection of myocardial necrosis and deep venous thrombosis (2-5). In addition to diagnostic applications, radiolabeled antibodies have been also used therapeutically (radioimmunotherapy) (2, 3).

However, the applications of radioimmunoscintigraphy and radioimmunotherapy are limited by a moderate target-to-background ratio. When a radiolabeled antibody is administered *in vivo*, it localizes in tumor to only a modest degree (in the range of 0.0007-0.01% of the injected dose per gram of tissue) and the majority of the administered dose is free to localize elsewhere, namely in blood, liver, kidney and other normal tissues (6-8). The consequence of this is an increase in the background radioactivity levels and an increase in the difficulty of detecting and treating malignant and non-malignant disorders, which is a major detriment to the use of radiolabeled antibodies for diagnosis and therapy.

In order to improve the ratio of target-to-background

radioactivity, either the tumor uptake of radiolabeled antibodies should be increased, or non-specific activity in normal tissues should be reduced, or both. To enhance tumor targeting and accretion by radiolabeled antibodies, various approaches have been attempted with limited success (9-16). The alternative to increase the ratio is the reduction of background radioactivity. In order to lower the high normal tissue background after administration of radiolabeled antibodies, either the uptake of the radiolabel must be decreased or its removal must be increased. These processes can be manipulated only if we have an understanding of the mechanisms involved in the uptake and metabolism of radiolabeled antibodies.

This work focuses on the mechanisms of biodisposition of directly-labeled ^{99m}Tc-antibodies.

An understanding of the metabolism of radiolabeled antibodies and elucidation of the metabolic products of ^{99m}Tc-antibodies may provide insights and approaches that would reduce the undesirable deposition of the labeled antibody in normal tissues. Thus, studies were designed to investigate the role of the circulating antibody, its metabolism and the fate of the ^{99m}Tc tracer. *In vivo* experiments were conducted to determine the nature of the labeled antibody in the serum, its metabolites in the liver and kidney tissues, and the metabolites secreted in the bile and urine of mice.

The accumulation of ^{99m}Tc radioactivity in liver and kidney is an interactive process between ^{99m}Tc-antibody and

the tissues of the recipient. In order to elucidate the mechanisms of uptake, a systematic study was required to investigate the roles of radionuclide (^{99m}Tc), protein moiety and the nature of tissues. Antibodies are radiolabeled with ^{99m}Tc by direct method only after reduction of endogenous disulfide bonds to sulfhydryls and ^{99m}Tc binding to one or two sulfhydryls (17). Sulfhydryl-containing molecules such as cysteine and glutathione are present in high concentration in plasma, liver and kidney (18, 19). Therefore, transchelation may be expected to occur *in vivo* after the administration of ^{99m}Tc-antibody. The role of thiol transchelation with ^{99m}Tc in tissue uptake of the radiolabel was investigated by studying the effects of sulfhydryl modulation on ^{99m}Tc-antibody behavior *in vivo* and the influence of *in vitro* challenge with thiol-containing compounds on association of ^{99m}Tc with the antibody. For the protein moiety, *in vitro* experiments were designed to investigate the roles of native antibody and two of its fragments [$F(ab')_2$, Fc] in the uptake of the radiolabel by hepatocytes. To avoid interference from other tissues, *in vitro* kidney binding studies were conducted. In addition, considering that liver is a blood-rich organ and that high blood radioactivity is observed in antibody biodistribution studies, the contribution of radiolabeled antibody f ›m blood pool to liver radioactivity was also assessed.

LITERATURE SURVEY

I. MONOCLONAL ANTIBODIES

A. Immunoglobulin Structure

Humans possess millions of different immunoglobulin (Ig) molecules. This provides the body with a broad immunologic diversity, since the antibodies collectively exhibit much variety in binding with many different antigen determinants, or epitopes. All human and mouse Igs are divided into five major classes: IgG, IgA, IgM, IgD, and IgE. IgG and IgA are divided further into subclasses or isotypes. There are four subclasses of IgG in humans (IgG1, IgG2, IgG3, and IgG4) and in mice (IgG1, IgG2a, IgG2b, and IgG3).

Each Ig molecule consists of two pairs of identical polypeptide chains, the heavy chain and the light chain. The monomer form of the Ig molecules have a molecular weight between 150 and 180 kd. Molecular integrity is maintained both by specific covalent bonding mediated through disulfide bridging and by strong noncovalent interactions between the two heavy chains and between each of the heavy-chain light-chain pairs. The monomeric Ig molecule, as exemplified by mouse IgG (Figure 1), is bivalent in that the amino terminal end of each heavy-chain light-chain pair contains an antigen binding site. The heavy chain is composed of four contiguous and homologous structural domains: the variable (V) domain and the constant (C) domains, C1, C2, and C3. The light chain is composed of a V and a C domain. The interface between the V domains of each of the heavy-chain light-chain pairs forms

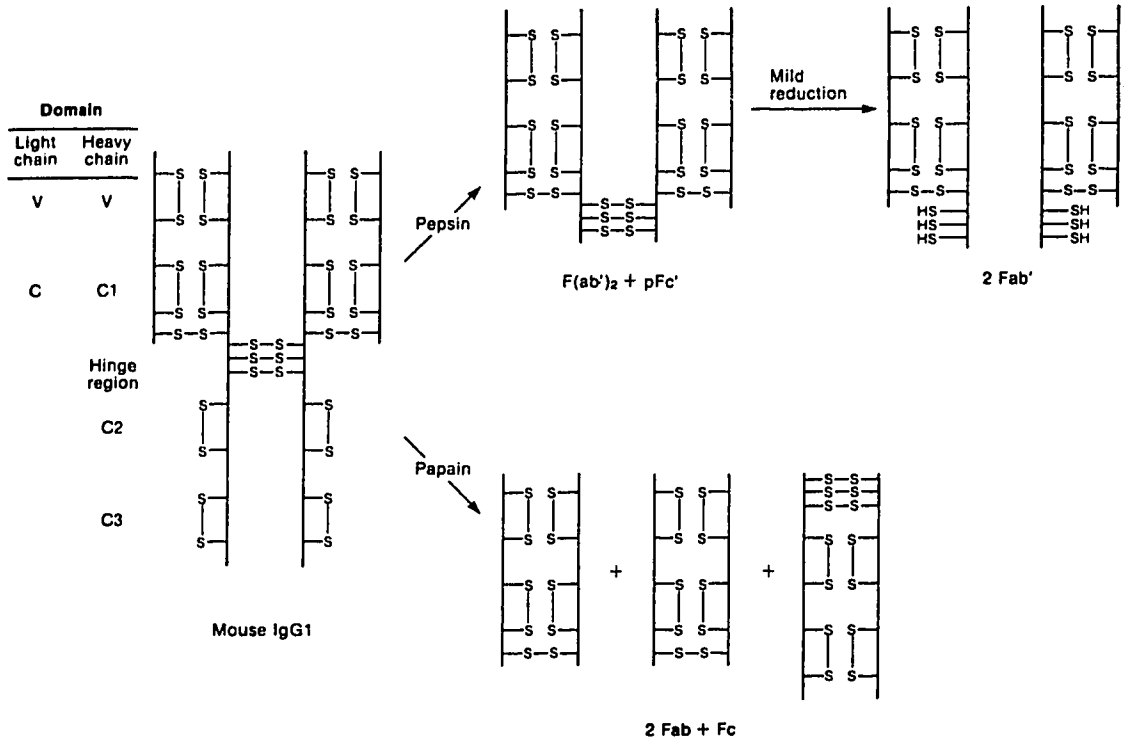

Figure 1. Structure of an IgG molecule. The two V regions bind to specific antigenic determinants and the C region interacts with the host immune system. Enzymatic digestion of the IgG with pepsin or papain produces a variety of fragments. The domain nomenclature for the light and heavy chain is shown on the left side of the figure. Intradomain and interchain disulfide bonding within the antibody and fragments are indicated by S-S and free cysteines generated in the Fab' are shown as -SH. [Adopted from Bogard *et al.* (20)].

the antigen binding sites. The C domains modulate certain effector functions such as antibody-dependent cell cytotoxity (ADCC), complement activation, and phagocytosis, and also exert an effect on the half-life of the antibody in serum (20).

IgG can be fragmented into smaller units, yielding Fab fragments ($F(ab')_2$, Fab' or Fab) and Fc fragments. The former are composed of variable (V_L) and constant (C_L) light domains and variable (V_H) and constant (C_H) heavy domains. Fc fragments contain heavy-chain domains (i.e., C_H2 and C_H3). Fab' and Fc fragments each weigh 50,000 daltons, while a $F(ab')_2$ fragment weighs approximately 100,000 daltons (21). IgG can be digested into two fragments, Fab and Fc, with a molar ratio of 2:1 with the proteolytic enzyme papain (22). When digested with pepsin, IgG divides into one large fragment and several smaller fragments. The larger fragment contains both of the antigen binding regions of the parent IgG molecule and is designated $F(ab')_2$. The smaller fragments are designated Fc pieces (pFc'). The $F(ab')_2$ fragment can be further divided into Fab' fragments (20).

Antibodies are glycoproteins with the carbohydrate content varying among different isotypes. One uniform feature of all IgG isotypes is that each H chain contains a single carbohydrate chain at Asn 298 in C_H2. Although the other chain pairs of C region domains in IgG interact noncovalently, the C_H2 domains are forced apart by the presence of carbohydrate. The carbohydrate is not only

important in maintaining the quarternary structure of the IgG, but also is essential for some effector functions (23).

B. Production of Monoclonal Antibodies

In 1975, Kohler and Milstein described the hybridoma technology to generate monoclonal antibodies (1). In this technique, antibody-forming cells (B lymphocytes) are fused to a tissue-culture adapted malignant plasma cell in order to make hybrids that retain the properties of both the normal antibody-forming cell and the myeloma fusion partner. The potential benefits of this technology are enormous. Pure antibodies can be generated against impure and even unknown antigen. A second major benefit of the hybridoma technology is that relatively large amounts of a single antibody molecule can be produced. A further benefit of the technology is the potential for selecting antibodies suited for a particular task (24).

Mouse Hybridoma Technology

In order to immortalize normal lymphocytes immunized by a particular antigen, they are fused with a suitable myeloma cell line so that ideally the hybrid myeloma/B lymphocytes acquire the genetic information for antibody production from the B lymphocytes and the unlimited dividing capacity from the myeloma cell. This enables the B-cell/myeloma hybrids (hybridoma) to produce antibodies of a desired specificity that are then cloned and expanded for large-scale MAb manufacture. First, mice are immunized with the antigen of

interest, usually with a limited immunization protocol. After the immunization, B lymphocytes, which have been committed to the production of antibodies specific for the antigen, are recovered from the spleen. These cells are then fused by the use of polyethylene glycol with a mouse myeloma cell line that lacks thymidine kinase activity. To select the hybrid cells, the cell mixture is suspended in hypoxanthine-aminopterin-thymidine (HAT) selective media. The unfused B lymphocytes live for only a few days in culture, and unfused myeloma cells are killed by the medium. The cells are then typically cloned by limiting dilution, and the desired hybridoma cells selected by immunoassay for the antibodies of interest.

Mouse monoclonal antibodies have some characteristics that may limit their usefulness as biological pharmaceutical reagents. The single largest issue is that mouse monoclonal antibodies, especially whole IgGs, are immunogenic in humans. This problem is being addressed from two different approaches: human monoclonal antibodies and chimeric monoclonal antibodies (20).

Human Monoclonal Antibodies

Human monoclonal antibodies can be generated by a procedure analogous to that used for making mouse monoclonal antibodies. The production of human MAbs for clinical applications lags behind that of murine MAbs because a number of obstacles have to be overcome: a source of sensitized human B lymphocytes, methods of immortalization and

stabilization clones, the selective screening of tumor reactive antibodies, and the production and purification of human MAbs for preclinical and clinical testing (25). These methods have been reviewed extensively (26-29). Many human MAbs, mostly IgM, have been obtained. The clinical results with human MAbs recently introduced in radioimmunoscintigraphy trials suggest that they do not elicit an antiglobulin response against the human antibody (HAHA), which could interfere with *in vivo* tumor targeting (25).

Chimeric Antibodies

Recombinant DNA techniques have been developed that make it possible to combine the V region of useful mouse monoclonal antibodies with the C regions of human monoclonal antibodies (23, 30). These reconstructed genes are then transfected into mouse myeloma cell lines or other cultured cells where they encode the synthesis and secretion of relatively large amounts of antibodies that will hopefully be less immunogenic in humans than the intact mouse monoclonal antibody. This technique has been used to create chimeric version of several murine monoclonal antibodies, including the 17-1A antibody specific for gastrointestinal cancer (31). Preliminary data demonstrate less immunogenicity for the chimeric 17-1A IgG when compared with the murine version (20).

Bispecific Antibodies

Bispecific antibodies — molecules combining two different

antigenic specificities — are currently being developed as new agents for immunotherapy and for basic studies in cell biology (32). Bispecific antibody can be prepared using three methods: chemically linking two antibody molecules or their fragments, by genetic manipulations and by fusion of either immune splenocytes with hybridomas or two different hybridomas (33-38). The latter procedure is often the method of choice as it yields hybrid hybridomas constantly producing bispecific antibodies or predetermined specificity, affinity and subtype.

Single-Chain Antibodies

This antibody molecule consists of variable-domain proteins from both the heavy chain and the light chain, linked by a peptide, thus giving it similar antigen-binding characteristics to the whole antibody. Absence of the Fc region decreases immunogenicity while retaining specific antigenic determinant properties. Because of its smaller size, the molecule is able to penetrate the target tissue, allowing for earlier localization while having decreased background (21).

Molecular Recognition Units

Researchers can now synthesize peptides that have the same amino acid sequences as the second or third (or other) hypervariable regions of the heavy chain of the parent antibody. These may have the greatest penetrating ability, since they are only a fraction of the size of the original

amino acid residues. Because of their size, they can reach sites in the body not normally accessible to the larger MAbs and are cleared rapidly from the circulation (21).

II. LABELING OF ANTIBODIES WITH RADIONUCLIDES

A. Choice of Radionuclides

The choice of a particular nuclide in a given system is governed by many key factors. The most important one is that the half-life of the isotope selected should be suitable for the study for which it is to be used. For example, the half-life of the nuclide should permit the localization of tumors with low background and at the same time limit long-range radiation exposure to the host tissue. Thus, shorter half-life is preferred. The energy of the radiation should be optimal for appropriate imaging, preferably between 100 and 200 keV, which is the ideal radiation energy for imaging devices currently available. However, for diagnostic purposes absorbed dose should be limited, while for therapeutic purposes the intensity of absorbed radiation is the most important factor. Last, good methodologies should be available for labeling antibodies with the chosen nuclide (39).

The four principal radionuclides studied for radioimmunoscintigraphy have been iodine-131 (^{131}I), indium-111 (^{111}In), iodine-123 (^{123}I), and technetium-99m (^{99m}Tc). Of these, the most desirable one is ^{99m}Tc, since it has a high intensity photon energy and it is readily available at very

low cost from an on-site generator. However, its short physical half-life of 6.02 h limits its use to early (less than 24 h) imaging. Although the other radionuclides, particular ^{123}I and ^{111}In, have favorable imaging properties, they are not generator-produced, and therefore need to be shipped from the production source, thereby being considerably more inconvenient and expensive than ^{99m}Tc. Dehalogenation of radioiodine and sequestration of ^{111}In in reticuloendothelial organs, particular the liver, are further disadvantages for these two radioisotopes. The physical characteristics of commonly used radionuclides and their advantages and disadvantages in immunoscintigraphy are listed in Table 1 and Tables 2-4, respectively.

A large selection of radionuclides is available for radioimmunotherapy (Table 5). Each radionuclide decays at a particular rate and with the release of particular radioactive emissions. They differ in the distance that their particle travels in tissue, depending upon the kinetic energy of discharge from the radioactive nuclide. The most important types of decay are gamma emissions, β decay, α decay, and electron capture.

Table 1. Selected Isotopes for Radioimmunoscintigraphy*.

Nuclide	T1/2	Mode of Decay	Gamma-Ray Energy (keV) (%Abundance)	Production
^{99m}Tc	6h	IT	140(90)	Reactor(^{99}Mo)
^{123}I	13.3h	EC	159(83)	Cyclotron
^{131}I	8.1d	β^-	80(2.6),284(5.4) 364(82),637(6.8) 723(1.6)	Reactor
^{111}In	2.8d	EC	173(89),247(94)	Cyclotron

* Adapted from Rayudu (40).

Table 2. Advantages and Disadvantages of ^{123}I**.

Advantages:

1. Well tried one-step methods of labeling
2. Ideal energy and high count rate give good quality images
3. Study completed in 24 h
4. Low absorbed radiation dose compared with ^{131}I and ^{111}In
5. Low liver and kidney activity due to deiodinases

Disadvantages:

1. Limited availability
2. Expensive
3. *In vivo* dehalogenation: thyroid blocking required

Table 3. Advantages and Disadvantages of ^{111}In**.

Advantages:
1. High count rate gives good quality images
2. Early and late images, up to 96 h, are obtainable
3. A T1/2 of 67 h allows labeling 1 or 2 days after delivery
4. No thyroid blockade required
Disadvantages:
1. Availability limited
2. High cost
3. Two-step labeling methods, metal-free reagents required, antibody cross-linking aggregation
4. Relatively high absorbed radiation dose
5. High bone marrow and liver uptake

Table 4. Advantages and Disadvantages of ^{99m}Tc**.

Advantages:
1. Ready availability on site
2. Very low cost
3. Rapid labeling available
4. Ideal energy and high count rate give high quality images
5. study completed within 24 h
6. Low absorbed radiation dose
Disadvantage:
1. Short T1/2 of 6 h limits the use to early imaging

** Adapted from Britton *et al.* (41).

Table 5. Selected Isotopes for Radioimmunotherapy[#].

	T1/2	Decay	Advantages	Disadvantages
^{131}I	8d	β	Inexpensive, images	Deiodination thyroid uptake
^{90}Y	2.5d	β	Indium chemistry	Bone uptake, no images
^{186}Re	3.5d	β	Tc chemistry images	Availability
^{188}Re	17h	β	Generator-produced, Tc chemistry, images	Availability
^{67}Cu	2.5d	β	Images	Availability
^{211}At	7h	α, EC	Iodine chemistry, short range	No images
^{125}I	60.4d	EC	Short range Auger electrons	Poor images

[#] Adapted from Goldenberg (42).

B. Radiclabeling of Antibodies with ^{99m}Tc

A large number of methods have been described for radiolabeling antibodies with ^{99m}Tc. These may be divided into two categories: direct labeling methods where the label is attached directly to the protein via endogenous groups, and indirect methods in which an exogenous chelator group is employed to facilitate the stable attachment of the label to the protein.

Direct Labeling Methods

A major advantage of the direct labeling method is that it can readily be reduced to a one-step labeling process, which is beneficial for making a marketable radiopharmaceutical preparation kit. Another advantage of this method is that the bond formed between the reduced technetium and the sulphydryl group is very strong.

Direct labeling of proteins with ^{99m}Tc comprises several steps, which can occur simultaneously or serially within the same reaction vial: (a) reduction of disulfide groups in the protein that is to be labeled in such a way that the biological characteristics of the protein are not altered; (b) preservation of the reactive sulphydryl groups created by the reduction of disulfide moieties; (c) reduction of pertechnetate ions to a redox state that is highly reactive with sulphydryl moieties; (d) preservation of the ^{99m}Tc in the required redox state as a reactive intermediate by the presence of an appropriate complexing agent; and (e) transfer

of reduced technetium from the reactive intermediate to the sulfide moieties of the protein (17). The reactions are shown in Figure 2.

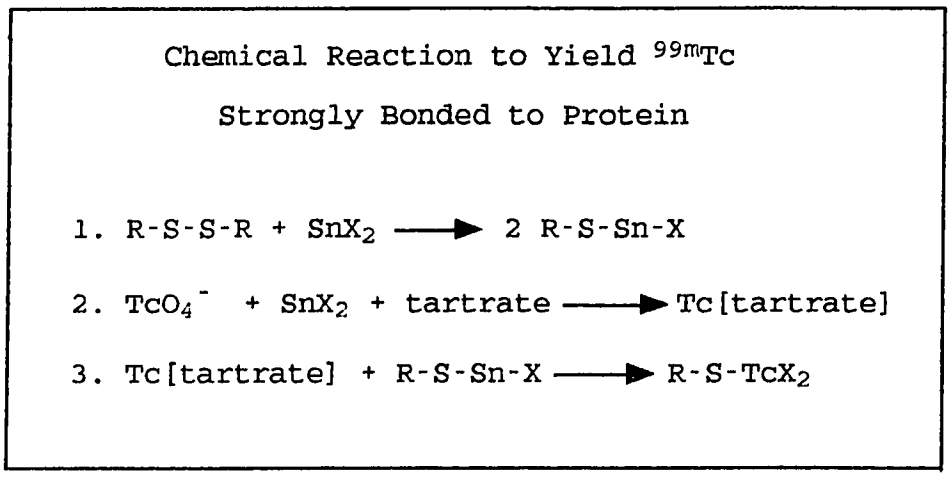

Figure 2. Direct labeling reactions to form strongly bonded ^{99m}Tc-proteins [Adapted from Rhodes (17)].

The protein to be labeled needs to contain sulfhydryl (-SH) groups or reactive monosulfides ($-S^-$ or -S-metal). These groups are also called thiols (43). Mono- and disulfides are a native part of most proteins and arise because one of the common amino acids, cysteine (the -SH-containing amino acid), is found as one of the units throughout the peptide backbone of most proteins. For many proteins, such as antibodies that are composed of several polypeptide chains, the native state of the protein is one in which most of the cysteine residues are linked to other cysteine residues, forming either intra- or inter-chain

disulfide bridges. The formation of these bridges occurs after polypeptide synthesis and is considered a primary mechanism involved in the folding of the polypeptide and in the interlinking of polypeptides into the secondary structure that imparts the overall shape and biological characteristics of the protein (44-46). These disulfide bridges are assumed to have a role in maintaining the structure of the mature, functioning protein.

Steigman *et al.*(47) were the first to suggest that sulfhydryl groups were responsible for the direct binding of ^{99m}Tc. Paik *et al.*(48) substantiated this hypothesis by titrating the number of SH groups produced by incubation with stannous ion. No free sulfhydryl groups could be detected before the addition of stannous ion. After incubation with stannous ion for 30 min, 5.5, 4.2 and 0.9 sulfhydryl groups per molecule were found in IgG, $F(ab')_2$ and Fab respectively. Pettit *et al.* (49) found that reducing the antibody with the disulfide-reducing agent increased the specific activity of the ^{99m}Tc-labeled antibody. If the antibody was dialyzed against Hg(II), which is known to block sulfhydryl groups, ^{99m}Tc labeling was blocked. As a control, antibody dialyzed against Mg(II), which does not block sulfhydryl groups, did not alter subsequent ^{99m}Tc labeling. Rhodes *et al.*(17) conclude, on the basis of the experiments of their own and others, that incubation of antibody with stannous salt solution reduces disulfide bonds and provides the $-S^-$ binding sites needed for the formation of strongly bonded ^{99m}Tc.

Generally, the disulfide groups in antibodies are distal to the hypervariable region, i.e. the antigen binding site. Hence, it seems unlikely that the immunoreactivity of the antibody would be changed unless the reduction caused either major structural alterations or fragmentation of the light and heavy chains, which would disrupt the hypervariable regions. When antibodies are reduced with various reducing agents for ^{99m}Tc labeling, only a small fraction of the available disulfide groups are reduced (50). ELISA (enzyme-linked immunosorbent assay) studies show that the immunoreactivity of the antibody is not changed by the pretinning process (17).

The method of reducing antibodies with stannous ions is named "pretinning", because it is assumed that the tin is fulfilling three roles: reduction of disulfides, co-ordination with $-S^-$ groups, and reduction of the pertechnetate.

It has been more than 10 years since Rhodes developed the direct labeling method by pretinning the antibody by overnight incubation with stannous chloride (51, 52, 238). This procedure is the conceptual basis for the many "direct labeling" methods being pursued today. In a recent improvement an optimum combination of $SnCl_2$, potassium phthalate and sodium potassium tartrate at pH 5.6 is incubated with the antibody for 21 h at room temperature. The pretreated antibody can be stored frozen at -70°C. Pertechnetate is added and incubated for 1 h at room

temperature before use.

Several variations of the direct-labeling method, all of which are generally successful, have been reported. These variations primarily involve alternate methods of antibody reduction.

The Schwarz method (53) involves the reduction of antibodies with monothiols such as 2-mercaptoethanol (2-ME). The essential feature of this method is that the antibody does not come into contact with the Sn(II)-containing reducing agent.

Reno *et al.*(54) reduced antibodies with dithiothreitol (DTT) then protected the free sulfhydryl groups with Zn(II) ions or other sulfhydryl derivatizing agents.

Recently ascorbic acid (AA) has been suggested as a better agent for the reduction of MAb disulfide bonds (56). A comparison with several reducing agents [Sn(II), DTT, dithioerythritol (DTE) and 2-ME] suggests that labeling IgM with these agents has an average efficiency of 55 to 65% while with AA the labeling efficiency is 96%.

A novel photoactivation process for direct labeling of MAbs with ^{99m}Tc has been developed by Sykes *et al.*(57). The process takes advantages of the effects of ultraviolet light exposure to facilitate ^{99m}Tc labeling of MAbs. MAbs in suitable vials with PBS are exposed to a selected spectral range (250-400 nm) from 3 watt low pressure mercury vapor lamps. The radiolabeled MAbs generated from an optimized process display high radiochemical purity (>90%), biochemical quality (>90%) and retention of immunological function (80%).

Photoactivation of MAbs provides a simple, rapid and compatible method which can be readily adapted for radioimmunopharmaceutical production.

Indirect Labeling Methods

This strategy, more commonly known as the bifunctional chelate (BFC) approach, involves the covalent attachment of a strong chelating agent on the antibody molecule at $-NH_2$, -SH or on the carbohydrate moiety. The chelating agents provide a known number of high affinity binding sites on the protein to which reduced technetium-99m may be strongly bound. The variations in the technique depend upon the type of bifunctional chelating agent employed, the point of attachment on the antibody molecule, and also whether the chelating agent is complexed with technetium-99m prior or subsequent to conjugation to the antibody (58).

A number of chelators have been described for this purpose. Derivatives of diethylenetriaminepentaacetic acid (DTPA) have been tested first, since the coupling methodology of this chelate to protein is already well established with other radionuclides. For this purpose, most investigators use DTPA anhydrides, either mixed anhydrides (59) or cyclic anhydrides (60). Attachment of the chelate immunoglobulin is usually through the epsilon amino group of the lysine residues. The isolated DTPA-conjugated MAb is then labeled with ^{99m}Tc either by reduction of ^{99m}Tc-pertechnetate with stannous chloride or sodium dithionate or by transmetallation using pre-reduced ^{99m}Tc in the form of ^{99m}Tc-glucoheptonate.

Metallothionein (MT) has also been tested as a protein derived chelating agent. This metal-binding protein, having a high proportion of cysteine which allows for efficient technetium-99m binding, can be attached to an immunoglobulin (61). The conjugation of the metallothionein to antibody molecule is achieved using glutaraldehyde as the cross-linker, and technetium-99m is incorporated into the conjugated antibody via a transchelation reaction with ^{99m}Tc-glucoheptonate (62). It has also been genetically engineered in the IgG structure whereby it provides a site-specific labeling point.

In yet another approach, antibodies have been pretreated with 2-iminothiolane so as to provide thiol reactive positions for the attachment of technetium using weak ^{99m}Tc chelates such as glucoheptonate or MDP (55).

Other bifunctional chelates have been designed and tested. These include: derivatives of bis-N-methylthiol semicarbazone (DTS) (63), diaminodithiol (DADT) ligand system (64), bifunctional aromatic hydrazines (65), diamide dithiolate chelating agent (66), SCN-derivatives of aromatic boronic acids (67), mercaptoacetyltriglycine (MAG_3) (68), and others.

C. Radioiodination of Antibodies

Various radionuclides of iodine have remained popular as MAb labels. This is due mainly to availability and cost. In particular, ^{125}I and ^{131}I, to a less extent ^{123}I, have become

available in sufficient quantities to carry out extensive investigations. The chemistry of protein radioiodination, in addition, is well established (69-71) and has guided the development of MAb iodination schemes.

Methods for iodination of antibodies include the common electrophilic substitution methods that use oxidants such as chloramine T, iodine monochloride, Iodogen, lactoperoxidase and electrolytic methods, as well as the classic Bolton-Hunter conjugation method in which the prosthetic group N-succinimidyl 3-(4-hydroxyphenyl) propionate is first iodinated using one of the above oxidants and then conjugated to the antibody (72, 73). Recently, new conjugation methods have been introduced and studied (74-76).

Direct electrophilic substitution methods involve oxidation of radioiodine to reactive cationic species that replaces a hydrogen atom on the carbon at the ortho position to the hydroxy group of a phenyl ring of MAb tyrosine (or histidine) residues. The various electrophilic radioiodination methods which have been used for antibody labeling are summarized in this section.

Chloramine T Method

Chloramine-T (N-chloro-4-methylbenzenesulfonamide sodium salt) is an oxidizing agent for the preparation of cationic I^+ from iodide and it was first used for protein iodination by Hunter and Greenwood (77, 78). Chloramine-T forms hypochlorous acid in the aqueous phase. This acid provides the mild oxidation needed. Iodination reaction conditions can

be easily controlled by appropriately choosing the concentration of reactants, temperature, and time. The chloramine-T-mediated iodination reaction can be terminated by the addition of an excess of reducing agent, usually sodium metabisulfite.

Iodogen Method

Fraker and Speck (79) first described the use of 1,3,4,6-tetrachloro-3α,6α-diphenylglycouril (Iodogen) as a reagent for the iodination of proteins. Iodogen is extremely stable and virtually insoluble in water, allowing rapid iodination in the solid phase with aqueous solutions of iodine and proteins. Procedurally, Iodogen is dissolved in chloroform or methylene chloride and then evaporated on the inside walls of a reaction vial. It can be stored in this form in a dessicator. The iodination mixture, containing the immunoglobulin and Na*I in the appropriate buffer, is added to the Iodogen-coated reaction vial. The reaction is allowed to proceed for 5 to 15 min and is terminated by the transfer of the reaction mixture to a non-coated tube. Therefore, there is no need for a reducing agent or centrifugation of the reaction mixture when this system is used for iodination. The procedure is rapid and offers many advantages over the chloramine-T procedure.

Lactoperoxidase Method

Marchalonis (80) first described an iodination method using enzymes to iodinate proteins and Thorell and Johansson

(81) modified the procedure to its present form. In this procedure, lactoperoxidase is used to convert I^- to I_2 and the reaction is started by the addition of H_2O_2 (82). The enzymatic procedure has the advantage in that it does not contain many chemical reagents except for a small amount of hydrogen peroxide. Hence, this procedure offers a comparatively gentle approach for the iodination of proteins to high specific activity. A disadvantage of this procedure is that the labeled proteins will be contaminated with small amounts of iodinated lactoperoxidase (39).

Electrolytic Method

Rosa *et al.*(83) described a method for electrolytic iodination and applied it to the labeling of fibrinogen. The reactive iodine needed for iodination of tyrosine residues can be generated by oxidation of I^- by careful choice of voltage and current. This procedure is rarely used.

III. RADIOIMMUNOSCINTIGRAPHY AND RADIOIMMUNOTHERAPY

A. Radioimmunoscintigraphy

Radioimmunoscintigraphy is the use of monoclonal antibodies, or their derivatives, labeled with radioactive materials for clinical diagnosis of cancer and many other diseases. The basic principle of this diagnostic modality is the specific reaction between radiolabeled monoclonal antibodies and the target antigen. After intravenous

injection, radiolabeled MAb passively diffuse into the extravascular compartment and progressively accumulate at sites where the target antigen is expressed. When a sufficient amount of radioactivity is carried to the target, it can be detected externally by gamma camera (84). The sensitivity thus is determined by the ultimate accumulation of the tracer.

1. Oncological Diagnosis

Using antisera against carcinoembryonic antigen (CEA), Goldenberg *et al.*(85) reported excellent sensitivities and specificities in whole body survey imaging using gamma camera methodology in a series of patients with colorectal tumors in 1978. It was the first large series of clinical studies of radioimmunoscintigraphy. About the same time, imaging of human renal cell cancer using radiolabeled antibodies was also reported (86). In more than 10 years since then, several thousands patients have been evaluated with radiolabeled antibodies in radioimmunoscintigraphy studies, in which the patients have been injected with a variety of antibodies, differing in nature and form (intact or fragments) and labeled with various radionuclides.

The prime question related to radioimmunoscintigraphy is whether cancer-specific antigens exist. At present no such antigens have been identified for carcinoma, and thus tumor-associated antigens are used instead. Most cancer antigens identified by anticancer antibodies appear to be quantitatively increased in neoplasia, and frequently are

associated with a wide range of carcinomas, so that antibodies raised against them are considered to be pancarcinoma in specificity. Indeed, it is rare to find an MAb that is specifically reactive with a single organ or tissue type, whether normal or neoplastic (3, 87, 88). Despite these limitations, numerous applications of MAbs in cancer diagnosis, detection, monitoring and prognostication have been identified or proposed (3).

Most studies of radioimmunoscintigraphy have focused on colorectal carcinomas (89, 90), ovarian cancer (91), lung cancer (92), and malignant melanoma (93). The potential clinical applications for radioimmunoscintigraphy of cancer are summarized by Goldenberg (3): (a). Presurgical staging of extent of disease; (b). Postsurgical evaluation of residual disease; (c). Confirmation of viable tumor known by other methods; (d). Disclosure of recurrence in a patient with a rising tumor-marker titer in the blood; and (e). Confirmation of tumor targeting of antibody to be used for immunotherapy. The results of thousands of patients indicate that usually between 60% and 90% of known lesions have been disclosed correctly, depending on the antibody and its form, the radionuclide, or the planar and/or tomographic scanning methods.

The current status of cancer radioimmunoscintigraphy showed some encouraging aspects. In over 10,000 patients studied worldwide, radioactive antibodies have been found to be safe. On a tumor-site basis, results between 60% and over 90% have been reported, with the highest accuracy rates found

for MAbs labeled with ^{131}I, ^{123}I, ^{111}In and ^{99m}Tc. Tumors as small as 0.4 to 0.5 cm have been disclosed with ^{99m}Tc-MAbs, especially with emission tomography, but the resolution is usually in the range of 1.0 to 2.0 cm. Some tumors missed by other methods, including computed tomography, have been revealed by antibody imaging. Antibody imaging can be positive even before the antigen titer in the blood is elevated (3).

2. Detection of Infection and Inflammation

Various nuclear medicine techniques are widely used to image foci of infection and inflammation. Among the relatively new radiopharmaceuticals for this purpose are radioimmuno-conjugates such as labeled murine monoclonal antigranulocyte antibodies and labeled human polyclonal nonspecific immunoglobulin G.

Presently, several monoclonal antibodies that bind to epitopes on granulocytes are under clinical investigation. Approximately 10% of the injected radiolabeled antibody is bound to circulating granulocytes that are functionally normal and in turn they may target an infection area. Approximately 19% of the injected radiolabeled antibody circulates as free Ig and has the same potential as labeled nonspecific human IgG. The uptake of free circulating Ig is probably not antigen related (4). Although the mechanism for accumulation of radiolabeled nonspecific human IgG in inflammatory and infectious foci may not be completely understood, it is likely related to increased vascular

permeability into an expanded excellular fluid space and to the chemical nature of the radiolabel (94).

The clinical results for immunoscintigraphy with radiolabeled granulocyte-specific antibodies and human nonspecific polyclonal IgG indicate their potential value for the detection of infectious and inflammatory processes (4, 95). Bone, lung and abdominal infectious processes can thus be visualized with great sensitivity within 24 h after injection.

3. Cardiovascular Applications

Progress in biotechnology combined with clinical need have spawned the commercial development of two monoclonal antibody products with application to cardiovascular diagnostic imaging (5). The first is an antimyosin antibody first developed by Khaw *et al.* (96, 97). This antibody is targeted against the heavy chain of human cardiac myosin, a large intracellular protein (500,000 daltons) that is present in cardiac muscle cells but is exposed only in cells that are irreversibly damaged. The second is an antifibrin antibody (T2G1s) (98). It is targeted against the seven amino acids at the amino terminus of the beta chain of fibrin, which is exposed when thrombin removes fibrinopeptides A and B from intact fibrinogen. The resulting antibody is therefore specific for insoluble fibrin expressed during the *in vivo* formation of an acute blood clot. The antimyosin and antifibrin antibodies have the potential to provide the clinician with unique markers of disease processes based on

physiological rather than morphological or indirect indicators of pathology (5).

B. Radioimmunotherapy

MAb immunotherapy can involve the administration of unconjugated antibodies for direct killing and as active immunogen (vaccines), or as carriers of drugs, toxins or isotopes. In contrast to drug and toxin immunoconjugates, radiolabeled MAbs can kill cells that are at a distance from the target, depending on the choice of radionuclide, without the MAb conjugate being internalized. Therefore, radiolabeled MAbs can distribute their cytotoxic energy to antigen-negative cells in the neighborhood of antigen-positive cells. The attractive feature of radioimmuotherapy is the prospect that most normal tissues are spared intensive radiation. Unfortunately, radioimmunotherapy has thus far failed to fulfill this promise. Based on clinical experience of over a decade, mostly with ^{131}I-labeled polyclonal and MAbs, it has been found that: partial and transient responses can be achieved in certain solid tumors; lymphoproliferative malignancies are generally more responsive to radioimmuno-therapy; and there is usually, but not always, a dose-dependent effect (3). Overall, the results of clinical studies with radioimmunotherapy are still inconclusive, being most encouraging for specific indications (2).

IV. LIMITATIONS AND STRATEGIES OF RADIOIMMUNOSCINTIGRAPHY AND RADIOIMMUNOTHERAPY

The main factors limiting the clinical application of immunoscintigraphy and immunotherapy are an often moderate target-to-background ratio in images, the immunogenicity of injected murine antibodies, heavy and costly industrial constraints and the fact that a true benefit for the patient has not yet been demonstrated (2).

A. Antibody Biodistribution and Targeting

One of the advantages of scintigraphic imaging in general is the ability to perform relatively rapid whole body scanning. In the same way, it would be desirable to use immunoscintigraphy to detect occult disease foci through the body. To be efficient, such systematic scanning requires high radioactive uptake in the target and the highest possible ratios between target and normal tissue activity. In the present state of the art, these conditions have not yet been met.

It is universally observed that following administration of the radiolabeled antibodies, only a tiny fraction of the radioactivity concentrates in tumor with the rest localizing in blood and in normal tissues such as liver, spleen and kidneys (6). In patients, the fraction of radiolabel on antibody which localizes in tumor following i.v. administration is generally in the range of 0.0007-0.01% of the injected dose per gram of tissue (7, 8). The essential

requirement for high resolution of the site of tumor uptake and for high sensitivity for subclinical and subradiological tumor detection is to obtain the highest achievable count rate from the target by the imaging system. Low tumor uptake of radiolabeled antibody results in low count rates from tumor sites. Low count rates give "noisy" images where the target is less separable from background and the high variability of the background itself may give "noise blobs" which may be falsely interpreted as target signals (41). In radioimmunotherapy, the total dose of radiation delivered to tumor is generally low, usually less than 2,000 cGy and often less than 1,200 cGy, especially with ^{131}I-labeled MAbs (3).

It has been suggested that the low levels of tumor radioactivity in patients may be the result, in part, of antibody dilution *in vivo*. If 20% of the injected radioactivity localize in a 1 g tumor in a mouse xenograft, then only about 0.01% ID/g may be expected to accumulate in a human because of the 3000-fold difference in body weight (6, 99).

In recent years, the peculiarities of tumor physiology have been recognized as determinants of antibody distribution (100). Three physiological barriers responsible for the poor localization of antibodies in tumors have been identified: (a) heterogeneous blood supply; (b) elevated interstitial pressure; and (c) large transport distances in the interstitium. The first barrier limits the delivery of blood-borne molecules to well-perfused regions of a tumor; the second barrier reduces extravasation of fluid and antibodies

in the high interstitial pressure regions and also leads to an experimentally verifiable, radially outward convection in the tumor periphery which opposes the inward diffusion; and the third barrier increases the time required for slowly moving macromolecules to reach distal regions of a tumor. Binding of antibody to an antigen further lowers the effective diffusion rate of the antibody by reducing the amount of mobile antibody. Due to micro- and macroscopic heterogeneities in tumors, the relative magnitude of each of these barriers would vary from one location to another and from one day to the next in the same tumor and from one tumor to another (100).

In order to improve the ratio of target-to-background activity, either the tumor uptake of radiolabeled antibodies should be increased, or non-specific activity in normal tissues should be reduced, or both. To enhance tumor targeting and accretion by MAbs, methods to increase tumor vascularization and permeability are under investigation, such as with external irradiation or vascular dilators (9-11). A simple approach has been the direct injection of the MAb into the tumor cavity, such as intraperitoneal or intrathecal applications (12, 14). This regional administration may increase antibody targeting. Other methods that may increase antibody accretion include use of combination of MAbs against different antigen targets (14), as well as methods to increase the expression of the antigen targets, such as by treatment with biologic agents (e.g., recombinant interferon) (15, 16).

Recombinant human interferons (rHu-IFNs) are potent immuno-modulatory compounds capable of altering the antigen phenotype of a variety of human cells (101). Preclinical studies have demonstrated that recombinant interferons can both increase the amount of tumor antigen expressed by a given tumor cell and increase the percentage of cells within the tumor cell population that express the antigen (101). Greiner *et al.*(15) have observed that rHu-IFN significantly increased ^{125}I-B6.2 binding to (a) human colon tumor extracts and (b) the localization of the radioconjugated MAb to the surface of the colon xenograft. Studies by Rosenblum *et al.*(102) have also shown that interferons can up-regulate tumor targeting of radiolabeled MAbs in patients in a clinical trial.

The effect of interleukin 2 (IL-2) on tumor uptake of ^{99m}Tc-labeled ZCE025, anti-CEA MAb, in nude mice bearing human gastric cancer has also been investigated (103). After pretreatment of the mice with IL-2 at doses of 1000 and 2000 units, there is 1.2-1.5 fold increase in tumor uptake of MAb that appears to be dose-dependent. This effect is probably related to the increase in vascular permeability of tumor endothelium.

Several methods have been proposed to reduce the normal tissue concentration of the radiolabeled antibody. In an attempt to speed up blood clearance, MAbs have been split up into bivalent or monovalent fragments or reduced to just the hypervariable region. However, this reduces their binding affinity. Antibody fragments, such as $F(ab')_2$ or Fab

fragments, have a faster blood clearance than whole antibodies, to the extent of allowing the use of short-lived radionuclides such as ^{99m}Tc. This improvement, however, does not yield tumor-to-background ratios high enough to allow good diagnostic sensitivity and low-risk therapeutic application (104). A useful approach towards reducing blood radioactivity levels is the administration of a second antibody, unlabeled, and specific for the radiolabeled first antibody (105). The immune complexes formed in the circulation are rapidly cleared into liver and spleen. A related approach, which does not suffer from the high RES backgrounds inherent in the use of a second antibody, employs bifunctional, or, bispecific, antibodies, where there is linkage of one antibody or fragment against the tumor target with another antibody or fragment against the chelated hapten (106). After injection of the unlabeled bifunctional antibody, the chelated isotope, which reacts with the second antibody arm, is injected once time has permitted the bifunctional antibody to clear from normal tissues. A two- or three-step targeting strategy involving the high-affinity (10^{15} M^{-1}) noncovalent binding between avidin (or streptavidin) and biotin is also being developed. This binding affinity can exceed that of antigen-antibody reactions by 1 million. Biotin is a vitamin found in low levels in tissues and blood, and avidin is a protein found in egg white. Either can be conjugated to targeting antibodies, and the other is then subsequently administered as a drug or isotope conjugate for capturing at the site of antigen (3, 107-109). Other

approaches for the reduction of background radioactivity include increasing the dose of antibody administered (110) and use of metabolizable chelate linkers (111).

B. Immunogenicity of Murine Antibodies

The clinical usefulness of the radiolabeled murine MAbs for diagnostic and therapeutic applications is limited by their immunogenicity. The development of a human antimouse antibody (HAMA) response in most patients after one, or at most a few, administrations of murine MAbs results in the formation of circulating immune complexes diverting the MAbs from their tumor targets to the reticuloendothelial system, especially liver and spleen, and the rapid excretion of the radioisotopes (25, 112-118). Under these conditions, the radiolabeled antibodies cannot reach their disease target, which is then generally not visualized. This is the major obstacle to their repeated use for radioimmunoscintigraphy and radioimmunotherapy. Another consequence of the presence of HAMA is their interference with tumor marker assays and the risk of false-positive results (119).

Removing circulating HAMA by plasmapheresis or suppressing HAMA formation with immunosuppressive agents or high doses of antibodies have been attempted with limited success (120-124). The alternative to immunosuppression is the development of less or nonimmunogenic antibodies. Mouse/human chimeric antibodies and humanized antibody fragments (HV or CDR constructs) produced by molecular engineering are in various stages of preclinical or clinical evaluation. The

results obtained with chimeric antibodies suggest that some of these products still elicit a clinically significant HAMA response and have limitations similar to murine MAbs (125-127). The human antibodies and humanized antibodies that are currently undergoing clinical evaluations showed that they do not elicit a significant human antihuman response (25). Their respective merits may depend on the repertoire of tumor-associated antigens they recognize. Human MAbs, being an expression of the immune response of the host, may confer an advantage to these antibodies in terms of identifying more relevant targets for cancer detection.

V. PHARMACOKINETICS AND METABOLISM OF RADIOLABELED ANTIBODIES

A. Variables in Pharmacokinetics and Metabolism of Antibodies

In considering the metabolism and pharmacokinetics of antibodies, three crucial variables must be considered: the nature of the Ig molecule studied, the species of the recipient, and the methods of antibody purification, labeling, and assay (24).

The Igs studied may be polyclonal, and therefore heterogeneous, or monoclonal and homogeneous. They may originate from a number of animal species. The Ig molecules are administered either intact or as Fab or $F(ab')_2$ fragments that have been generated by proteolytic or chemical cleavage. More recently, mutant monoclonal antibodies arising through

deletions or recombination between different constant region genes have also been examined (24).

The species of the recipient of the passively administered Ig represents a crucial variable. Many studies have been carried out in which Igs from one species are administered to another species (heterologous recipient). The interpretation of these studies using heterologous antibody are especially complicated because the T1/2 of an animal's own homologous Ig is inversely proportional to the size of the species, i.e., mouse Ig has a much shorter T1/2 in mice than human Ig has in humans (128). While this is usually attributed to the inherent metabolic characteristics of species, the structural properties of the Ig may also be important (129). Ig of one species administered to another is literally a foreign antigen, and may encounter preformed cross-reacting antibodies and elicit a significant immune response affecting its intravascular metabolism. If the recipient bears a tumor or other target antigen, the size of the species and resultant dilution of the administered antibody will be a large determinant of the rate of interaction with the target (130).

Final important variables in the studies that have been reported are the methods of purification, labeling, and quantification of the administered Ig. Radiolabeled antibodies are most frequently used in biodistribution studies because of the ease of quantification. Overly harsh isolation and purification of antibody may cause structural damage and accelerated antibody catabolism (131). The number

of substituted radioactive groups per antibody molecule can range from less than one, in which case some antibodies are unmodified, to much greater than one, which increases the risk of denaturation.

In spite of all the biological and technical variables involved, previous studies of Ig metabolism have clearly demonstrated that plasma levels of Ig are tightly regulated. This is mediated in large part by a mechanism that recognized the concentration of Ig in the plasma and changes the rate of intravascular metabolism is response to that level, suggesting the presence of some type of receptor to mediate these changes (24, 132, 133).

B. Pharmacokinetics of Radiolabeled Antibodies

Radiolabeled MAb distributes fairly rapidly throughout the blood pool following intravenous injection. The intact Ig has a biologic half-life in serum between 16 and 50 hours (mean, 31 hours). Fragments have an appreciably shorter half-life: between 20 min to three hours (mean, 83 min) for Fab fragments and between seven and 15 hours (mean, 12 hours) for the $F(ab')_2$ fragment. Plasma clearance of MAbs will depend both on the nature of the MAb (intact Ig vs fragment) and on the nature of the antigen-antibody system; different antigenic sites also will show differences in MAb handling (93). Larson *et al.*(134) observed significant differences in serum clearance as well as major differences in hepatic uptake of Fab directed against two distinct antigenic systems (the HAWA and p97 antigens).

Various studies have fit the pharmacokinetic data to different compartment models. Rosenblum *et al.* (135) described the analysis of pharmacokinetic data for a radioindium labeled anti-p97 MAb96.5 in 28 patients. They observed that the label was cleared from the plasma monoexponentially and closely fit an open, one-compartment mathematical model. The plasma half-life for ^{111}In label varied from 27 h for 1-mg dose to 39 h for the 20-mg dose; the overall mean plasma T1/2 was 32 h. Although there appeared to be some variability in the calculated T1/2 for the various dose levels, these differences were not statistically significant and did not appear to be dependent upon either the total dose of antibody or upon the dose of ^{111}In label. The apparent volume of distribution (Vd) varied with the dose administered from 7.8 to 3.0 liters at the 1- and 20-mg doses, respectively. The decrease in the Vd at higher doses is perhaps due to saturation of extravascular binding compartments. The Vd approximated the total blood volume at lower dose (1-2 mg) and approximated the total plasma volume at higher doses (5-20 mg). Analysis of the ^{111}In label in spleen, liver, heart, and kidney showed that the concentration of label in liver tissue was reduced with increasing antibody doses and coincided with changes in the apparent volume of distribution. The cumulative urinary excretion of the ^{111}In label over 48 h was between 12 and 23% of the total administered dose.

The pharmacokinetics and biodistribution of a ^{131}I-labeled

mouse/human chimeric MAb (C-17-1A) was studied in six patients by Meredith *et al.* (136). The serum disappearance of radioactivity in all six patients best fit a two-compartment model with an α T1/2 of 17.6 h and β T1/2 of 101 h. The pharmacokinetic parameters based on two independent measures (serum MAb concentration vs serum radioactivity) of ^{131}I labeled chimeric antibody are quite similar. Another chimeric MAb, B72.3, composed of the V-regions of murine B72.3 and the constant regions of human immunoglobulin G4 heavy and k light chain, was administered as a ^{131}I labeled conjugate to 12 patients. The plasma disappearance curve of the chimeric MAb was best fit by a two-compartment model with an α T1/2 of 18 h and a β T1/2 of 224 h (137). Other radiolabeled antibodies whose *in vivo* kinetics in patients fit two-compartment model with various α T1/2 and β T1/2 include radioiodinated anti-ovarian carcinoma MAb MOv18 (138), tritium labeled anti-transferrin receptor antibody OX-26 (139), and indium-111 labeled MAb BW431/26 (140). When the latter is labeled with ^{99m}Tc, it is eliminated linearly over time, indicating that the radionuclide moiety also plays a role in the *in vivo* disposition of the radioimmunoconjugates (140).

A pharmacokinetic comparison of the murine and chimeric forms of the ^{99m}Tc-labeled MAb174H.64 has been made by McQuarrie *et al.*(141) in a phase II clinical trial. A two-compartment model of the form: $C(t) = C_1 e^{-\lambda 1 t} + C_2 e^{-\lambda 2 t}$ was found to best describe the distribution of activity of both the murine and chimeric MAbs. The distribution half-lives

were 2.9 ± 0.7 h and 2.7 ± 0.2 h and the terminal elimination half-lives were 17.6 ± 3.8 h and 22.5 ± 1.3 h for the murine and chimeric MAbs, respectively. No significant difference was found between the kinetic model parameters of two MAbs at the 95% confidence level.

Based on their observations and known immunoglobulin kinetics, Eger *et al.*(142) developed a nonlinear compartmental model to describe the biodistribution of ^{111}In-9.2.27 and the other coinjected ^{111}In-associated compounds in humans. The model included (a) three compartments representing intact ^{111}In-9.2.27 (Plasma, nonsaturable, and saturable binding compartments), (b) four compartments representing ^{111}In-diethylenetriaminepenta-acetic acid, and (c) one compartment representing ^{111}In in an undetermined chemical form (extravascular delay compartment). Analysis of the rate of urinary excretion relative to plasma concentration indicated that the saturable binding compartment was a site for catabolism of monoclonal antibody. The model indicated that to fill the saturable sites would require a dose of approximately 0.5 mg and suggested that >3.5 mg would maintain saturation for 200 h. Computer integration of gamma camera counts over the spleen revealed a clear saturable component of uptake, whereas integration over the liver showed no such pattern. The bone marrow also showed saturable uptake.

The pharmacokinetics of a radioiodinated immunoglobulin G1 (MOPC-21) and its $F(ab')_2$ and Fab' fragments following

i.v. administration in mice has been studied by Covell *et al.* (143) using a physiologically based, organ-specific model to describe antibody biodistribution, catabolism, and excretion. The model includes the processes related to (a) circulation of plasma, (b) exchange of antibody across the capillary wall, (c) return of antibody from the interstitial space to the bloodstream via lymph, (d) interaction of antibody with "cell-associated" material, and (e) formation of metabolic products. This analysis is comparable to that of fitting a three-compartment linear model to the data for each organ. The investigators concluded that the whole IgG (a) remains in the body for 8.3 days, the majority of time in the carcass (53% of the total residence time); (b) has a distribution volume exceeding that of plasma plus interstitial fluid; (c) distributes into these volumes rapidly for most enteral organs; and (d) has the greatest percentage of its catabolism due to the gut (73%), followed by the liver (21%), then the spleen (4%). When compared with whole IgG, the Fab' fragment (a) is cleared from the body 35 times faster; (b) has a larger total distribution volume; (c) distributes more rapidly into this volume; and (d) is catabolized principally by the kidney (73% of total catabolism), followed by the gut (23%), then the spleen (3%). The $F(ab')_2$ fragment has pharmacokinetic characteristics that fall between those of whole IgG and Fab'.

C. Factors Modulating Rate of Antibody Catabolism

1. Structural Determinants of Intravascular Half-life

Class- and subclass-specific rates of antibody catabolism imply that the location of the rate-determinating area is in the C region of antibody molecule (144, 145). Spiegelberg and Fishkin's (146) finding that the Fc fragments of all four human IgG subclasses have identical fractional catabolic rates suggested that structures outside the Fc fragment were responsible for the accelerated catabolism.

2. Modified Antibodies

Ig molecules can be modified by genetic and biochemical means. The modified antibodies may have different pharmacokinetics from their parent Igs.

Carbohydrate side chains in Fc portion have an important bearing on antibody half-life. Removal of the terminal sialic acid residue from carbohydrate side chain of homologous mouse IgG1 resulted in a rapid T1/2 of approximately ten to 20 min. The possible reason is that exposed terminal galactose residues mediate antibody binding to the hepatic galactose receptors (24). Rapid intravascular clearance and hepatic uptake of IgG-antigen complex was uniquely inhibited by coinjection or preinjection of galactose terminal glycoproteins, confirming a role for the hepatic galactose receptor system in immune clearance (147).

The role of interchain disulfide bonds on catabolism was examined by reduction and alkylation of rabbit gamma globulin. Slightly increased catabolism of these molecules in

the rabbit was observed (148).

3. Serum Ig Levels

IgG catabolism rate is proportional to the serum concentration, termed the concentration-catabolism phenomenon. The higher the serum level of IgG (as in inflammatory disease or myeloma), the greater the rate of catabolism. Conversely, states with reduced IgG level (hereditary or acquired) have decreased rates of catabolism. Subclass-specific elevation of IgG1, IgG2, and IgG3 each results in increased catabolism of all the IgG subclasses (149-153).

The existence of the concentration-catabolism phenomenon has implications beyond one of many determinants of the catabolic rate. It implies the presence of some type of receptor that recognizes IgG and modulates catabolism, resulting in specific regulation of metabolism.

4. Metabolic and Systemic Factors

Because of the variation of Ig half-life dependent on the size of the animal studied, it is hypothesized that metabolic rate is a major determinant of antibody survival. This hypothesis is confirmed by making rabbits hyperthyroid with a resultant decrease in gamma globulin half-life. In the rat, variation in thyroid function correlates with rate of gamma globulin catabolism. Age of the recipient may affect antibody half-life (128).

D. Metabolism of Radiolabeled Antibodies

1. ^{99m}Tc Labeled Antibodies

Hnatowich *et al.*(154) have investigated the *in vivo* (mouse) and *in vitro* properties of ^{99m}Tc when labeled to antibodies via direct (via stannous ion reduction) and indirect (via the hydrazino nicotinamide chelator) method. Radiochromatograms obtained by size-exclusion HPLC analysis of serum and homogenates of liver and kidneys after administration of labeled MAbs showed radiolabeled antibodies, with various radioactive metabolites in liver and kidneys. The direct label was more prone to transchelation to cysteine and glutathione *in vitro* and *in vivo*. Following intravenous administration, urinary excretion of activity was threefold greater for the direct label and was almost exclusively labeled cysteine and glutathione. Significant differences in the biodistribution of ^{99m}Tc were also observed: liver levels were lower, kidney levels were higher and clearance of label from blood and tissues was faster for the direct label.

2. Radioiodinated Antibodies

The *in vivo* fate of radioiodinated MAb ^{131}I-B72.3 (anti-TAG-72) in 27 patients was studied by Colcher *et al.*(155). High performance liquid chromatography and SDS-polyacrylamide gel electrophoresis demonstrated that the radionuclide is remaining in association with the MAb in serum following i.v. administration to patients. Similar results have been

observed in patients following i.p. administration of ^{131}I-B72.3. In most cases, very little free ^{131}I-labeled fragments are detected with the exception of one patient where 4-22% of the radiolabel is determined as free ^{131}I. This does not preclude, however, the possibility that degradation of MAb B72.3 is occurring. Degradation products or free ^{131}I may not be detected due to rapid clearance from the circulation. Other investigations (129, 156-159) confirmed that there is *in vivo* dehalogenation of radioiodinated antibodies. As much as 50% of the injected radioactivity has been reported as appearing in patient urine in 24 h (129), presumably either as free iodide ion or as a low molecular weight iodinated protein fragment (156). This dehalogenation occurs in liver, spleen, bone marrow, and lymph nodes (157, 159).

3. Indium-Labeled Antibodies

In an effort to understand the nature of nontarget uptake of indium-labeled antibodies Himmelsbach and Wahl (160) have evaluated the molecular weight of ^{111}In species retained in several tissues by radio-FPLC (sizing chromatography) following injection of ^{111}In-DTPA-5G6.4, a murine MAb, into normal mice. The proportion of ^{111}In-containing species was found to vary with the tissue and with time. Analysis of blood showed only radiolabeled antibody. In the liver, several ^{111}In species were identified with molecular weights compatible with intact antibody, ^{111}In-transferrin, and low molecular weight complexes, with an increase in the

proportion of latter two species occurring over time. While the same molecular weight species were also identified in the kidneys, the kidneys contained the largest percentage of low molecular weight species which increased with time. Other investigators (161-163) observed similar metabolic fate of ^{111}In-labeled antibodies.

VI. MECHANISMS OF HEPATIC UPTAKE OF RADIOLABELED ANTIBODIES

A. Morphology and Physiology of Liver

Although liver is the largest internal organ, it is, in a sense, only one to two cells thick. This is because the hepatocytes (parenchymal or polygonal cells) form one-to-two-cell thick plates that are separated from each other by large capillary spaces called sinusoids. The sinusoids are lined with hepatic sinusoidal cells (including Kupffer cells, endothelial cells, fat-storing cells, and pit cells) which form the wall of the hepatic sinusoids and located between blood in the lumen of the sinusoids and hepatocytes. The large intercellular gaps between adjacent sinusoidal cells make these sinusoids more highly permeable than other capillaries and permit blood plasma containing endogenous and exogenous substances to enter the space of Disse, i.e. between sinusoidal membrane and hepatocytes, and to have direct contact with the microvilli of the parenchymal cell membrane. Red blood cells cannot pass into the space of Disse (164-166).

The hepatic plates are arranged into functional groups

called liver lobules. Due to the structure of the lobule, blood entering the liver from the portal vein and hepatic artery at the periphery of the lobule flows past 12 to 24 cells before entering a central vein. The central veins of different liver lobules converge to form the hepatic vein, which carries blood from the liver to the inferior vena cava (166, 167).

The normal young adult rat has two main cell types, hepatic parenchymal cells and sinusoidal cells. Parenchymal cells constitute 90-95% of total liver weight but only 60-65% of total cell population, while reticuloendothelial cells (sinusoidal cells) represent 5-10% of liver by weight and 35-40% of total cellular population (168).

The hepatocyte knows no rival in terms of its complexity of function. It shares responsibility for total body homeostasis of fats, carbohydrates, and proteins; the liver cell closely monitors their utilization and synthesis in order to both regulate plasma levels and meet its own metabolic requirements. Hormones, immunoglobulins, lipoproteins, and effete substances are among the macromolecules that are taken up specifically by receptor-mediated endocytosis, either for degradation, secretion into the bile, or utilization by the hepatocyte (167).

Bile is produced by hepatocytes and secreted into bile canaliculi located within each hepatic plate. The bile canaliculi are drained at the periphery of each lobule by bile ducts, and these in turn drain into the hepatic duct, which carries the bile to the gallbladder (via the cystic

duct) and to the intestine (via the common bile duct) (166).

Hepatic sinusoidal cells perform an enormous diversity of functions. Kupffer cells and endothelial cells form part of a cooperative system that interacts with hepatocytes. Some of the functions of sinusoidal cells are: particle phagocytosis, endocytosis of bacteria and endotoxin, clearance of cellular debris after trauma, clearance of antigens and immune complexes, etc. (165).

B. Mechanisms of Hepatic Uptake of Radiolabeled Antibodies

Since antibodies are proteins of relatively high molecular weight, their elimination from the body is usually a slow process. Thus if the radiolabeled antibody localizes in tumor to only a modest degree, the majority of the administered dose is free to localize elsewhere, namely in blood, liver and other normal organs. The consequence of this is an increase in the background radioactivity levels and an increase in the difficulty of detecting tumor (6).

Most investigators have focused on the liver as the organ of concern with regard to excessive background radioactivity levels. It appears that the uptake by the liver of IgGs and clearance through the kidney of the antibody fragments are the major routes of elimination. Accumulation of radionuclides in these organs is a major detriment to the use of radiolabeled monoclonal antibodies for diagnosis and therapy. A more complete understanding of the uptake, clearance, and radioisotopic sequestration mechanisms may lead to the development of alternative labeling procedures

which may circumvent some of these problems.

Accumulation of radioactivity in liver after administration of radiolabeled antibody has been attributed to clearance of antibody molecules denatured during the labeling process (6, 169). The liver accumulation increases with increasing denaturation of antibodies. With improvement of labeling techniques, denaturation of antibodies only plays limited role in the liver accumulation of radiolabels.

Accumulation of radiolabel in liver may result from clearance of antigen-antibody complexes. Radioactive immune complexes of murine antibody may form with circulating human anti-mouse antibodies or the antigen shed from tumor into serum after the *in vivo* administration of radiolabeled antibodies. Studies in mice have shown that the level of circulating antigen have a major impact on the pharmacokinetics of radiolabeled antibody (170). The pharmacokinetics of ^{111}In and ^{125}I anti-CEA was determined in athymic mice bearing tumors which secreted different amount of CEA. In the animals bearing lower tumor secreting levels of CEA, the blood anti-CEA activity at 24 h was 15% ID per gram for both isotopes. This contrasts with a blood level of 2% ID per gram for the ^{125}I-labeled anti-CEA seen in animals with high CEA secretory rates. Liver values of ^{111}In were also markedly increased in these animals. Beatty *et al.*(171) demonstrated that much of the liver uptake is related to the formation of antigen-antibody complexes and the normal liver intensity can be decreased by inhibition of radiolabeled complex formation. In their study, antigen-antibody complexes

have been formed *in vitro* with CEA and murine monoclonal anti-CEA antibodies. The behavior of these complexes *in vivo* is very similar to the behavior of indium-111-labeled anti-CEA MAb when injected into a tumor bearing animal. As a result of complex formation liver uptake of ^{111}In increased and the rate of clearance of indium-111-labeled anti-CEA MAb from the circulation was more rapid. Further indirect evidence of the importance of antigen-antibody complex formation in liver uptake is that high affinity antibodies were more prone to form antigen-antibody complexes and resulted in increased liver uptake. The role of antigen-antibody complexes in liver uptake is strongly supported by HPLC radiochromatograms of liver homogenates at different times following administration of indium-labeled anti-CEA MAb in normal and tumor bearing mice (163). Liver uptake of ^{111}In in mice without tumor was low (8-12% ID/g) and both IgG and a low molecular weight metabolite were found in the liver homogenates. Liver uptake in tumor bearing mice increased dramatically (15-40% ID/g) with size of tumor and in addition to the IgG and low molecular weight components, a high molecular weight compound was identified. Administration of CEA-^{111}In-anti-CEA MAb complexes to non-tumor bearing mice produced the same HPLC and SDS-PAGE patterns as those seen in mice with large (>1 g) tumors. Liver homogenates from tumor bearing mice given specific antibody pretreatment showed the same patterns seen with non-tumor bearing mice (no high molecular weight peak). In conclusion, radioactive antigen-antibody complexes are formed in tumor bearing mice and

rapidly cleared by the liver.

Beyond those mentioned above, it is possible that foreign proteins such as xenogeneic antibodies may themselves be cleared by the liver (i.e., natural process of clearance). As is described above, liver uptake of radiolabeled MAb in normal mice (without tumor) is still very high (163).

Liver uptake of radiolabeled antibodies is probably related to the Fc portion on the antibody. Fc receptors and carbohydrate receptors which bind immunoglobulin have been localized on both parenchymal and nonparenchymal cells (172-176). Consequently, both may contribute to the hepatic uptake of a radioisotope which is attached to a monoclonal antibody. The mechanism for the *in vivo* uptake of foreign compounds such as human IgG by mouse hepatocytes is thought to involve binding to a receptor followed by macropinocytosis (177). Studies using the radiolabeled $F(ab')_2$ have shown reduced accretion of radionuclide by the liver. When the Fc portion of the antibody was removed by pepsin digestion, and the resulting $F(ab')_2$ radiolabeled with ^{111}In and ^{125}I and administered into mice, at 1 h after injection the absolute uptake in the liver of ^{111}In was reduced from 0.61 ± 0.04% (SD) of the injected dose/g of liver to 0.16 ± 0.06% of the injected dose. Similarly, the uptake of ^{125}I was reduced from 0.23 ± 0.06 to 0.11 ± 0.01 (162). One possible explanation for the reduced liver uptake is that the more rapid clearance from blood reduces the available $F(ab')_2$ for the liver accretion. Studies by Sands (178) have shown that this is not

the case. Reduced uptake of both radioiodine and radioindium were seen both *in vivo* and in rat livers perfused *in vitro*. These data strongly suggest that liver cells have receptors for a component of the Fc portion of the antibody which is responsible for the non-antigen specific liver uptake of radiolabeled murine monoclonal antibodies. It is not known at present if these receptors are for the carbohydrate, which is found predominantly on the Fc, or for a protein component of the Fc (178).

Jones *et al.*(162) have identified the liver cell types responsible for radiolabeled antibody uptake. Following perfusion with collagenase and separation by Percoll gradient, two liver cell fractions of rat were visually identified on the basis of cell size as parenchymal and nonparenchymal cells. Each fraction contained at least 95% of the designated cell type. Further identification of these cell fractions was accomplished by the use of cell markers, Microlite and Hepatolite, which were used to functionally identify the two cell fractions. The majority of the ^{99m}Tc-Microlite and ^{99m}Tc-Hepatolite were recovered in the nonparenchymal and parenchymal fractions, respectively. One hour after radiolabeled (^{111}In or ^{125}I) antibody injection, approximately equal amounts of each radionuclide were associated with each cell type, as calculated on a per cell basis. Since the majority of liver cells are parenchymal cells, the largest fraction of both radionuclides were found within the parenchymal cells of the liver. Similar results have been found by Beatty *et al.*(171).

In addition to the protein moiety, the isotope moiety also plays a role in the liver accumulation of radiolabel after administration of radiolabeled MAb. The time course of rat liver uptake of a murine antibody radiolabeled with either ^{125}I or ^{111}In showed that antibody accretion at early time points (0 - 1 min) was equal regardless of the radiolabel. Differences occur with time; i.e., radioiodine accretion decreases with time while that of the radioindium increases with time. This result was most likely due to the trapping of metabolized radioindium in the liver and extrusion of the freed raioiodine out of the liver (178). The dual-labeled (^{125}I and ^{111}In) antibody biodistribution (1 - 48 h) in other studies showed similar results (179). There was a very rapid and prolonged retention of ^{111}In by the liver accompanied by the rapid accumulation and prolonged retention of ^{111}In by the spleen. Iodine-125 radiolabeled antibody was also taken up rapidly by liver and spleen, while the radiolabel left both organs quickly. It has been suggested that the increased background levels of ^{111}In radioactivity in liver may be a direct consequence of transchelation with the labeled transferrin localizing in the liver (180). In conclusion, the murine antibodies radiolabeled by currently available methods rapidly accumulate in the liver. Differences in liver content of radioactivity are due to inherent differences in the manner by which the radioisotope is subsequently handled.

C. Strategies of Reducing the High Liver Background

In order to lower the high liver background after administration of radiolabeled antibodies, either the uptake of the radiolabel must be decreased or its removal must be increased. With the increase in understanding of the liver mechanisms by which radiolabeled antibodies are taken up and cleared, various approaches have been proposed to reduce the liver radioactivity background.

As liver accumulation is related to the Fc portion on the antibody, it has been suggested that the removal of the Fc fragment of an antibody will reduce uptake into liver and other tissues possessing specific receptors for the Fc fragment. The use of radiolabeled $F(ab')_2$ fragment in place of the intact IgG antibody does reduce the absolute liver uptake of the radiolabels (162).

Formation of antigen-antibody complexes is a significant factor in the increased uptake of radiolabel by the liver in tumor bearing animals (171). To neutralize the circulating antigen with unlabeled antibody will result in an increased production of unlabeled complexes and a decreased production of labeled complexes and hence will decrease the liver uptake of radiolabel. Beatty *et al.*(181) described that pre-treatment of tumor bearing mice with high doses of unlabeled antibody altered the biodistribution of ^{111}In-labeled antibody and resulted in a significant reduction of radioactivity in the liver. This effect was found to be antibody specific and dose dependent. The most significant decrease in liver uptake of the radiolabel was obtained when the unlabeled antibody

was identical to the labeled antibody or had a higher affinity than the labeled antibody.

An alternative approach to decrease accumulation of label in liver is to alter the way in which the antibodies are radiolabeled. Brechbiel *et al.*(182) synthesized a chelate, SCN-Bz-DTPA (a DTPA analogue), for antibody labeling with ^{111}In. Animal biodistribution studies with the same antibody coupled with the cyclic anhydride of DTPA and with SCN-Bz-DTPA have consistently shown lower liver levels following administration of the latter (183, 184). These improved biodistribution results have been attributed to improved stability of the ^{111}In label resulting in decreased transchelation to transferrin and subsequent decreased localization of ^{111}In-transferrin in liver (183). Another labeling approach reported by Wang *et al.*(185) also showed reduced hepatic accumulation of radiolabeled MAb with Indium-111-thioether-poly-L-lysine-DTPA-MAb.

VII. MONOCLONAL ANTIBODY MAb170

MAb170 is a IgG1 murine monoclonal antibody derived from mice immunized with the terminal disaccharide of asialo-GM1, the beta anomer of the Thomsen-Friedenreich antigen (TF-antigen) (186-188). Although the TF-antigen is expressed by a large proportion of human carcinomata (189-191), subsequent screening of clones demonstrated no binding of MAb170 with asialo-GM1. However, the MAb reacts *in vitro* with over 90% of adenocarcinoma tested (186-188).

MAb170 has been successfully radiolabeled with ^{99m}Tc, ^{111}In and radioiodines, and its clinical trials are currently under way (192-194). Biodistribution studies in mice of both ^{111}In and ^{99m}Tc labeled MAb170 shows that the latter has a faster clearance. At 6 h after administration, ^{99m}Tc radioactivity levels in blood, heart, lungs, liver, spleen, kidney and muscle are lower than those observed in mice which are injected with ^{111}In-MAb170. On the other hand, intestinal uptake levels of ^{99m}Tc are significantly higher than those of ^{111}In. Of interest is that some biliary excretion of ^{99m}Tc radioactivity has been noted in mice which are injected with ^{99m}Tc MAb170 (186). Analysis of the *in vivo* data obtained from patients indicated that a two-compartment model would adequately fit the MAb170 data labeled with both ^{99m}Tc and ^{111}In (195). The terminal elimination phase half-life of the ^{99m}Tc was calculated to be approximately 18.8 ± 0.9 h and of ^{111}In-MAb approximately 57.5 ± 20 h. These values can be used to estimate optimal postinfusion imaging times when used in conjunction with the observed r[illegible]mum organ/tumor uptake.

^{99m}Tc radiolabeled MAb170 has been evaluated in patients with cancers of breast, colon, ovary, bladder, prostate and other tissue origins (187, 192, 193, 196). Overall clinical accuracy with the radiolabeled antibody is 88-92%, with the antibody appearing to have particular clinical utility in gynaecological and breast cancers (195, 196). It was concluded that MAb170 has significant potential as a new

radiopharmaceutical in the evaluation of patients with a range of adenocarcinomata.

A thorough study of the distribution of the antigen CA170 in normal and cancer tissues showed a highly restricted pattern with a primary expression on a subset of simple epithelial cells. A variety of cells of gastrointestinal origin as well as the collecting tubules of the kidney, liver bile ducts, and the epithelial cells of the lungs and prostate showed moderate expression of CA170. The strong expression of CA170 was noted in breast, colon, endometrial, lung, ovarian, and prostatic carcinoma. Biochemical investigations on the nature of CA170 suggested that the epitope recognized by MAb170 on the natural antigen is associated with cytoskeletal proteins (186), but the exact nature of the antigen has not been elucidated.

MATERIALS AND METHODS

I. SOURCES OF MATERIALS

Monoclonal antibody MAb170 was a gift from Biomira Inc., Edmonton, Canada.

Human immunoglobulin G (HIgG) and fragments of $F(ab')_2$ and Fc were purchased from Calbiochem, USA. HIgG was supplied in the form of lyophilzed powder containing D-mannitol and NaCl, and the label purity was stated as greater than 99% of total protein content. $F(ab')_2$ was prepared by pepsin digest of purified human IgG. Fc was prepared by papain digest of purified human IgG. As stated by the supplier, both $F(ab')_2$ and Fc were determined as homogeneous by electrophoresis and their protein contents were greater than 90% by dye-binding assay.

Sodium pertechnetate ($Na^{99m}TcO_4$) and sodium iodide ($Na\ ^{125}I$) were purchased from the Edmonton Radiopharmaceutical Center, Edmonton, Canada.

The sources of variety of chemicals and culture media used in this work are specified in the text immediately after the description of the chemical or the medium.

Adult male Balb/c mice were obtained from University of Alberta Health Sciences Laboratory Animal Services, University of Alberta, Edmonton, Canada. Mice weighing 20-25g were used for biodistribution studies, others weighing 25-30g were used for isolation of hepatocytes. Animals were housed four to five per cage and given water and food *ad libitum.*

II. PREPARATION AND QUALITY CONTROL OF RADIOLABELED ANTIBODIES

A. Preparation of Radiolabeled Antibodies

1. ^{99m}Tc-MAb170

MAb170 was provided by Biomira Inc. as a solution consisting of 5 mg/mL in phosphate buffered saline (PBS, 0.05 M phosphate buffer, 0.15 M NaCl). The pretinned direct labeling method was employed. This method consisted of the mixture of a 0.27 mL solution containing 2 mM $SnCl_2.2H_2O$, 10 mM potassium phthalate, and 100 mM sodium potassium tartrate at pH 5.6 which was added to 0.4 mL of 5 mg/mL MAb170 and incubated for 24 h at room temperature. The required amount of sodium pertechnetate (^{99m}Tc) was added and incubated with the above mixture for 15 min at room temperature. ^{99m}Tc-MAb170 preparation was purified on a centrifuged sephadex G-50 mini-column with saline wash before using.

2. ^{99m}Tc-HIgG

^{99m}Tc-HIgG was prepared and purified using the same methods as described above.

3. Radioiodination of MAb170

MAb170 was radioiodinated using 0.1 mg of protein in PBS and 10 µg of tube-coated Iodogen (Pierce) with 74 MBq (2 mCi) of Na^{125}I for 5 min. The free radioiodine was separated using an Excellulose GF-5 desalting column (Pierce). ^{125}I-MAb170 was

stored in a shielded container at 2-8°C and used within 24 h.

B. Quality Control of Radiolabeled Antibodies

In the preparation of radiolabeled antibodies there are undesirable radiochemical impurities which include free radionuclide and radiolabeled antibody fragments. After the purification of radiolabeled antibody preparation with G-50 mini-column or GF-5 desalting column, quality control must be performed to ensure that only the desired radioactive antibody is recovered. The following methods were used in this study for quality control.

1. High Performance Liquid Chromatography (HPLC)

The purified preparations of radiolabeled antibody were analyzed using a size-exclusion HPLC system (TSK G3000sw column) to determine the radiochemical purity. The column was eluted with a solvent mixture containing 0.1 M NaH_2PO_4, 0.1 M Na_2SO_4 and 0.65% NaN_3 at pH 7.2 and a flow rate of 1 mL/min.

2. Trichloroacetic Acid (TCA) Precipitation

The percent radioactivity bound to antibody was determined using TCA precipitation technique. Aliquots of purified preparations of radiolabeled antibody (3-5 µL) were added to Eppendorf centrifuge tubes containing 0.5 mL of 1% bovine serum albumin (BSA) in PBS and 5 µL of 1 M NaI solution. The solution in the tube was treated with 0.5 mL of 20% TCA solution and mixed thoroughly. The dissolved protein could be precipitated from the solution by the addition of TCA. The

precipitate was isolated by centrifugation and the radioactivity of both the precipitate and the supernatant was determined by gamma counting. The percent of the radioactivity present in the precipitate was the percent bound radioactivity.

3. Instant Thin Layer Chromatography (ITLC)

The purified preparations of radiolabeled antibody were analyzed by instant thin layer chromatography (Silica gel, Gelman Sciences, Ann Arbor). Acetone and 85% methanol (MeOH)/normal saline were used as solvent systems. Two microliters of the sample were applied to the origin of the gel plate. After drying, the plate was developed, cut at the center and assayed for radioactivities of the two strips. ITLC would show the radioactivity bound to the protein and the free unbound radionuclide.

III. DETECTION OF ^{99m}Tc AND ^{125}I RADIOACTIVITY

Both ^{99m}Tc and ^{125}I are the radioisotopes used in this project. The radioactivity of the isotopes was measured using two types of Na(Tl) gamma detection equipment and associated electronics: Beckman gamma 8000 counter and MINAXI Auto-Gamma 5000 series gamma counter.

^{99m}Tc is generated from the ^{99}Mo-^{99m}Tc generator system. The 6-h half-life isomeric state of ^{99m}Tc at 142 keV primarily (99% probability) decays to another isomeric state at 140

keV. It decays almost instantaneously to the ground state by the emission of a 140 keV gamma ray or a corresponding conversion electron. The ground state or the nuclide ^{99}Tc itself is a radionuclide. However, its half-life is so long that for all practicall purposes it may be considered stable (197). Based on its decay scheme, the gamma emissions of ^{99m}Tc were counted with an energy window of 100 - 300 keV. The two sigma % error was set to be 2.0%. The radioactivity was expressed as counts per minute (CPM). The decay corrections of the radioactivity were performed according to the equation of decay of law:

$$Rt = Ro\ e^{-\lambda t}$$

where Ro and Rt are the radioactivity count rates at time zero and t, repectively; λ is the decay constant and t the elapsed time.

^{125}I decay scheme is complex and its disintegrations fall in three categories. In 7% of the disintegrations there is no detectable radiation produced since the X-rays produced are of too low energy to interact with the crystal. A further 39.8% of the disintegrations produce a single photon due to either a 27.5 keV X-ray (K-shell filling of ^{125}Te after electron capture in ^{125}I) or a 35.5 keV gamma ray (emission from excited state of ^{125}Te). The remaining 53.2% of the disintegrations give 2 photons with a sum peak at 55.0 keV (K-shell X-ray after electron capture plus a K-shell X-ray after internal conversion) or a sum peak at 63.0 keV (K-shell X-ray after electron capture plus gamma ray from ^{125}Te)

(198). Based on its decay scheme, the radioactivity of ^{125}I was detected with two energy windows, one ranging 15 to 40 keV for the lower energy singles photopeak and the other 40 to 80 keV for higher energy coincidence photopeak. The two sigma % error was set to be 0.5%. The radioactivity was expressed as disintegrations per minute (DPM) using an appropriate calculator.

In the case of dual label (^{99m}Tc and ^{125}I) counting, two energy windows were set, one for ^{125}I (15 to 80 keV) and the other for ^{99m}Tc (100 to 200 keV). The spill-over radioactivity to the ^{125}I window from ^{99m}Tc was corrected using "Dual Label Spillover Correction" program in the Beckman gamma 8000 counter. The two sigma % error was set to be 2.0%. The radioactivity of both ^{99m}Tc and ^{125}I was expressed as counts per minute.

IV. BIODISTRIBUTION STUDY OF ^{99m}Tc-MAB170 IN MICE

The biodistribution of ^{99m}Tc-MAb170 was conducted in normal Balb/c mice. Radiolabeled antibody (0.1 mL) was intravenously injected in the tail vein of experimental mice. At various time intervals the mice were exsanguinated by cardiac puncture under CO_2 (dry ice) anesthesia. Tissues were dissected from the carcass, blotted to remove adhering blood, weighed and counted for radioactivity in a multi-sample NaI (Tl) gamma counter against an aliquot of the injectate. Final data were routinely expressed as either percent of the

injected dose per gram or per organ. Each experiment consisted of a group of 3 mice.

V. STUDIES OF METABOLISM OF ^{99m}Tc-MAb170 IN MICE

A. Animal Studies and Tissue Homogenates

Balb/c mice were used for metabolic studies of ^{99m}Tc-MAb170. ^{99m}Tc-MAb170 (0.1 mL, 20 µg, 2.22-3.70 mBq) was injected into the tail vein of mice. At different time intervals following ^{99m}Tc-MAb170 administration, urine samples were collected. The animals were sacrificed at 1, 3, 6 and 24 hour by exsanguination after CO_2 anaesthesia. Blood was collected and the livers and kidneys were excised. The urine and tissue samples were kept on ice before further processing.

The blood and urine were centrifuged at 3,000 rpm for 15 min. The resulting supernatants were then passed through a 0.22µ Millipore filter and the filtrates were stored in a refrigerator.

The liver and kidney were homogenized in normal saline (3 to 5 times tissue weight) with a glass homogenizer. The homogenate was centrifuged at 10,000 rpm for 15 min in an Eppendorf table centrifuge. The ^{99m}Tc activities in the total homogenate and the supernatant were determined. About 50-60% of the ^{99m}Tc radioactivity was recovered in the supernatant. The supernatant was then centrifuged for 15 minutes. The

resulting supernatant was passed through a 0.22μ Millipore filter.

Mouse gallbladders were removed at 1 h after ^{99m}Tc-MAb170 administration. Seven gallbladders were put in an Eppendorf tube containing 1 mL of saline, cut into pieces and shaken with a Vortex mixer for 2 min so that the bile would be released in saline. The tube was then centrifuged in an Eppendorf table centrifuge at 10,000 rpm for 15 min. The resulting bile supernatant was also filtered.

B. High Performance Liquid Chromatography (HPLC) Analysis

Size-exclusion HPLC analyses were performed with a TSK guard column, TSK G3000sw column (7.8 mm x 30 cm), pump, manometric module, UV monitor and radioisotope flow detector. The column was eluted with a solvent mixture containing 0.1 M NaH_2PO_4, 0.1 M Na_2SO_4 and 0.65% NaN_3 at pH 7.2 and a flow rate of 1 mL/min. The column was calibrated for molecular weight by analysis of a set of standards consisting of thyroglobulin (670,000 daltons), IgG (150,000 daltons) and carbonic anhydrase (31,000 daltons). The standard molecular weights were plotted against the retention times to obtain a standard curve. The column was also calibrated with ^{99m}Tc-MAb170 and $Na^{99m}TcO_4$.

Twenty μL of filtered samples (blood, urine, liver and kidney homogenates) was loaded and eluted through the HPLC. The fractions were collected and counted in a multi-sample Beckman gamma 8000 counter.

C. Sephadex G-50 Chromatography

Sephadex G-50 open column chromatography was performed principally to estimate the molecular weights of ^{99m}Tc antibody catabolites. A 1 x 50 cm column of G-50 (Dry bead diameter: 50-150 μ. Fractionation range: 1,500-30,000 daltons. Sigma Chemical Co.) was eluted with 0.25 M PBS, pH 7.2. The column was calibrated for molecular weight by the analysis of carbonic anhydrase (31,000 daltons), chymotrypsinogen A (25,000 daltons), ribonuclease A (13,700 daltons) and vitamin B12 (1,350 daltons). The void volume (Vo) was determined with blue dextran (2,000,000 daltons). The column was also calibrated with $Na^{99m}TcO_4$. The standard molecular weights were plotted against Ve/Vo (Ve = elution volume, Vo = void volume) to obtain a standard curve.

Filtered samples (100-300 μL) of blood, urine, liver and kidney homogenates were eluted through the column. The fractions were collected into test tubes using fraction collector and counted in a Beckman gamma 8000 counter.

D. Bio-Gel P2 Chromatography

Bio-Gel P2 open column chromatography was performed to separate and identify smaller molecular weight ^{99m}Tc antibody catabolites. A 1 x 50 cm column of Bio-Gel P2 (62 μ, fine, fractionation range: 100-1,800 daltons. BIO-RAD) with a pump and UV monitor was used for sample separation. The various catabolites were eluted with 0.25 M PBS, pH 7.2. The column was calibrated for molecular weight ranges by the assay of

vitamin B12 (1,350 daltons), glutathione disulfide (GSSG, 613 daltons), reduced glutathione (307 daltons), uracil (112 daltons) and sodium azide (65 daltons). The column was then calibrated with ^{99m}Tc-glutathione, ^{99m}Tc-cysteine and $Na^{99m}TcO_4$.

Labeling of ^{99m}Tc-Glutathione (GSH)

GSH (Sigma) was radiolabeled with ^{99m}Tc according to Fritzberg *et al.*(199). A solution of GSH was prepared by dissolving 180 mg of the material in approximately 2.8 mL of distilled water, adjusting the pH to 7.5 with 1 N NaOH, and bringing the volume to 3 mL. After purging with nitrogen for 5 min, 1.5 mL of this solution was mixed with 1.5 mL of $Na^{99m}TcO_4$ diluted with saline and the final solution heated at 60-65°C for 15 minutes.

Preparation of ^{99m}Tc-Cysteine

Cysteine (Sigma) was radiolabeled with ^{99m}Tc according to the procedures of Johannsen *et al.*(200) and Mardirossian *et al.*(201). To 100 µL of 10 mg/mL solution of cysteine in 0.5 M acetate buffer, pH 6, was added about 10 µL of $Na^{99m}TcO_4$ solution in saline and 2 µL of a fresh 0.1 M HCl solution containing 2 mg/mL of $SnCl_2.2H_2O$ (Sigma). The cysteine solution was mixed and allowed to react for a few minutes.

Small volumes (50-200 µL) of the selected samples of ^{99m}Tc-GSH, ^{99m}Tc-cysteine, radioactive filtered urine, liver and kidney homogenates as well as 800 µL of bile supernatant obtained after administration of radiolabeled MAb170 were eluted through a Bio-Gel P2 column. The fractions were collected and counted in a Beckman gamma 8000 counter.

The mouse urine collected at 3 h after ^{99m}Tc-MAb170 administration underwent G 50-Bio-Gel P2 serial analyses. The filtered urine was first eluted through G-50 column. The eluates from 35 mL to 38 mL were collected and mixed. One mL of the eluate mixture was then applied to the Bio-Gel P2 column. The fractions were collected and counted in Beckman gamma 8000 counter.

E. Sephacryl S-200 Chromatography

An open column of Sephacryl S-200HR (Dry bead diameter: 25-75 µ. Fractionation range: 5,000-250,000 daltons. Pharmacia) was employed to study the metabolites of antibody present in liver homogenates. The column (1 x 50 cm) was eluted with 0.25 M PBS and was calibrated with a series of standards of blue dextran (2,000,000 daltons), MAb170 (150,000 daltons), chymotrypsinogen A (25,000 daltons) and ribonuclease A (13,700 daltons).

The filtered liver homogenates obtained from mice at 24 hour after ^{99m}Tc-MAb170 administration were eluted through the column. The fractions were collected and counted in a Beckman gamma 8000 counter.

F. Instant Thin Layer Chromatography (ITLC)

The filtered serum, urine and the supernatants from liver and kidney homogenates obtained after administration of radiolabeled MAb170 were analyzed by ITLC (Silica gel, Gelman Sciences, Ann Arbor). ITLC was performed with two solvent systems: acetone and 85% MeOH/normal saline. Two microliters of each sample were spotted at the origin and developed until the solvent migrated to the solvent front line. The silica gel plates were cut at the center point, placed in vials, and assayed for radioactivity in a Beckman 8000 gamma counter. The percent radioactivity remaining at the origin after development was calculated.

VI. ANALYSIS OF GROSS LIVER ^{99m}Tc RADIOACTIVITY AND DISTRIBUTION OF ^{99m}Tc RADIOACTIVITY IN BLOOD

A. Contributions of ^{99m}Tc Radioactivity in Blood to the ^{99m}Tc Radioactivity in Liver

The contributions of radioactivity in blood to the ^{99m}Tc radioactivity in liver at various times after the injection of ^{99m}Tc-labeled MAb170 was studied in healthy male Balb/c mice. The mice were injected intravenously with 0.1 mL of ^{99m}Tc-MAb170 (555 kBq). At 1 h and 24 h after the injection, the mice underwent three kinds of treatments:

(1) Ligated group: The mice were sacrificed with an overdose of sodium pentobarbital. All of the afferent and efferent

blood vessels of the liver were ligated immediately, so that the blood volume in the liver remained the same as that if the mice were alive.

(2) Exsanguinated group: The mice were anesthetized with sodium pentobarbital (100 mg/kg). The heart was exposed and the blood was withdrawn with syringe by cardiac puncture until the animal was completely exsanguinated. This procedure was similar to that used during routine biodistribution studies.

(3) Perfused group: After the anesthesia of the mice with sodium pentobarbital, the thoracic inferior vena cava was cannulated via the right atrium and the liver was perfused in a retrograde manner (for details, see section of Hepatocyte Isolation and Culture) with normal saline at a rate of 5 mL/min for 5 min. The blood pool in the liver was completely washed out by the perfusion. At this time, the liver had a pale and light yellow appearance.

After the above treatments, the livers were dissected from the carcasses, blotted and counted for radioactivity in a NaI (Tl) well counter against an aliquot of the injectate. The percent ID/organ was calculated.

B. Distribution of ^{99m}Tc-MAb170 Radioactivity in Blood

The mice were injected intravenously with 0.1 mL of ^{99m}Tc-MAb170 (555 kBq). At 0.1, 1 and 3 h after the injection,

0.6-1.0 mL of blood samples were obtained by cardiac puncture after CO_2 anesthesia and added to the test tube containing 0.12 mL of 3.8% sodium citrate. The test tubes were centrifuged after addition of 1 mL of 0.9% saline at 3000 rpm for 15 min in a Dynac II centrifuge. The supernatant was transferred to another test tube. The cell pellet was washed twice with 0.9% saline. The blood cell pellets and the pooled supernatants were measured for radioactivity. Based on this measurement, the proportions that the blood cells and plasma contributed to the whole blood radioactivity at different time points after injection of radiolabeled MAb were calculated.

VII. ROLE OF TRANSCHELATION IN THE UPTAKE OF ^{99m}Tc-MAb170 IN MOUSE LIVER AND KIDNEY

A. *In Vitro* Thiol Transchelation

Equal volumes of ^{99m}Tc-MAb170 solution and transchelators (cysteine, glutathione and metallothionein) in PBS were mixed and incubated at room temperature for 24 h. The molar ratio of MAb to transchelator was equal to 1:50 (cysteine), 1:100 and 1:1000 (GSH), and 1:10 for metallothionein (MT). At various time intervals, the activity of ^{99m}Tc bound to MAb170 was determined by running aliquots of the mixture through a sephadex G-50 mini-column or size exclusion high performance liquid chromatography (TSK 3000 column).

B. Effects of *In Vivo* Cysteine Administration on Tissue Levels of ^{99m}Tc

Effect of Dose

Mice were injected intravenously via the tail vein with different doses of cysteine (1, 2, 3, 4, and 5 mg/25 g body weight) 1 h after the ^{99m}Tc-MAb170 injections (22 µg, 1.30 mBq, i.v.). At 3 h after cysteine administration, animals were sacrificed and tissues (blood, liver and kidney) were removed and counted for ^{99m}Tc radioactivity in a gamma counter.

Effect of Time

Mice were injected intravenously with cysteine (4 mg/25g body weight) at 1, 6, and 21 h after ^{99m}Tc-MAb170 injection. At 24 h post-injection of ^{99m}Tc-MAb170, all animals were sacrificed and tissues (blood, liver and kidney) were removed and counted for radioactivity.

C. Effects of Pretreatment with Thiol-Modulating Agents

1. (-)-2-Oxothiazolidine-4-carboxylate (OTC) Experiment

Mice were injected intraperitoneally with OTC (a prodrug of cysteine; 6.5 mmol/kg; Sigma) in PBS. Two hours later, the mice were given i.v. injections of ^{99m}Tc-MAb170 (22 µg, 2.22 mBq). The animals were sacrificed at 1 h and 4 h post-injection and various tissues (blood, liver and kidney) were removed and counted for radioactivity in a gamma counter.

2. DL-Buthionine-[S, R]-sulfoximine (BSO) Experiment

Mice were injected intraperitoneally with BSO (an inhibitor of γ-glutamylcysteine synthetase; 4 mmol/kg; Sigma). At 4 h after BSO injection, the mice were given i.v. injections of ^{99m}Tc-MAb170 (22 μg, 2.22 mBq). The mice were sacrificed at 1, 6 and 24 h after ^{99m}Tc-MAb injection and tissues (blood, liver and kidney) removed and measured for radioactivity.

3. Metallothionine (MT) Experiment

Mice were pretreated with $ZnSO_4$ (an MT inducer) in distilled water (50 mg Zn/kg, s.c.) 24 h prior to the injection of ^{99m}Tc-MAb170 (22 μg, 2.22 mBq). The mice were sacrificed at 1 and 24 h after ^{99m}Tc-MAb injection and tissues (blood, liver and kidney) removed and measured for radioactivity.

D. Biodistribution of ^{99m}Tc-MAb170 after Challenging with Cysteine

Solution of cysteine was added to a solution of ^{99m}Tc-MAb170 so that the molar ratio of MAb to cysteine in the final solution was 1:50. An aliquot of ^{99m}Tc-MAb170 to which PBS was added was used as the control. At 4 h after incuabtion at room temperature, the preparations of labeled MAb under different treatments were purifed using G-50 mini-column. The resultant ^{99m}Tc-MAb solutions were used for biodistribution study in mice.

The biodistribution of ^{99m}Tc at various times post-intravenous administration for both radiolabeled MAb170 preparations was established in normal Balb/c mice. Each mouse received about 8 μg of antibody with 0.25 mBq of ^{99m}Tc by tail vein administration. After sacrifice, samples of tissues were obtained and counted for ^{99m}Tc activity. The uptake of ^{99m}Tc was expressed as percent ID/organ.

E. Identification of ^{99m}Tc-Labeled Thiols in Bile, Urine and Kidney

At various times after ^{99m}Tc-MAb170 was injected into mice, the animals were sacrificed and samples of the bile, urine and kidney were obtained. The kidney was homogenized with a small amount of saline (3 to 5 times tissue weight) and the supernatant fraction separated for analysis. All samples were analyzed by Bio-Gel P2 chromatography. The Bio-Gel P2 column was calibrated with ^{99m}Tc-GSH, ^{99m}Tc-cysteine, $Na^{99m}TcO_4$ and a series of standards. (For details, see section V: Studies of Metabolism of ^{99m}Tc-MAb170 in Mice).

VIII. ROLES OF LIVER RECEPTORS, Fc, F(ab')$_2$, AND INTACT ANTIBODY IN THE UPTAKE OF ^{99m}Tc-LABELED ANTIBODIES BY LIVER

A. *In Vitro* Binding Studies of ^{99m}Tc-Labeled Antibody to Mouse Hepatocytes

1. Solutions for the Preparation and Culture of Hepatocytes

(1) Preparation of Hanks' Solution for Liver Perfusion (Hanks'-EGTA)

Hanks'-EGTA is calcium- and magnesium-free Hanks' balanced salt solution (HBSS, Gibco) containing 0.5 mM ethylene glycol-bis-(β-aminoethyl) N, N'-tetraacetic acid (EGTA, Sigma) and 0.05 M N-2-hydroxyethylpiperazine-N-2-ethane sulfonic acid (HEPES, Sigma).

The Hanks'-EGTA solution was prepared as follows. Fifty mL of 10 x HBSS was taken to a beaker aseptically. Three mL of distilled water, 5.95 g of HEPES and 5 mL of 50 mM EGTA were added to the beaker and mixed well. The pH was then adjusted to 7.4 using NaOH. The solution was made up to 500 mL, filtered into a sterile bottle (Nalgene filter unit, 0.2 μ), and stored at 4°C.

(2) Preparation of Collagenase Solution (L15-Collagenase)

Fifty milligrams of collagenase (Type I, Sigma) was dissolved in 100 mL of Leibovitz's L15 liquid medium with L-glutamine (Gibco) containing 10% heat inactivated fetal bovine serum (FBS, Gibco), insulin (0.01 mg/mL, Sigma), penicillin (100 u/mL) and streptomycin (100 μg/mL). The

solution was used immediately after preparation (within one hour after preparation).

(3) Preparation of Hepatocyte Culture Medium

Leibovitz L15 medium (pH 7.4) containing 10% FBS, insulin (0.01 mg/mL), penicillin (100 u/mL) and streptomycin (100 µg/mL) was used for this experiment.

2. Hepatocyte Isolation and Culture

Hepatocytes were isolated from male Balb/c mice using a two-stage perfusion of the liver. The techniques of Klaunig *et al.* and Renton *et al.*(202-204) were used with modifications. Mice were anesthetized with sodium pentobarbital (100 mg/kg, intraperitoneally), the abdomen was opened, the intestines were displaced to the left, and the portal vein was exposed. The chest was opened, and the inferior vena cava was cannulated in retrograde fashion via an incision in the right atrium with a 20-gauge plastic cannula (OD 1.27 mm, ID 0.86 mm) connected to a peristaltic pump (LKB, Pharmacia) that was delivering Hanks'-EGTA solution (37°C) at a rate of 5 mL/min before the cannula was inserted. The hepatic portal vein was cut to allow the perfusion fluid to escape. In mice weighing 25-30 g, the 20-gauge cannula fits tightly enough so that a ligature is not required. After 5 min, the perfusion solution was switched to L15-Collagenase (37°C). The perfusion was continued for another 10 min at the same rate. The perfusion cannula was disconnected, and the liver was excised and transferred to a

60-mm Corning tissue culture dish. The liver was homogenized with scissors and transferred to a 50 mL centrifuge tube containing about 15 mL of L15-Collagenase solution. The tube was shaken for 1.5 min in the 37°C water bath. The collagenase action was stopped by adding L15 culture medium to 50 mL in the tube. The resulting cell suspension was filtered through five layers of sterile gauze. The cells were sedimented by centrifugation at 50 g for 5 min and suspended in 40 mL of L15 culture medium.

A 0.2 mL of portion of the cell suspension was combined with 0.2 mL of trypan blue dye solution (0.4% in isotonic saline) and allowed to incubate for 5 min at room temperature. The viable and non-viable cells were counted in a hemocytometer using trypan blue dye exclusion as the criterion of viability. The total number and percentage of viable cells isolated was calculated.

The cell suspensions were plated on angled neck tissue culture flasks (80 cm^2/260 mL, Nunclon). The cultures were maintained at 37°C in a humidified 5% CO_2/95% air incubator. The medium was changed after 3-4 h in culture and at 24 h. The plated cells were used 24-48 h after plating.

3. Binding Assays

(1) Harvest of Hepatocytes

Flasks of cells were washed repeatedly with L15 medium and sterile PBS to remove any non-viable cells. 5 mL of 0.25% trypsin with 0.02% EDTA was then applied to each flask. After a digestion of 2 to 3 min, the trypsin solution was discarded

and replaced with L15 medium. The hepatocytes were harvested with a gentle blow to the flask, washed, and resuspended in L15 medium without FBS added. The viability of the cells was determined with trypan blue dye exclusion technique. Only those batches of hepatocytes with a viability of >90% were used for binding assays.

(2) Binding Assays

a) Binding Studies of ^{99m}Tc-MAb170 to Mouse Hepatocytes

An aliquot of 2-3 x 10^5 cells in 1 mL of L15 medium were added to tubes containing ^{99m}Tc-labeled MAb170, with or without unlabeled MAb. The mixtures were incubated for different durations at 37°C. Triplicate tubes were used for each data point. After incubation, the contents of each tube were centrifuged at 10,000 rpm for 2 minutes. The cell pellets were washed once. Both the cell pellets and the supernatants were counted for radioactivity in a gamma well counter. The uptake of ^{99m}Tc-MAb170 by hepatocytes was measured by counting the radioactivity of the cell pellets and expressed as total CPM of the pellets.

Effect of Time

Aliquots of 1 mL of the cell suspensions were added to the tubes containing 0.1 mL of ^{99m}Tc-MAb170 (37 kBq/1 μg). The mixtures were incubated at 37°C for 5, 10, 15, 20, 30, and 60 min. At the end of the incubation periods the content of each tube were centrifuged and processed as described above.

Effect of Dose

Aliquots of 1 mL of cell suspensions were added to the tubes containing 0.1 mL of ^{99m}Tc-MAb170 with different antibody concentrations. The doses of 0.1 mL of ^{99m}Tc-MAb were 37 kBq/1 µg, 74 kBq/2 µg, 389 kBq/10 µg, and 777 kBq/20 µg. The mixtures were incubated at 37°C for 15 min and processed as previously described.

Effect of Unlabeled Specific MAb

Aliquots of 1 mL of cell suspensions were added to the tubes containing 0.1 mL of ^{99m}Tc-MAb170 (37 kBq/1 µg), with 0, 50, and 100 µg of unlabeled native MAb170. The mixtures were incubated for 15 min at 37°C and processed as previously described.

b) Effect of Unlabeled HIgG, F(ab')$_2$ and Fc on ^{99m}Tc-HIgG Uptake by Mouse Hepatocytes

An aliquot of 2-3 x 10^5 hepatocytes in 1 mL of L15 medium were added to tubes containing 0.1 mL of ^{99m}Tc-HIgG, with various amounts of unlabeled native HIgG, F(ab')$_2$ or Fc fragments (Table 6). Triplicate tubes were used for each data point. The mixtures were incubated in a incubator at 37°C for 15 min. After incubation, the contents of each tube were centrifuged at 10,000 rpm for 2 min. The cell pellets were washed once. Both the cell pellets and the supernatants were counted for radioactivity in a gamma well counter. The uptake of ^{99m}Tc-HIgG by hepatocytes was expressed as the amount of

radioactivity (CPM) associated with the cell pellets.

Table 6. Amounts of Native Proteins Used in the Study of the Effects on ^{99m}Tc-HIgG Uptake by Mouse Hepatocytes.

Unlabeled Proteins	Incremental Concentrations of Labeled HIgG in the Reaction Mixture			
	0 x	10 x	50 x	100 x
HIgG (μg)	0.0	10.0	50.0	100.0
$F(ab')_2$ (μg)	0.0	6.7	33.5	67.0
Fc (μg)	0.0	3.4	16.8	33.5

B. *In Vivo* Interventional Biodistribution Studies of ^{99m}Tc-MAb170

1. Effects of Unlabeled and Aggregated Soluble Specific MAb on ^{99m}Tc-MAb Distribution

Aggregated MAb has shown a higher affinity to antibody binding sites (205). A soluble aggregated MAb170 solution was prepared by heating a MAb solution (10 mg/mL) at 63°C for 20 min according to Sancho *et al.*(206). The previous article reported a higher affinity of such aggregated antibody to liver binding sites (205).

The present study was designed to investigate if

unlabeled and aggregated specific MAb had competitive inhibitory effects on the biodistribution of ^{99m}Tc-MAb170. 0.5 mg of unlabeled monomeric or aggregated MAb170 in 0.1 mL of PBS was administered 2 h prior to the injection of ^{99m}Tc-MAb170 into groups of mice (3 mice each data point). Control mice were pre-injected with 0.1 mL of saline. Thirty minutes after injection of ^{99m}Tc-MAb170, the mice were sacrificed and tissues such as blood, liver and kidneys were obtained and counted for ^{99m}Tc radioactivity. The uptake in tissues was expressed as %ID/organ.

2. Effect of Cyclophosphamide on ^{99m}Tc-MAb170 Biodistribution in Mice

Cyclophosphamide (which enhances Fc receptor-mediated functions) was administered (200 mg/kg) intra-peritoneally 48 hours prior to the injection of ^{99m}Tc-MAb170 into groups of mice. Mice were sacrificed at 1, 6 and 24 h after the injection of radiolabeled MAb. Blood, liver and kidneys were obtained and counted for ^{99m}Tc radioactivity. The uptake of radioactivity by the tissues was calculated and expressed as %ID/organ.

IX. BINDING STUDIES OF RADIOLABELED MAB WITH KIDNEY SLICES

A. Preparation of Krebs-Bicarbonate Buffer

The following chemicals, NaCl 6.90 g, $MgSO_4.7H_2O$ 0.29 g, KCl 0.35 g, $CaCl_2$ 0.28 g, $NaHCO_3$ 2.10 g, KH_2PO_4 0.16 g, and Dextrose 2.00 g, were dissolved in 1000 mL of ddH_2O and the pH was adjusted to 7.4. The Krebs-bicarbonate buffer was stored in a refrigerator and used within 24 hours.

B. Preparation of Kidney Tissue Slices

Conventional Balb/c male mice were anesthetized with dry ice and sacrificed by exsanguination. The kidneys were removed and stored in ice-cold Krebs-bicarbonate buffer. Then the kidney was properly seated in the Rodent Organ Matrix (Activational Systems Inc., USA) and the sections were sliced serially (about 1 mm thick) through the entire extent of the kidney. The kidney slices were gently transferred to the Slice Saver (SS-1100, Activational Systems Inc.) for binding studies.

C. The Stability of ^{99m}Tc-MAb170 in an Oxygen Environment

While the tissue binding studies were performed, oxygen was supplied to keep the cells alive. Because of the importance that ^{99m}Tc-MAb remains stable in an O_2 environment, therefore, the stability of ^{99m}Tc-MAb was tested when O_2 was applied to establish the potential non-metabolized products

in the media. The solution was found to be stable under the conditions of our experiment.

MAb170 was radiolabeled with ^{99m}Tc using the pre-tinned technique. The labeled MAb was purified using a Sephadex G-50 mini-column to produce >98% trichloroacetic acid (TCA) precipitable product.

One mL of ^{99m}Tc-MAb170 (9.62 mBq/220 µg) was added to the Slice Saver containing 4.5 mL of Krebs-bicarbonate buffer. One Slice Saver was supplied with carbogen (95/5% O_2/CO_2), the other with nitrogen (N_2). ^{99m}Tc-MAb170 (0.1 mL) was mixed with 0.45 mL of PBS without any treatment. Incubations were conducted at room temperature. At various time intervals, the percentage of ^{99m}Tc bound to protein was determined using the TCA precipitation technique.

D. Binding Studies of Radiolabeled MAb with Kidney Slices

The binding studies of radiolabeled antibody with kidney slices were also performed in Slice Saver chambers. The Slice Saver chamber was pre-filled with Krebs-bicarbonate buffer and was supplied with carbogen (95/5% O_2/CO_2) between 5-10 psi. The gas flow control was adjusted until the desired degree of bubbling was achieved within the holding chamber.

1. Comparisons of Data from Two Slice Saver Chambers

As the two Slice Saver chambers were employed as treatment and control, respectively, the data obtained should be

comparable. The protocol was designed to study their comparability. Two Slice Saver chambers were designated as A and B. In each chamber of the Slice Saver, 4 kidney slices (one kidney) or 8 slices (two kidneys) were incubated with 4.75 mL of Krebs-bicarbonate buffer and 0.25 mL of ^{125}I-MAb170 (1.67 mBq). For each study, the contents in chamber A was exactly same as in B. At different incubation intervals, the tissues were transferred to petri dishes and washed with Krebs-bicarbonate buffer three times. Then, the slices were weighed and counted for ^{125}I radioactivity. The difference of counts between the tissues in A and B was tested using the paired t test.

2. ^{125}I-MAb170 Binding Kinetics to Kidney Slices

Kidney slices were incubated with 0.25 mL (1.67 mBq) of ^{125}I-MAb170 and 4.75 mL of Krebs-bicarbonate buffer in the Slice Saver chamber. For each time point, 4 kidney slices were used. At different incubation intervals, the tissues were removed from the Slice Saver chamber, washed three times, and counted for ^{125}I radioactivity against an aliquot of ^{125}I-MAb170 standard. The uptakes of % dose/gram were calculated.

3. Time-Course of ^{125}I-MAb170 Uptake or Binding to Kidney Slices

Kidney slices were incubated with 0.1 mL of ^{125}I-MAb170 (3.7 mBq/3 μg) and 5 mL of Krebs-bicarbonate buffer in the

Slice Saver. Eight slices of kidney were used for each data point. Two batches of slices were incubated for 15 and 30 min, respectively. The other two batches of slices were taken out of the Slice Saver chamber after 30 min of incubation, washed three times, transferred tc the clean Slice Saver chamber containing fresh buffer (no ^{125}I-MAb170 was added), and incubated for another 15 and 30 min, respectively. All of the tissue slices were washed three times and counted for ^{125}I radioactivity.

4. Radioactivity Released by Kidney Slices in Fresh Buffer

Kidney slices were incubated with 0.2 mL of ^{99m}Tc-MAb170 (1.85 mBq/40 µg) and 4.8 mL of Krebs-bicarbonate buffer for 15 min. The slices were washed three times, transferred to a clean Slice Saver chamber containing fresh Krebs-bicarbonate buffer, and incubated for another 15 min. The radioactive species in the fresh buffer released from kidney slices was measured with the TCA precipitation technique. The percent precipitation was calculated.

5. $Na^{99m}TcO_4$ Kinetics Binding to Kidney Slices

The procedures were same as described in (3) except that the radiolabel was $Na^{99m}TcO_4$ (0.1 mL, 1.85 mBq) instead of ^{125}I-MAb170.

6. Dual Tracer Binding of Kidney Slices with ^{99m}Tc- and ^{125}I-MAb170

Kidney slices were incubated in the solution of mixture of 0.4 mL of ^{99m}Tc-MAb170 (2.70 mBq/84 µg), 0.1 mL of ^{125}I-MAb170 (3.7 mBq/3 µg) and 4.5 mL of Krebs-bicarbonate buffer in the Slice Saver chambers. At different incubation intervals, the tissue slices were taken out of the Slice Saver chamber and washed (x3). The tissue slices were counted for ^{99m}Tc and ^{125}I radioactivity in Beckman Gamma 8000 counter using dual label counting technique with spillover corrections. The activity ratios of ^{99m}Tc/^{125}I in kidney slices were calculated.

7. Effect of Chloroquine on the Uptake of ^{99m}Tc-MAb170 by Kidney Slices

The effect of chloroquine (which interferes with receptor recycling) on the uptake of ^{99m}Tc-MAb170 was studied by pretreatment of kidney slices with chloroquine (2 mM, 5.16 mg in 5 mL of Krebs-bicarbonate buffer) for 30 min. Then 0.2 mL of ^{99m}Tc-MAb170 (2.22 mBq/45 µg) was added. After 15 min of incubation, the tissue slices were washed (x3) and counted for ^{99m}Tc radioactivity. The uptake of radioactivity by the treated kidney slices was compared with that of the untreated control.

8. Effect of Protein G on the Uptake of ^{99m}Tc-MAb170

Protein G is an immunoglobulin-binding molecule which binds to the Fc part of IgG. ^{99m}Tc-MAb170-protein G complex was prepared by adding 0.2 mL of protein G (Sigma) in PBS (0.25 mg/mL; binding capacity is approximately 4.8 mg of human IgG per mg protein G) to a vial containing 0.2 mL of ^{99m}Tc-MAb170 (0.2 mg/mL). The reaction solution was gently mixed and incubated for 5 min at room temperature.

Kidney slices were incubated with 0.3 mL of ^{99m}Tc-MAb170-protein G complex and 4.7 mL of Krebs-bicarbonate buffer for 15 min. Then the slices were washed (x3) and measured for radioactivity. The uptake of radioactivity by kidney slices which were incubated with ^{99m}Tc-MAb170 in PBS and Krebs-bicarbonate buffer was used as the control.

X. STATISTICAL ANALYSIS

Standard statistical analysis of the data was carried out to reveal the relationship between various sets of data. The analysis required the determination of the mean and corresponding standard deviation (SD) values as well as the size of the samples (or the number of observations). The statistical methods employed in this work were based on the nature of the data and the testing purposes. In the case of testing the difference of mean between two independent samples, the students t test was used at various levels of significance. A paired-difference test was performed using

paired samples and the t test. The t test statistics can be used for a small size of samples (less than 30) by assuming the populations to be normally distributed (207). The resultant p (probability) values are indicated with asterisks. The correlation analysis was employed to test the statistical relationship and the strength of the linear association between two variables (207).

RESULTS AND DISCUSSION

I. RADIOLABELING OF THE ANTIBODIES AND QUALITY ASSURANCE

Monoclonal antibody MAb170 and human IgG (HIgG) were radiolabeled with ^{99m}Tc using the direct labeling method via stannous ion reduction, and purified using a centrifuged G-50 mini-column. For both antibodies, approximately 80% of the added radioactivity was recovered from the mini-column. After purification in this manner, the radiochemical purity as determined by HPLC, ITLC and TCA precipitation was >98%.

MAb170 was radioiodinated using the Iodogen method and purified with an Excellulose GF-5 desalting column. After purification, the radiochemical purity as determined by HPLC and TCA precipitation was >98%. Specific activity was in the range of 148-444 kBq/μg (4-12 μCi/μg).

II. BIODISTRIBUTION STUDY OF ^{99m}Tc-MAB170 IN NORMAL MICE

The purpose for conducting the biodistribution study of ^{99m}Tc-MAb170 was to reveal the distribution pattern of the antibody and provide the kinetic data in specific organs or tissues. The distribution pattern of ^{99m}Tc-MAb170 can then be used as a reference for the interventional biodistribution studies where various physiological factors are manipulated to alter the distribution of the radiolabel and to investigate the mechanisms of localization of radiotracer in tissues. The kinetic data would then provide the clues for

sampling time in a variety of studies.

Table 7 presents the biodistribution data of ^{99m}Tc-MAb170 in normal Balb/c mice at various times after the administration of radiolabeled antibody. High uptake of the radioactivity was observed in blood, liver, kidney, intestines and bone.

Blood

In blood, the highest percent ID/organ was observed at all time points. From an initial level near 70% of the administered radioactive dose, there was a rapid decrease of ^{99m}Tc-MAb170 in blood during the first hour after injection. This rapid decline was followed by a gradual decrease over 6 to 24 h. Compared with the biodistribution data of ^{125}I-MAb170 (data not shown), the value of % ID/organ in blood at 6 h for ^{99m}Tc-MAb170 was only half of that for ^{125}I-MAb170. The difference in uptake was also noticed in other tissues between two radiolabels, although same amount of uptake was observed in some tissues between the two. These suggests that different mechanisms might be invoved in the disposition of ^{99m}Tc- and ^{125}I-labeled antibodies.

Liver

The uptake of ^{99m}Tc-MAb170 by liver was lower than that in blood and higher than in all other organs. The profile for ^{99m}Tc-MAb170 radioactivity in liver was similar to that in blood. This similarity implied that the levels of MAb170

activity in the liver might be accounted partly by blood level contribution.

Kidney

In kidney, the radioactivity showed a rapid rise in the first hour to a peak value, followed by a gradual decline thereafter. The increase in radioactivity might be indicative of a continuous uptake of radiolabeled MAb and/or appearance of radioactive metabolites from other organs.

Intestines

The profile for radioactive species in intestines was similar to that for kidneys and showed peak values between 3 and 6 h. The radioactive peak was first noticed in duodenum and in turn in small and large intestines. The increase in radioactivity was probably due to the excretion of radioactive catabolites from the hepato-biliary system.

Bones

High uptake of ^{99m}Tc radioactivity was also observed in bones, which was the result of accumulation of the radiolabel by bone marrow. The mechanism involved in this accumulation is not known. The high percentage of bone in whole body weight may also contribute to the high values in the uptake expressed as the percent of injected dose per organ. The ratio of bone/blood radioactivity increased with time, suggesting the blood pool contribution to bone radioactivity may be less important.

Table 7. Biodistribution of ^{99m}Tc-MAb170 in Normal Mice.*

Tissues	% ID/Organ**				
	0.1 h	1.0 h	3.0 h	6.0 h	24.0 h
Blood#	67.9±7.3	46.7±2.0	33.0±2.6	26.0±3.8	11.8±1.3
Liver	25.0±3.3	19.3±0.9	14.5±0.8	12.2±1.7	6.4±0.5
Kidneys	5.8±0.8	6.2±0.5	5.9±0.4	5.9±0.6	3.5±0.6
Intestines	1.9±0.2	3.9±0.4	4.0±0.4	4.0±0.5	1.5±0.3
Lungs	2.0±0.4	1.4±0.1	1.1±0.4	1.2±0.6	0.7±0.3
Heart	1.3±0.1	1.1±0.1	0.9±0.1	0.8±0.1	0.3±0.1
Spleen	0.9±0.2	0.9±0.1	0.6±0.1	0.5±0.1	0.3±0.3
Stomach	0.5±0.1	0.6±0.1	0.6±0.1	0.7±0.2	0.3±0.1
Bladder	0.2±0.1	0.2±0.1	0.1±0.1	0.1±0.1	0.1±0.1
Testis	0.3±0.1	0.5±0.1	0.6±0.1	0.6±0.1	0.3±0.1
Salivaries	0.5±0.1	0.5±0.1	0.5±0.1	0.6±0.1	0.4±0.1
Bone#	5.6±1.1	5.4±0.3	4.8±0.6	4.4±0.6	3.1±0.5

* Dose = 740 kBq/20 µg/0.1 mL.

** Mean ± SD, n = 3.

Blood (organ mass) = 0.065 x body mass, bone (organ mass) = 0.15 x carcass mass. Based on: Maddalena DJ, TISCON, a BASIC computer program for the calculation of the biodistribution of radionuclide-labeled drugs in rats and mice, Lucas Heights Research Laboratories, Australia, 1983.

III. STUDIES OF METABOLISM OF ^{99m}Tc-MAb170 IN MICE

A. HPLC Analysis

The HPLC radiochromatogram of ^{99m}Tc-MAb170 prior to injection is shown for reference in Figure 3. For ^{99m}Tc-MAb170, the peak of the radioactivity eluted at a molecular weight of approximately 150,000 daltons. As shown in Figure 5, the calibration of molecular weight vs retention time was very good. (Figures 3 and 5).

The HPLC analysis of ^{99m}Tc substances present in serum at 1, 6 and 24 h after injection of ^{99m}Tc-MAb170 into mice revealed that the radioactivity was present predominantly in a single peak associated with antibody at each time point. A very small fraction (about 1%) eluted at a lower molecular weight. (Figure 6 a, b and c).

Figure 3. Size exclusion HPLC radiochromatogram obtained by analysis of ^{99m}Tc-MAb170 after radiolabeling.

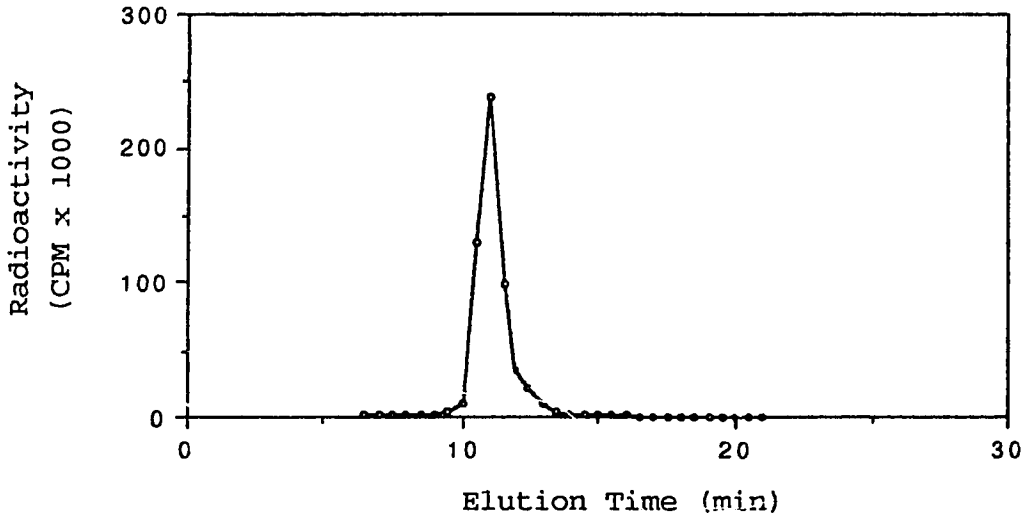

Figure 4. Size exclusion HPLC radiochromatogram of $Na^{99m}TcO_4$.

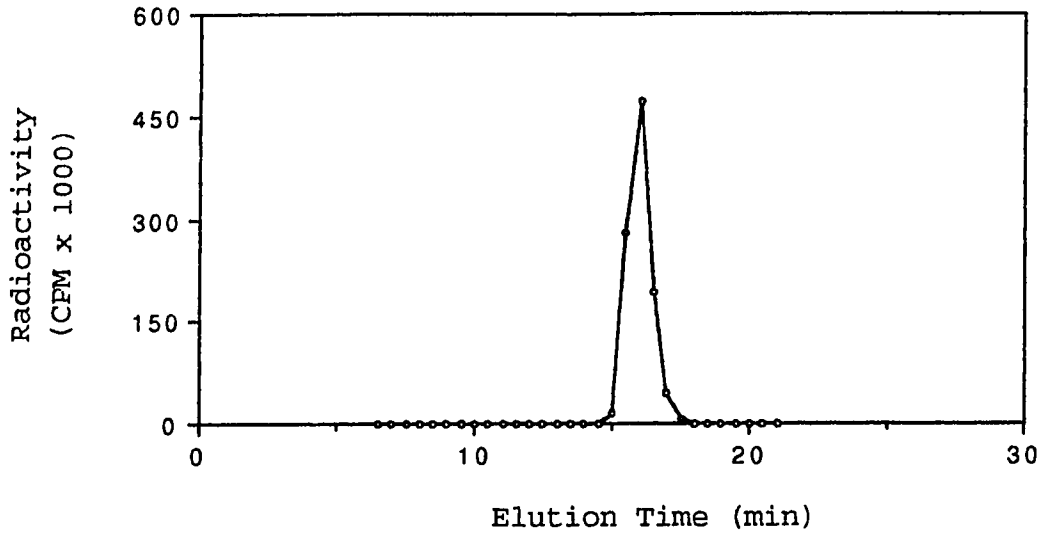

Figure 5. Molecular weight calibration of TSK 3000SW HPLC column.

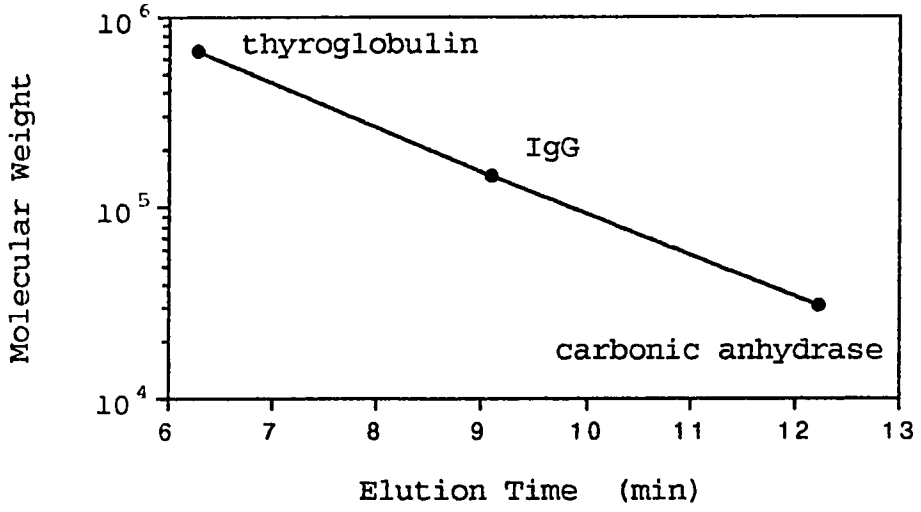

Approximately 50-60% of the total ^{99m}Tc activity in the liver and kidney was extracted into the supernatant when either organ was homogenized. The radiolabeled components present at 1, 6 and 24 h in liver homogenates of mice given injections of ^{99m}Tc-MAb170 are shown in Figure 7 a, b and c. The liver homogenates showed two major peaks of radioactivity eluted from the HPLC column. The first was native MAb170, which decreased from 70% of the total activity in the eluate at 1 h to 42% at 24 h. The second was a low molecular weight (LMW) material that increased from 30% at 1 h to 58% at 24 h. The activity profiles for kidney extracts (Figure 8 a, b and c) were similar to those of the liver and the radioactivity was also distributed between two major peaks. The native MAb170 decreased from 30% of the total activity in the eluate at 1 h to 26% at 24 h. The LMW ^{99m}Tc-containing species increased from 70% at 1 h to 74% at 24 h.

In the urine, most of the measured radioactivity appearing in multiple peaks was associated with LMW species. Little evidence for labeled antibody in urine was apparent. The patterns of activity profiles for urine were similar at all time points. (Figure 9 a, b and c).

Figure 6. Size exclusion HPLC radiochromatograms obtained by analysis of mouse serum obtained at 1, 6 and 24 h post-administration of ^{99m}Tc-MAb170.

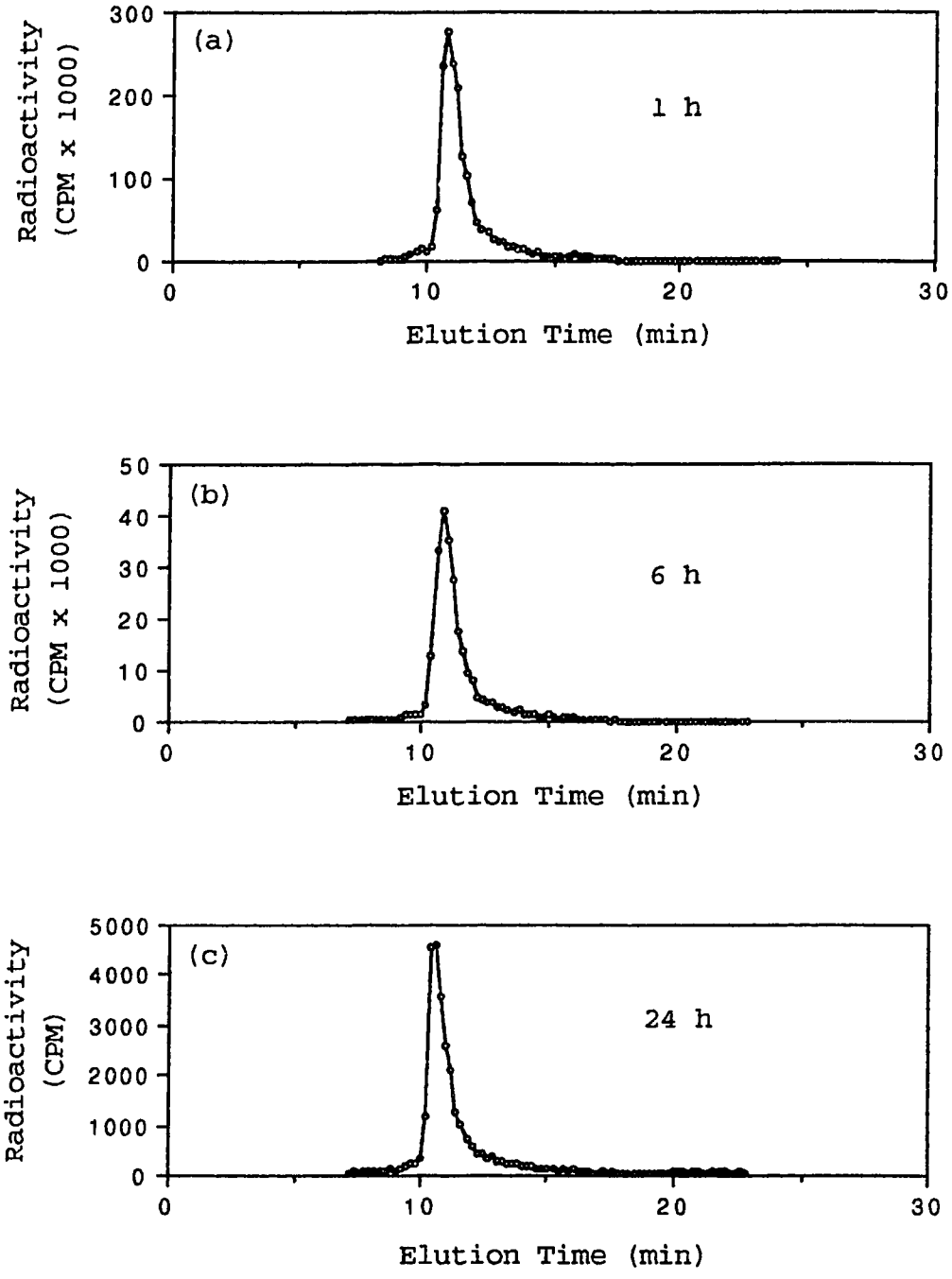

Figure 7. Size exclusion HPLC radiochromatograms obtained by analysis of mouse liver homogenates obtained at 1, 6 and 24 h post-administration of ^{99m}Tc-MAb170.

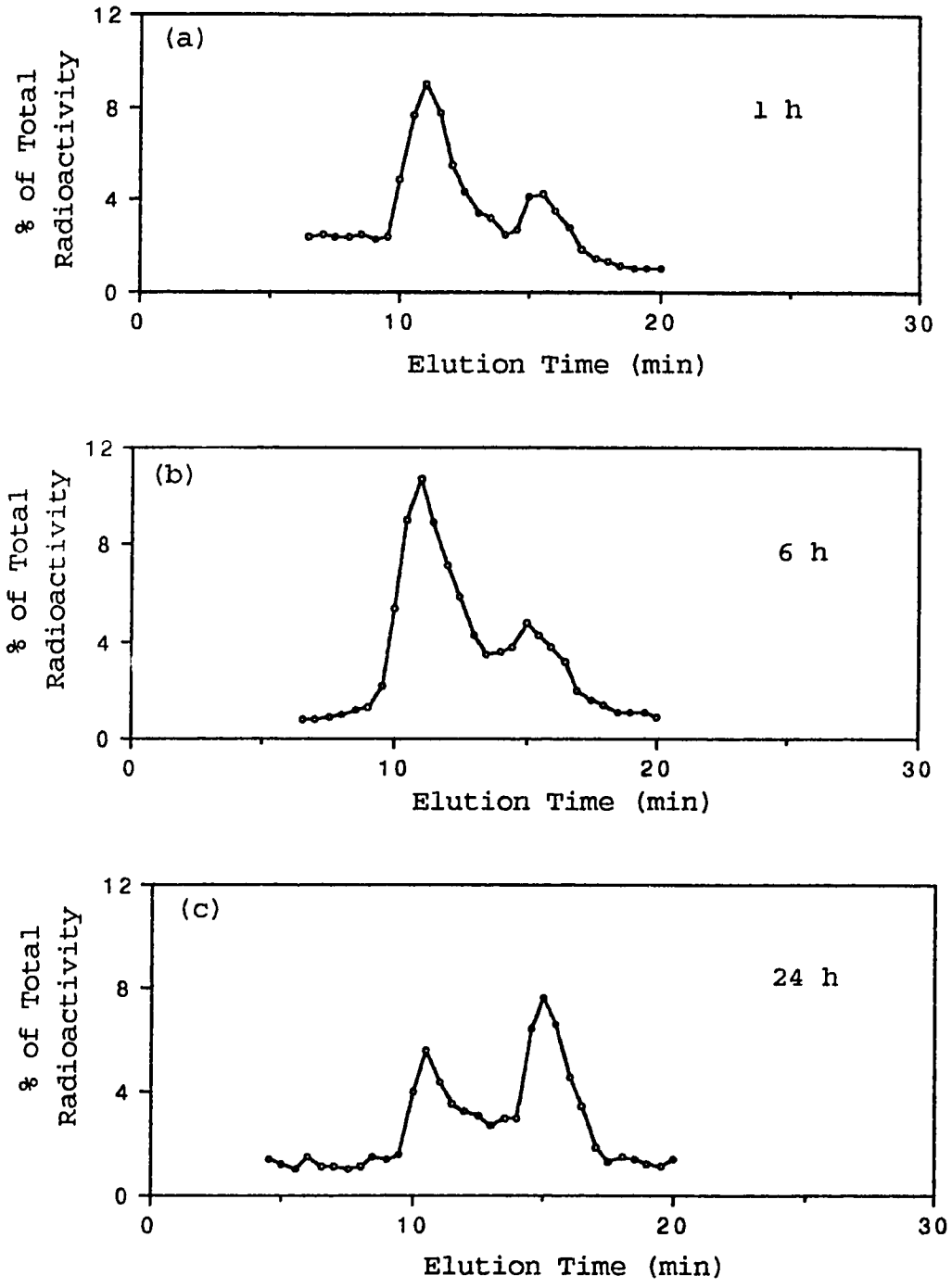

Figure 8. Size exclusion HPLC radiochromatograms obtained by analysis of mouse kidney homogenates obtained at 1, 6 and 24 h post-administration of ^{99m}Tc-MAb170.

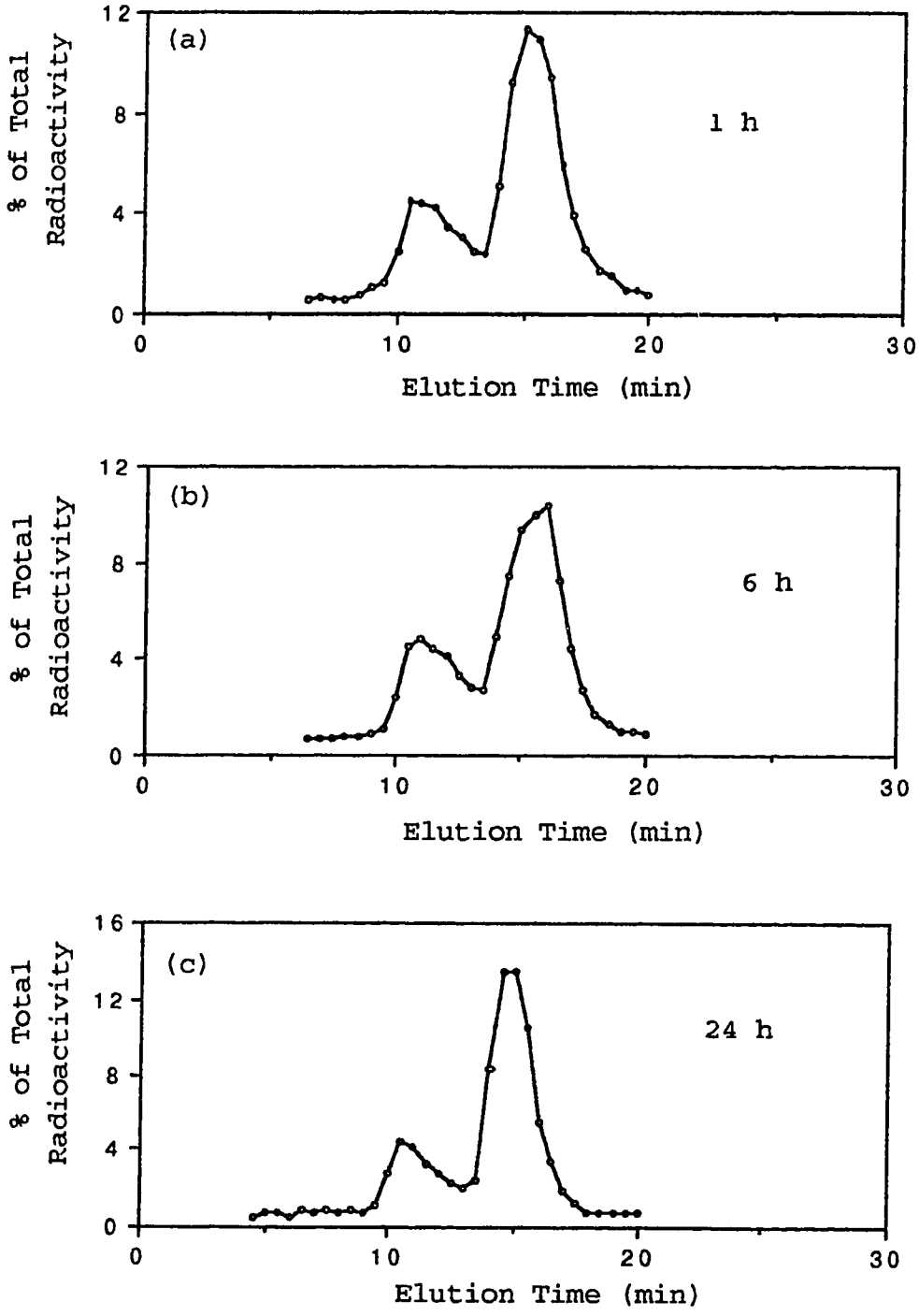

Figure 9. Size exclusion HPLC radiochromatograms obtained by analysis of mouse urine obtained at 1, 6 and 24 h post-administration of ^{99m}Tc-MAb170.

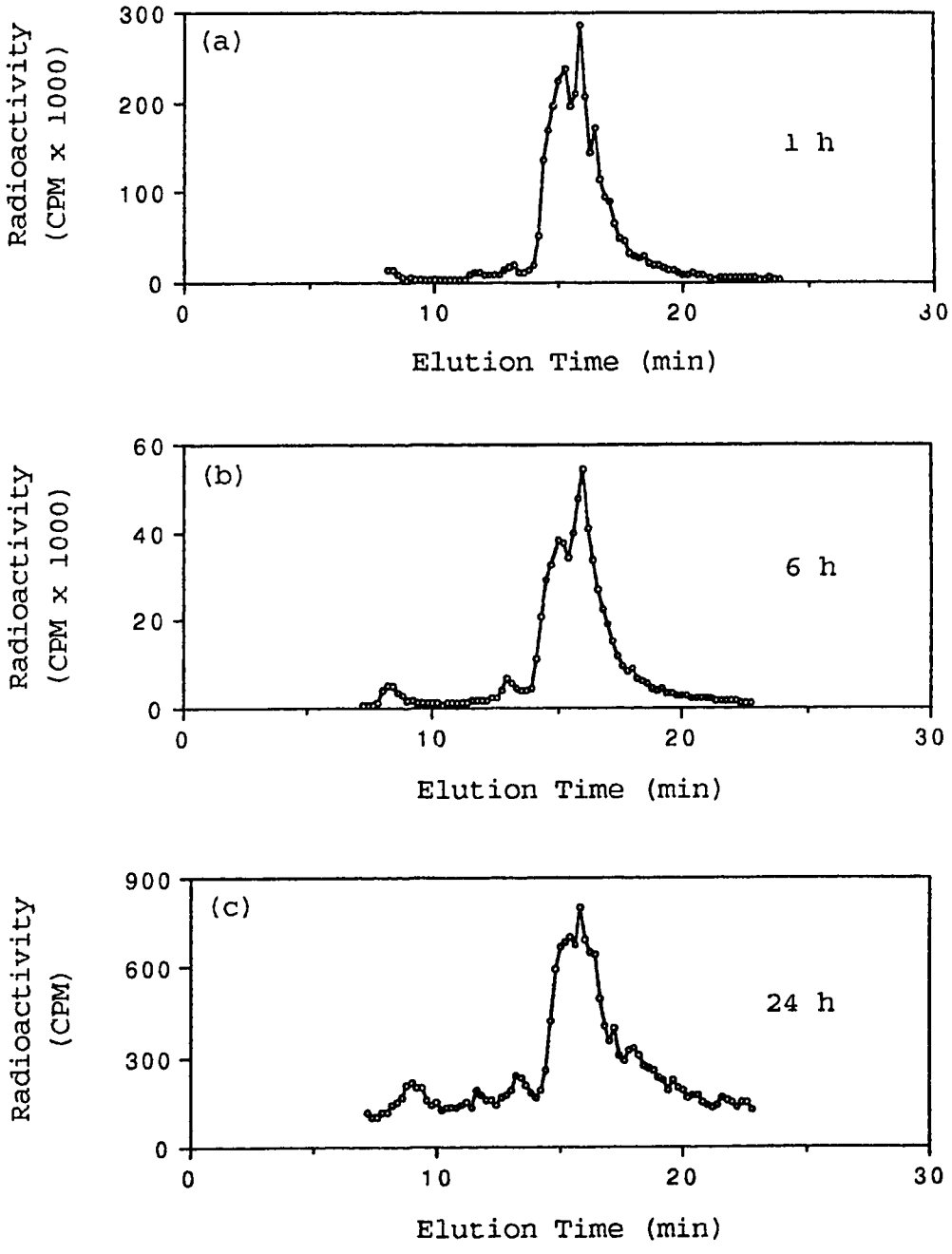

In contrast to the ^{99m}Tc-MAb170, radioactive biological samples obtained from the mice injected with ^{125}I-MAb170 show different patterns of HPLC radiochromatograms. Although the data are not shown, a single peak was observed in liver, kidney and urine as well as in blood. The radioactive peaks of liver, kidney and blood coeluted with the native MAb170. The radioactive substance in urine eluted as a low molecular weight compound, presumbly free iodide. The differences in radiochromatography between the two labeling methods suggest that the radionuclide moiety may play a role in the biodisposition of radiolabeled antibody.

All of the peaks of ^{99m}Tc-radiolabeled LMW species from liver, kidney and urine appeared with retention times of around 15 min. Even very small molecules such as $^{99m}TcO_4^-$ eluted from the HPLC at this position (Figure 4). Thus it is difficult to identify these LMW species on the basis of HPLC results exclusively with this particular size exclusion column.

B. Sephadex G-50 Chromatography

A column of G-50 was calibrated with a series of standards. A linear relationship between logarithm of molecular weight (log MW) and Ve/Vo was observed (Figure 10). The column could be used to estimate the molecular weight of small catabolites.

Figure 10. Molecular weight calibration of sephadex G50 column.

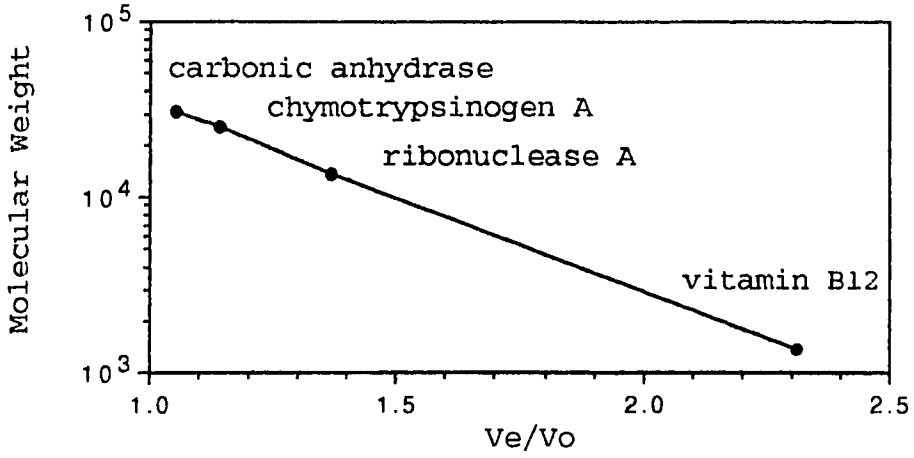

Figures 11 and 12 present radiochromatograms obtained by analysis on the G-50 column of liver homogenate samples from mice at 3 h and 24 h after injection of ^{99m}Tc-MAb170. The radioactivity was present predominantly in a single peak around the void volume (exclusion limit of G-50: 30,000 daltons) at both time points. A very small fraction (about 3%) eluted at a much lower molecular weight at 3 h but was not observed at 24 h post-injection of ^{99m}Tc-labeled MAb170.

The G-50 radioactivity profile of kidney homogenate obtained at 3 h post-injection of ^{99m}Tc-MAb170 was different from that of the liver (Figure 13). The radioactivity was distributed between two major peaks. One peak eluted near the void volume. The other eluted at a much lower molecular weight and was centered at molecular weights of 600 to 700

Figure 11. Radiochromatogram obtained by G50 gel filtration chromatography of mouse liver homogenate obtained at 3 h post-administration of ^{99m}Tc-MAb170.

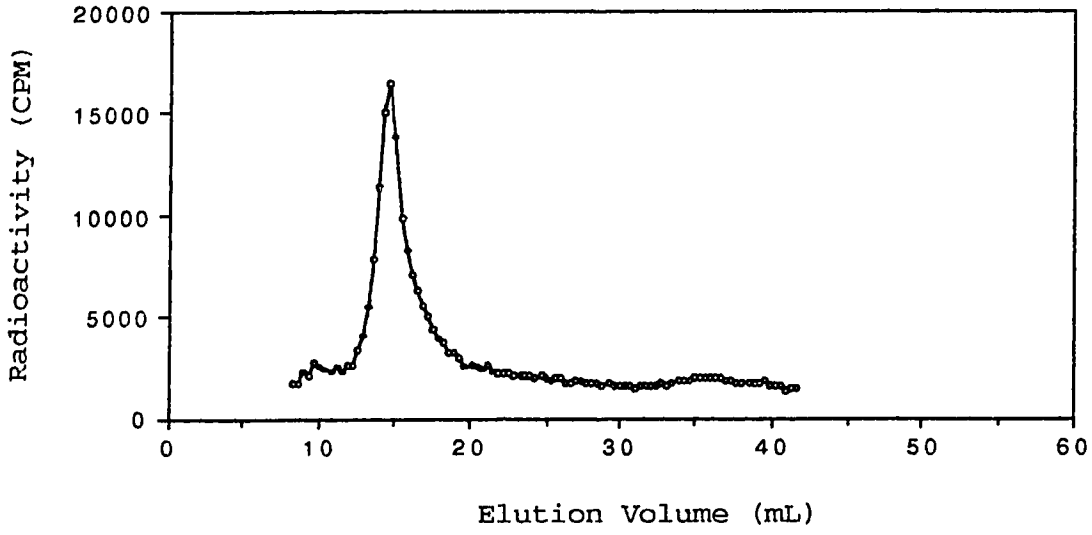

Figure 12. Radiochromatogram obtained by G50 gel filtration chromatography of mouse liver homogenate obtained at 24 h post-administration of ^{99m}Tc-MAb170.

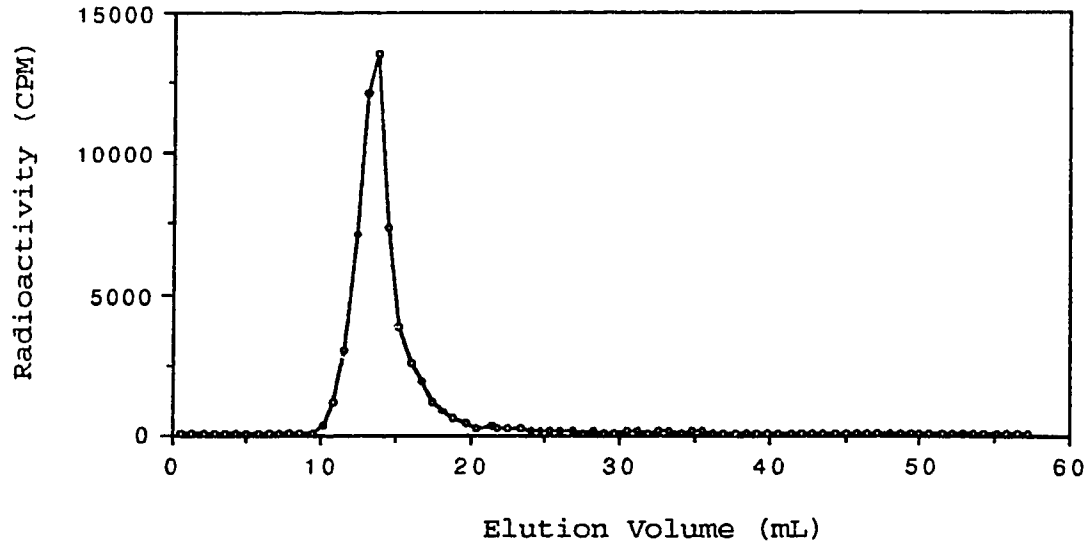

Figure 13. Radiochromatogram obtained by G50 gel filtration chromatography of mouse kidney homogenate obtained at 3 h post-administration of ^{99m}Tc-MAb170.

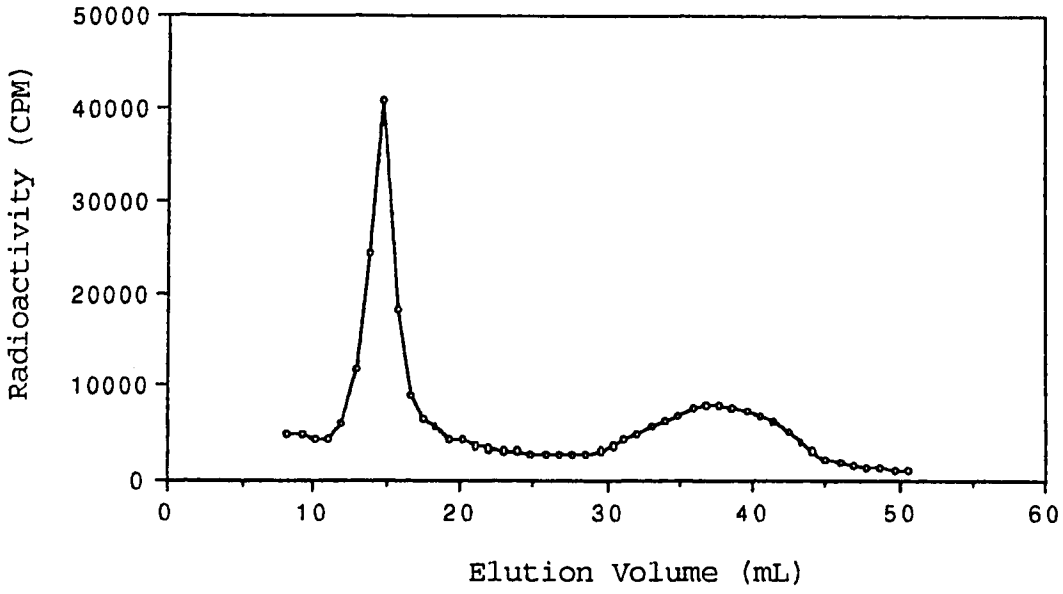

Figure 14. Radiochromatogram obtained by G50 gel filtration chromatography of mouse urine obtained at 3 h post-administration of ^{99m}Tc-MAb170.

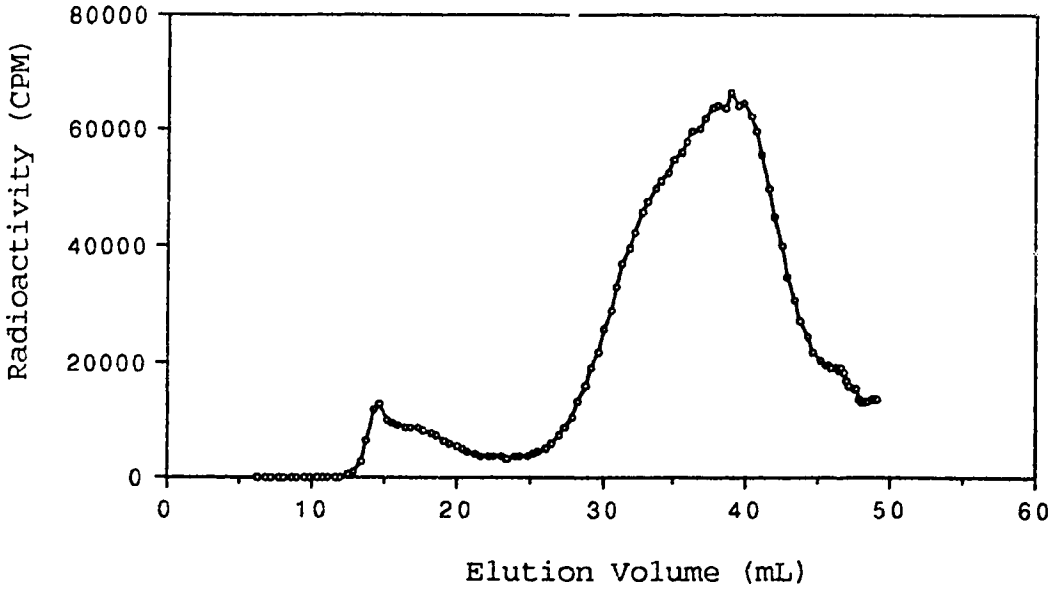

daltons. As this peak was quite broad, it is likely that it consisted of a mixture of radioactive species with different molecular weights equal to, as well as greater and lower than 600-700 daltons.

In the urine collected at 3 hour after ^{99m}Tc-MAb170 injection, the radioactivity was recovered in 3 (three) major peaks (Figure 14). The first peak came off the G-50 column around the void volume. The species of the second peak had a molecular weight of about 22,000 daltons. Both peaks were much smaller compared with the third one. The third was the LMW species that was centered at molecular weight of 600-700 daltons (Ve = 38 mL). Due to its large size and broadness, it was presumed to be the collection of multiple species with different molecular weight.

Figure 15. Radiochromatogram obtained by G50 gel filtration chromatography of $Na^{99m}TcO_4$.

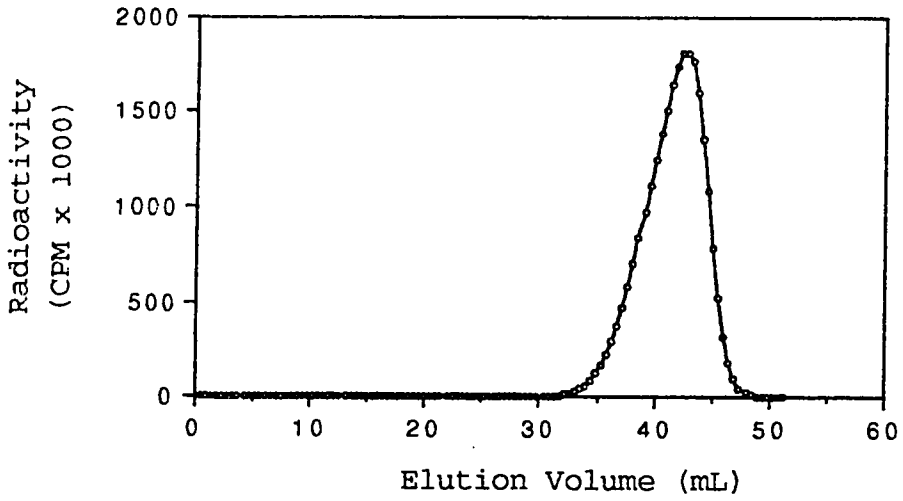

Free pertechnetate was eluted off the G-50 column with a retention time of 43 mL (Figure 15). However, the results of Bio-Gel P2 and TLC analysis of the biological samples did not support the *in vivo* formation of pertechnetate.

C. Bio-Gel P2 Chromatography

A column of Bio-Gel P2 was calibrated with a series of standards. No linear relationship between log MW and Ve/Vo was observed. Figures 16, 17 and 18 present radiochromatograms obtained by analysis on this column of ^{99m}Tc-cysteine, ^{99m}Tc-GSH and ^{99m}Tc-pertechnetate, respectively. ^{99m}Tc-cysteine was eluted off the P2 column as two radioactive peaks (peak A and B) with elution volumes of 21.5 mL and 43.0 mL. ^{99m}Tc-GSH eluted off the column as two peaks (a and b; not completely separated) presumably representing the dimer (Ve = 15.9 mL) and monomer (Ve = 18.3 mL) of ^{99m}Tc labeled glutathione, which is supported by the UV absorption peaks in the analysis of unlabeled GSH and GSSG on this column. Analysis of $^{99m}TcO_4^-$ on this column showed a single peak with an elution volume of 25.7 mL.

The Bio-Gel P2 radioactivity profile of liver homogenates showed a single peak eluted around the void volume. The profiles at 3 h, 6 h and 24 h (Figure 19) after ^{99m}Tc-MAb170 administration were similar to each other.

The Bio-Gel P2 profile of radioactivity obtained from the bile supernatant of mice at 1 h after injection of ^{99m}Tc-MAb170 showed 4 (four) radioactive peaks (Figure 20). Peaks 1

Figure 16. Radiochromatogram obtained by Bio-Gel P2 chromatography of ^{99m}Tc-labeled cysteine.

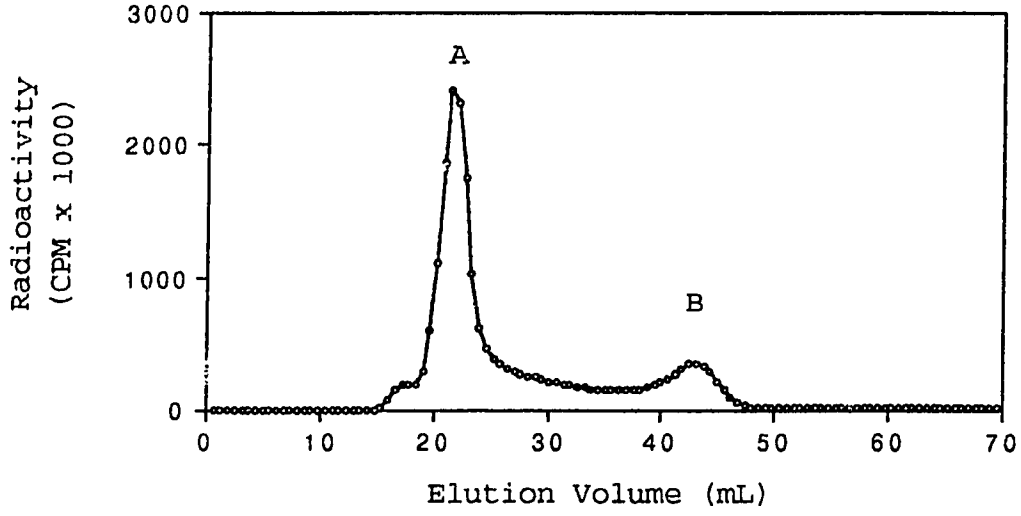

Figure 17. Radiochromatogram obtained by Bio-Gel P2 chromatography of ^{99m}Tc-labeled glutathione.

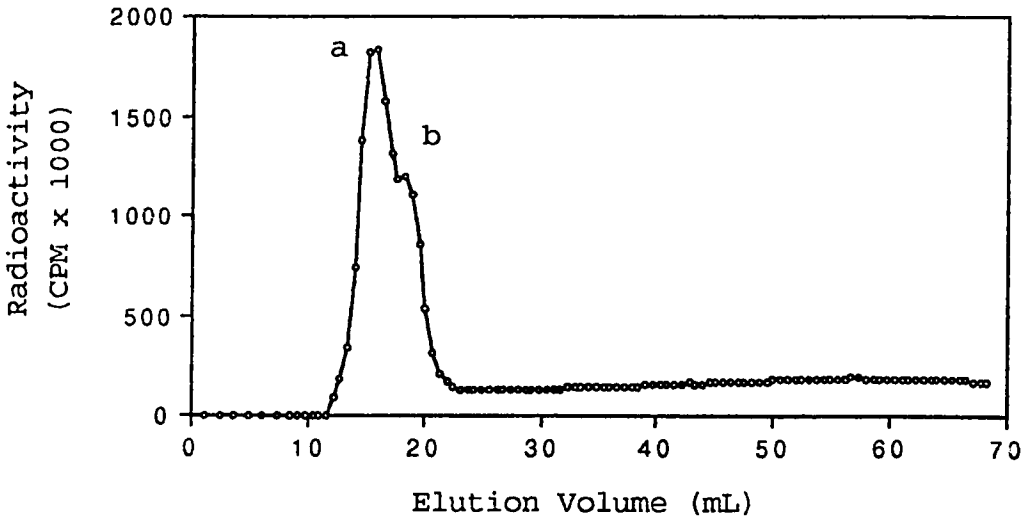

Figure 18. Radiochromatogram obtained by Bio-Gel P2 chromatography of $Na^{99m}TcO_4$.

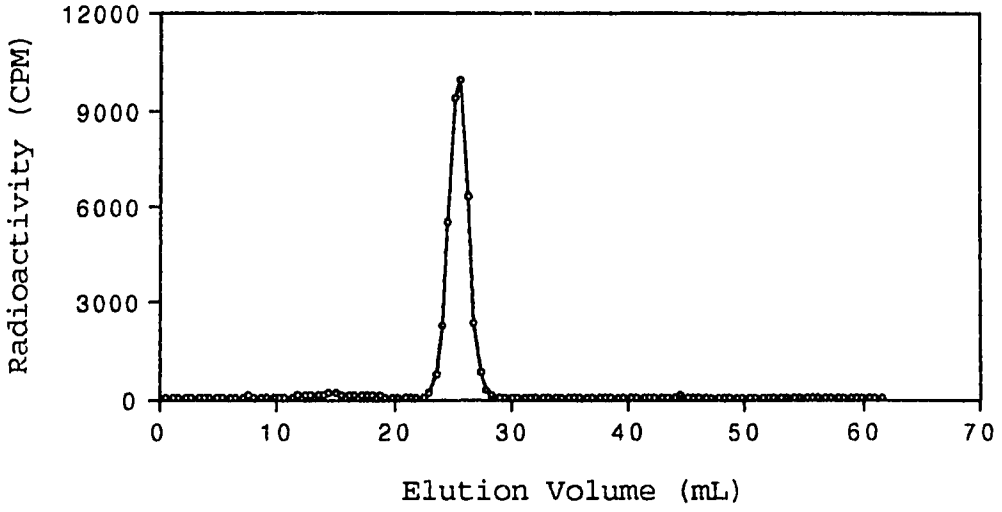

Figure 19. Radiochromatogram obtained by Bio-Gel P2 chromatography of mouse liver homogenate obtained at 24 h post-administration of ^{99m}Tc-MAb170.

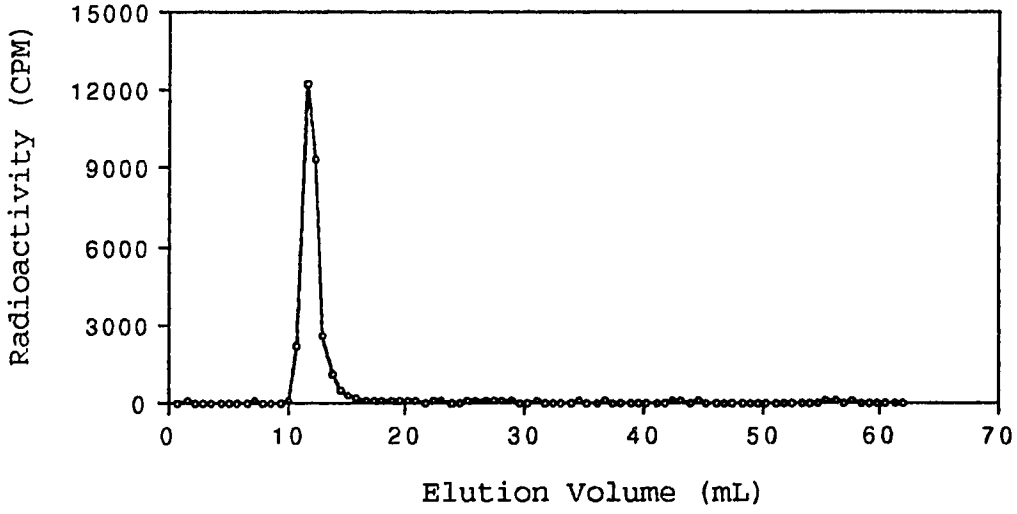

and 2 were eluted off the column at void volume and an elution volume of 13.1 mL, respectively. The species responsible for peak 3 coeluted with one peak (peak b) in the analysis of ^{99m}Tc-GSH. The species responsible for peak 4 coeluted with peak B in the analysis of ^{99m}Tc-cysteine.

The Bio-Gel P2 analysis of kidney homogenate at 3 hour post-injection of ^{99m}Tc-MAb170 showed 3 (three) radioactive peaks (Figure 21). Peak 1 was eluted off the column at void volume and was in large size. Peak 2 was quite broad and coeluted with the peak A of ^{99m}Tc-cysteine and peaks of ^{99m}Tc-GSH on this P2 column. Species responsible for peak 3 coeluted with the peak B in the analysis of ^{99m}Tc-cysteine.

Figure 22 presents radiochromatograms obtained by analysis on this column of mouse urine collected at 3 h post-injection of ^{99m}Tc-MAb170. ^{99m}Tc species in the urine were eluted as 3 (three) major peaks (peak 1, 2 and 3). Peak 1 eluted the column at void volume. Peak 2 was quite broad. Peaks 2 and 3 accounted for the majority of the radioactivity in the urine. The species responsible for the first two-thirds of peak 2 coeluted with the peaks in the analysis of ^{99m}Tc-GSH. The last third of peak 2 was superimposable with the peak A of ^{99m}Tc-cysteine. Species in peak 3 coeluted with the peak B of ^{99m}Tc-cysteine on Bio-Gel P2 analysis.

Figure 20. Radiochromatogram obtained by Bio-Gel P2 chromatography of mouse bile obtained at 1 h post-administration of ^{99m}Tc-MAb170.

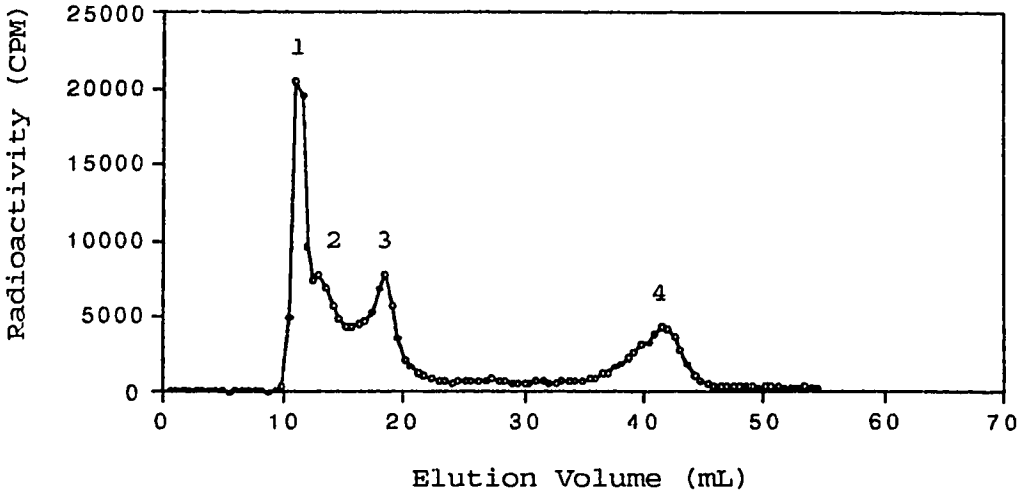

Figure 21. Radiochromatogram obtained by Bio-Gel P2 chromatography of mouse kidney homogenates obtained at 3 h post-administration of ^{99m}Tc-MAb170.

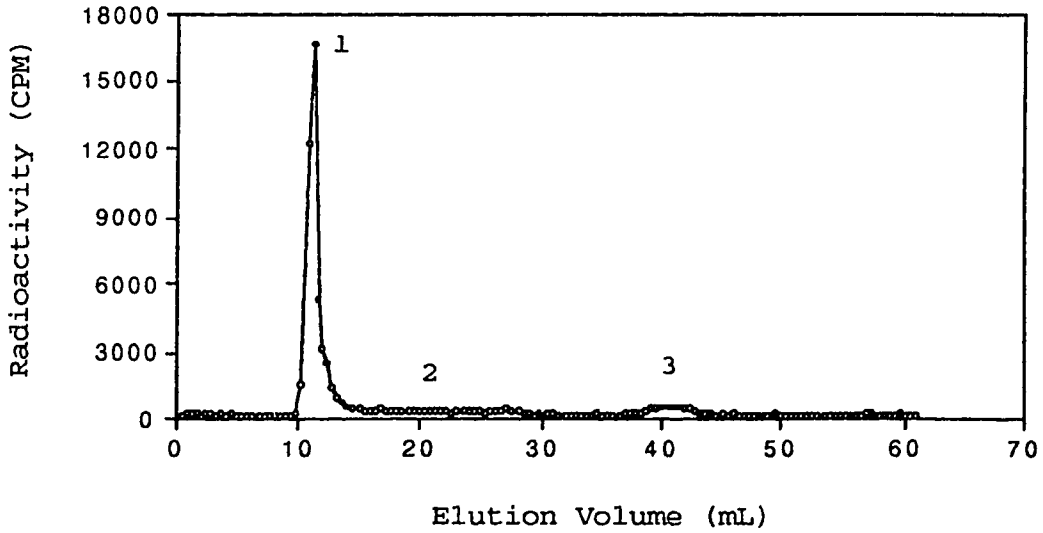

Figure 23 presents Bio-Gel P2 profile of post-G50 urine at 3 h after ^{99m}Tc-MAb170 administration. The mouse urine was first analyzed on G-50 column. Four mL of eluate of Ve 35-38 mL from the third peak on G-50 column were collected and mixed. One mL of this mixture was applied to Bio-Gel P2 column. The Bio-Gel P2 radioactivity profile showed 3 (three) major peaks (Figure 23). No radioactivity was eluted from the P2 column at void volume. The species responsible for the first two-thirds of peak 1 coeluted with the peaks in the analysis of ^{99m}Tc-GSH. The last third of peak 1 was superimposable with the peak A of ^{99m}Tc-cysteine. Species in peak 3 coeluted with peak B of ^{99m}Tc-cysteine. Species in peak 2 has yet to be identified.

D. Sephacryl S-200 Chromatography

A column of Sephacryl S-200 was calibrated with a series of standards so that the column could be used to estimate the molecular weights of catabolites (Figure 24).

The Sephacryl S-200 profile of radioactivity obtained from liver homogenate at 24 hour after ^{99m}Tc-MAb170 administration is shown in Figure 25. The radioactive species were present predominantly in a range with molecular weights from 25,000 to 150,000 daltons. There appeared to be three radioactive peaks, but they were not well resolved.

Figure 22. Radiochromatogram obtained by Bio-Gel P2 chromatography of mouse urine obtained at 3 h post-administration of ^{99m}Tc-MAb170.

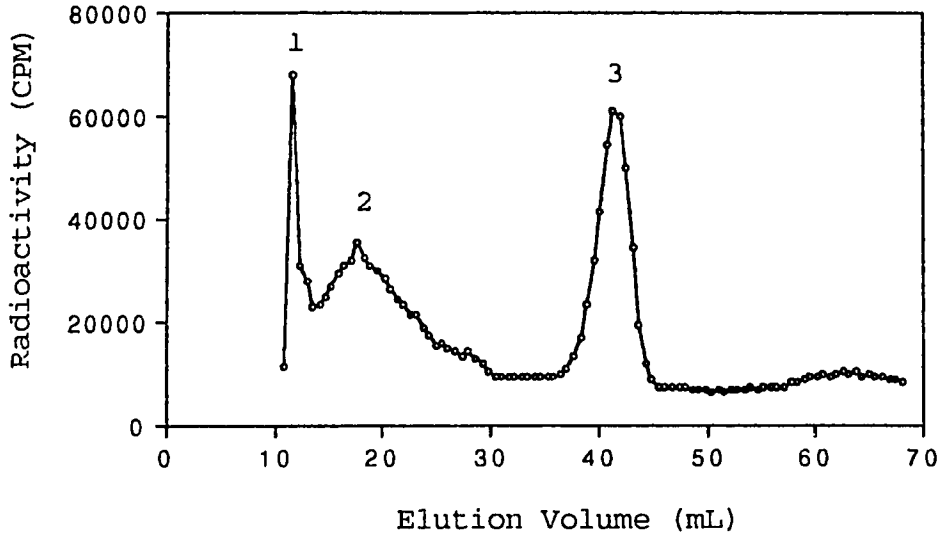

Figure 23. Radiochromatogram obtained by Bio-Gel P2 chromatography of fractions from sephadex G50 chromatography of mouse urine obtained at 3 h post-administration of ^{99m}Tc-MAb170.

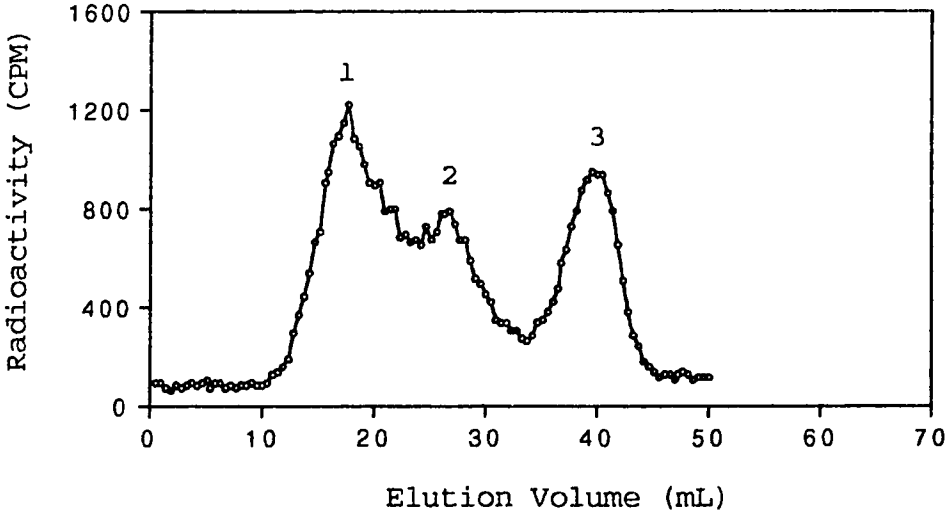

Figure 24. Molecular weight calibration of sephacryl S-200 column.

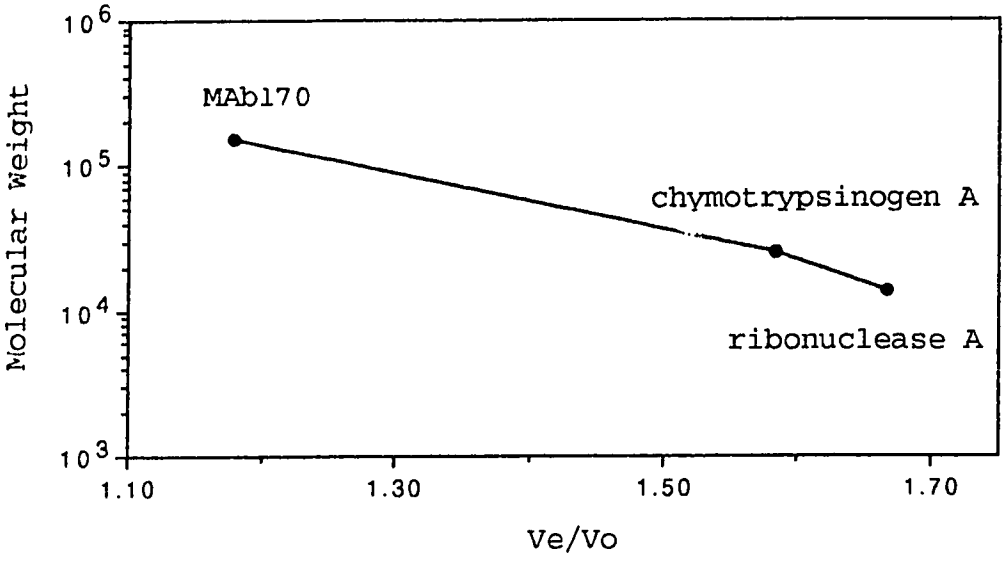

Figure 25. Radiochromatogram obtained by sephacryl S-200 chromatography of mouse liver homogenate obtained at 24 h post-administration of ^{99m}Tc-MAb170.

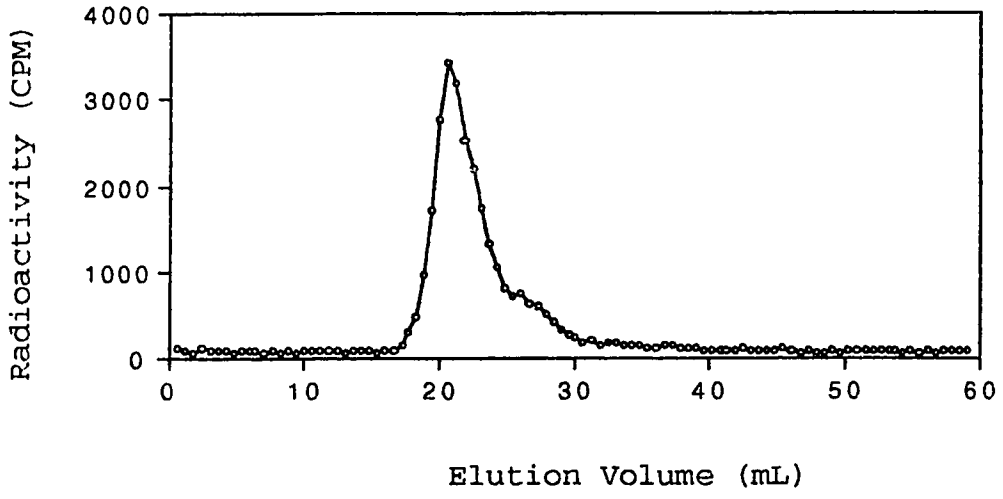

E. Instant Thin Layer Chromatography

ITLC analysis was performed by using two solvent systems, i.e., acetone and 85% MeOH/normal saline (NS). In general, free pertechnetate moves to the solvent front, whereas "reduced and hydrolyzed" ^{99m}Tc (R-Tc) and bound ^{99m}Tc radioactivity remains at the spot of origin in the acetone system. In the 85% MeOH/NS system, protein and R-Tc are precipitated at the origin of the chromatogram, whereas the free pertechnetate ($^{99m}TcO_4^-$) and non-protein bound ^{99m}Tc move with the solvent front. In this investigation, ^{99m}Tc-MAb170 was purified with Sephadex G-50 column prior to the injection into mice. Therefore, the presence of R-Tc *in vivo* would be negligible. It followed that the percent radioactivity at the origin represented bound ^{99m}Tc in ITLC-acetone and accounted for protein bound ^{99m}Tc in ITLC-85% MeOH/NS.

Table 8 shows the results of thin layer chromatographic analysis of radioactivity in mouse serum, urine and tissue extracts. The majority of the activity in serum, liver and kidney homogenates obtained at 1, 6 and 24 h after ^{99m}Tc-MAb170 administration remained at the origin of the chromatograms in both ITLC-acetone and ITLC-85% MeOH/NS assays. However, the majority of the activity in urine collected at all time points remained at the origin in ITLC-acetone but migrated to the solvent front in ITLC-85%MeOH/NS analysis. About 99% of the radioactivity in serum at 1, 6 and 24 h was associated with protein bound ^{99m}Tc. At all time points, 95-96% of radioactivity in liver homogenate was

Table 8. Silica gel thin layer radiochromatographic analysis of mouse serum, urine and homogenates of liver and kidneys obtained at various time intervals after administration of ^{99m}Tc-MAb170.

Sample	% Radioactivity at Origin*					
	1 h		6 h		24 h	
	Acetone	85%MeOH/NS	Acetone	85%MeOH/NS	Acetone	85%MeOH/NS
Serum	99.8±0.1	98.9±0.2	99.7±0.1	99.5±0.1	99.2±0.2	98.7±0.5
Urine	99.3±0.5	28.2±9.3	97.7±1.0	28.2±4.0	93.3±3.0	18.5±0.9
Liver	95.8±2.4	95.0±1.6	96.7±1.4	96.2±0.9	98.5±1.7	95.9±4.1
Kidney	94.8±1.5	87.9±2.5	94.4±1.9	86.6±1.8	97.9±2.0	93.0±1.7

* mean ± SD, n = 3.

associated with protein. However, 2.6% of the radioactivity in liver homogenates at 24 h post-administration was associated with non-protein bound ^{99m}Tc. In kidney homogenates at 1, 6 and 24 h, 87-93% of the ^{99m}Tc radioactivity was protein-bound and 5-8% was associated with a non-protein fraction. In the urine collected at 1 h and 6 h, 28% of the ^{99m}Tc radioactivity was protein-bound ^{99m}Tc while 70% was associated with non-protein fraction. In the urine collected at 24 h post-administration, only 18% of the radioactivity was protein-bound and 75% was non-protein bound ^{99m}Tc. 3-7% of activity from free pertechnetate was observed in analysis of urine at 24 h, liver and kidney homogenates at 1 h and 6 h. This might be due to the oxidation, presumably during TLC analysis, to ^{99m}Tc pertechnetate.

In the present study, radioactive species in mouse blood, urine, bile, liver and kidney homogenates obtained after ^{99m}Tc-MAb170 administration were analyzed with various chromatographic techniques. Attempts have been made to identify the ^{99m}Tc-containing species in these samples.

Size-exclusion HPLC of the serum taken from mice at different time points revealed that about 99% of the radioactive species was ^{99m}Tc-MAb170. Only about 1% accounted for ^{99m}Tc-labeled LMW which might represent material metabolized in the tissues that was in transit in the serum. The TLC analysis of serum was in agreement with the results of HPLC.

In contrast to the serum, HPLC analysis indicated that the radioactivity in liver homogenate was characterized by two distinct peaks. One was native-size IgG (MAb170), and the other was a LMW species. The native MAb peak decreased while LMW peak increased with time. G-50 profile of liver homogenate showed the radioactivity was present predominantly in a single peak around the void volume. If both the HPLC and G-50 analysis were taken into consideration, it was likely that there were radioactive metabolites in liver with MW around or greater than 30,000 daltons. Sephacryl S-200 analysis of liver extract confirmed this hypothesis. In S-200 profile of liver homogenate obtained at 24 h after ^{99m}Tc-MAb170, in addition to native MAb, there were two ^{99m}Tc-labeled metabolites, one with a MW of 26,000 and the other greater than 30,000 daltons. These metabolites were all ^{99m}Tc-labeled proteins and eluted the Bio-Gel P2 column at void volume.

Bio-Gel P2 analysis of mouse bile collected at 1 h after ^{99m}Tc-MAb170 injection presented an interesting profile. Four radioactive peaks were eluted off the column. Two major peaks presumably represented ^{99m}Tc-GSH and ^{99m}Tc-cysteine, respectively. However, we were unable to determine the types of ^{99m}Tc-GSH and ^{99m}Tc-cysteine complexes. ^{99m}Tc-labeled GSH and cysteine might be generated by transchelation in liver and thereafter excreted into bile. One peak appeared at the void volume, which was, at least in part, supposed to be ^{99m}Tc-labeled native MAb170. It was understandable that intact

MAb was present in bile supernatant. MAb170 does bind to bile ducts (186), and at the same time, MAb in blood vessels on gallbladder might be released during the preparation of bile supernatant. Another peak eluted the column immediately after the void volume. This ^{99m}Tc-containing species had a MW of less than 1,800 daltons and was yet to be identified.

The assay of liver homogenates showed only 3% of radioactive species with very low MW eluted the G-50 column at 3 h but not at 24 h after ^{99m}Tc-MAb170 injection. Bio-Gel P2 analysis of liver extracts obtained at 24 h post-injection of ^{99m}Tc-MAb170 showed no ^{99m}Tc-containing species present after void volume. These results indicated that ^{99m}Tc-labeled metabolites found in bile were excreted rapidly from the liver. This also meant that the methods which enhance the bile flow and bile output would have no effect on the excretion of radioactive species after the injection of labeled MAb.

Biodistribution studies of ^{99m}Tc-MAb170 in mice showed high level radioactivity in liver, gallbladder and intestines after injection of ^{99m}Tc-MAb170 (data for gallbladder not shown). This result, together with metabolism studies in the present investigation, indicated that hepatic-biliary route was an important metabolic pathway of ^{99m}Tc-MAb170.

The HPLC radioactivity profiles of kidney homogenates obtained after ^{99m}Tc-MAb170 injection were similar to those of liver extracts. Two distinctive radioactive peaks were eluted

off HPLC. One was native MAb170 which decreased with time, and the other was LMW ^{99m}Tc-containing species which increased with time.

G-50 analysis of kidney homogenate showed two major radioactive peaks. One was eluted around void volume, which was thought to represent ^{99m}Tc-MAb170 and/or ^{99m}Tc-containing species with a MW of equal to or greater than 30,000 daltons. The other was broad and centered at 600-700 daltons. This latter peak, according to the Bio-Gel P2 analysis of kidney extracts, was thought to consist of ^{99m}Tc-GSH and ^{99m}Tc-cysteine.

Three radioactive peaks were eluted off the Bio-Gel P2 column from kidney homogenates obtained at 3 h after ^{99m}Tc-MAb170 injection. One peak, in large size at void volume, represented ^{99m}Tc-MAb170 and/or ^{99m}Tc-containing species with a MW greater than 1,800 daltons. The other two smaller broad peaks were composed of ^{99m}Tc-GSH and ^{99m}Tc-cysteine. Two types of ^{99m}Tc-GSH and two types of ^{99m}Tc-cysteine were present. We were unable to determine what forms of ^{99m}Tc-GSH or ^{99m}Tc-cysteine were present at this time.

ITLC assays of kidney extracts showed 5-8% of radioactivity was from non-protein bound ^{99m}Tc, which was thought to be labeled GSH and cysteine. The majority of the radioactivity was protein bound ^{99m}Tc. Considering the large-size LMW peak in HPLC profile, there might be a ^{99m}Tc labeled proteinous metabolite which was not resolved by the methods

in this investigation.

HPLC analysis of mouse urine collected at various time points after ^{99m}Tc-MAb170 administration showed multiple ^{99m}Tc-bound LMW species. TLC analysis revealed that majority of the radioactivity in urine were from non-protein bound ^{99m}Tc, while only 18-28% from protein-bound ^{99m}Tc.

G-50 assays of urine collected at 3 h after ^{99m}Tc-MAb170 injection showed two smaller radioactive peaks (eluted off the column at void volume and 22,000 daltons, respectively) and one large broad peak centered at 600-700 daltons. Further analysis of this third peak with Bio-Gel P2 revealed three major radioactive peaks, of which two were composed of ^{99m}Tc-GSH complexes and two forms of ^{99m}Tc-cysteine , respectively. Another peak in smaller size eluted the P2 column between ^{99m}Tc-GSH and ^{99m}Tc-cysteine, and was yet to be identified.

Bio-Gel P2 results indicated that the majority of radioactivity in urine were from ^{99m}Tc-labeled GSH and cysteine. This was in agreement with TLC results, i.e., most of the radioactivity from non-protein bound ^{99m}Tc.

^{99m}Tc labeled GSH and cysteine found in kidney homogenates and urine after ^{99m}Tc-MAb170 injection might be generated by transchelation in kidney and thereafter released to urine. But we cannot exclude that some ^{99m}Tc-GSH and ^{99m}Tc-cysteine might be produced in other organs and transported to the kidney and then to the urine.

Summary of Metabolism of ^{99m}Tc-MAb170 in Mice

Accumulation of radionuclide in liver and kidney is a major detriment to the use of ^{99m}Tc radiolabeled monoclonal antibodies for diagnosis and therapy. The elucidation of the metabolic products of the ^{99m}Tc-MAb170 conjugate may provide insights and approaches that would reduce the undesirable deposition of labeled MAb in normal tissues. In this investigation, the radiolabeled species in blood, urine, bile and extracts of liver and kidney obtained at different time after the injection of ^{99m}Tc-MAb170 into mice were analyzed with various chromatographic methods. The following summarizes the main results in the present study.

(1) Ninety-nine to 100% of the radioactivity in serum was associated with intact MAb170. About 1% of the activity in serum at 1 h after ^{99m}Tc-MAb170 injection was eluted off the HPLC as LMW species.

(2) The radioactivity in liver homogenate was distributed between native MAb170 and LMW species. With the passage of time, the former decreased while the latter increased. Of the LMW species, two ^{99m}Tc-labeled proteins were observed, one with a MW of 26,000, and the other greater than 30,000 daltons. The protein bound ^{99m}Tc accounted for the majority of the radioactivity in liver homogenates. In addition, about 3% of radioactive species with very low MW (in hundreds) was found in liver extract at 3 h but not at 24 h after ^{99m}Tc-

MAb170 injection.

(3) At least four ^{99m}Tc-radiolabeled species were postulated present in mouse bile after ^{99m}Tc-MAb170 injection: intact MAb170, ^{99m}Tc-GSH, ^{99m}Tc-cysteine, and one metabolite with a MW of less than 1,800 daltons and yet to be identified. ^{99m}Tc-MAb170 in bile probably came from the MAb binding to bile ducts and circulating in gallbladder blood vessels. The two major metabolic components in bile, ^{99m}Tc-GSH and ^{99m}Tc-cysteine, might be generated by transchelation in liver and thereafter excreted into bile. All these LMW ^{99m}Tc-containing species were excreted rapidly from the liver.

(4) In kidney extracts, the majority of the radioactivity was protein bound ^{99m}Tc. Only 5-8% of the activity was from non-protein bound ^{99m}Tc. The ^{99m}Tc-containing species in kidney homogenates were postulated to be: native MAb170, ^{99m}Tc-GSH, ^{99m}Tc-cysteine, and a possible proteinous metabolite which was not resolved by the methods in this investigation. The labeled MAb170 decreased but the catabolites increased with time.

(5) At least five ^{99m}Tc-containing species were postulated present in mouse urine after ^{99m}Tc-MAb170 administration: ^{99m}Tc-GSH, ^{99m}Tc-cysteine, two metabolites with a MW of 22,000 and greater than 30,000 daltons, respectively, and another

catabolite which came off between ^{99m}Tc-GSH and ^{99m}Tc-cysteine and was yet to be identified. The majority of the radioactivity in urine were from non-protein bound ^{99m}Tc, while only 18-28% from protein bound ^{99m}Tc. ^{99m}Tc-labeled GSH and cysteine, which accounted for the majority of the radioactivity in urine, might be generated in kidney and / or in other organs, and then transported to the urine. Little evidence for labeled antibody in urine was apparent.

(6) No evidence for the *in vivo* formation of ^{99m}Tc-pertechnetate in mouse blood, liver, kidney, bile and urine was observed.

The work of Hnatowich *et al.*(154) supports our conclusions. These authors have investigated the *in vivo* and *in vitro* properties of ^{99m}Tc when labeled to antibodies via direct stannous reduction and indirect hydrazino nicotinamide chelation method. It was found that ^{99m}Tc attached to antibodies with either method could be transchelated to cysteine and glutathione *in vitro* and *in vivo*. However, when labeled to antibodies by direct method, ^{99m}Tc was unstable towards transchelation relative to the indirect method. The *in vivo* data showed that urinary excretion of radioactivity was threefold greater for the direct label and was almost exclusively labeled cysteine and glutathione. Significant differences in the biodistribution of ^{99m}Tc were also observed between the two labeling methods (154).

IV. ANALYSIS OF GROSS LIVER ^{99m}Tc RADIOACTIVITY AND DISTRIBUTION OF ^{99m}Tc RADIOACTIVITY IN BLOOD

A. Contributions of Radioactivity in Blood Compartment to the ^{99m}Tc Activity in Liver

The liver is a blood-rich organ. One of the hepatic functions is that the human liver acts as a "blood reservoir", containing 0.5 to 1.0 L of blood, that can be shunted to the circulation (208). The mean hepatic blood flow in fasting humans is estimated to be 1,530 ± 300 mL per minute; this is nearly 25% of the cardiac output (209). About 75% of the influx consists of portal venous blood, and the remaining 25% represents hepatic artery flow. The biodistribution study of radiolabeled antibody demonstrated that there was very high %ID/organ of ^{99m}Tc radioactivity in blood after the injection of ^{99m}Tc-MAb, 46.7% at 1 h and 11.8% at 24 h. Therefore, it is reasonable to assume that the radioactivity in the blood pool would also make a significant contribution to total liver radioactivity *in vivo*. In the experiments conducted on ligated, exsanguinated, and perfused livers, our data proved that this assumption was correct. In Figures 26 and 27 are presented the results of liver uptake with and without the blood pool. Figures 28 through 31 show the proportions that the blood pool and liver tissue contributed to total liver activity at different time points after the injection of radiolabeled MAb. Liver blood pool contributed about two-thirds of the *in vivo* liver radio-

Figure 26. Liver uptake of ^{99m}Tc radioactivity in normal mice with ligated, exsanguinated, and perfused liver at 1 h post-administration of ^{99m}Tc-MAb170.*

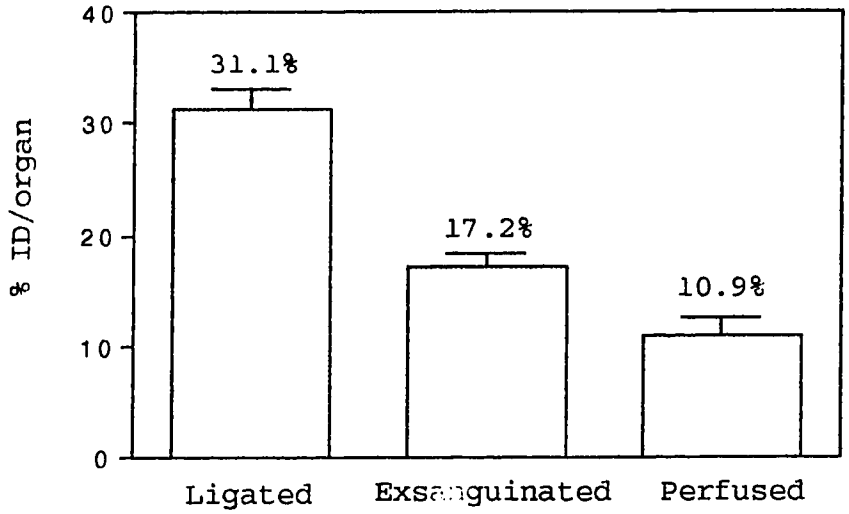

* Uptakes are expressed as mean ± SD, n = 3.

Figure 27. Liver uptake of ^{99m}Tc radioactivity in normal mice with ligated, exsanguinated, and perfused liver at 24 h post-administration of ^{99m}Tc-MAb170.**

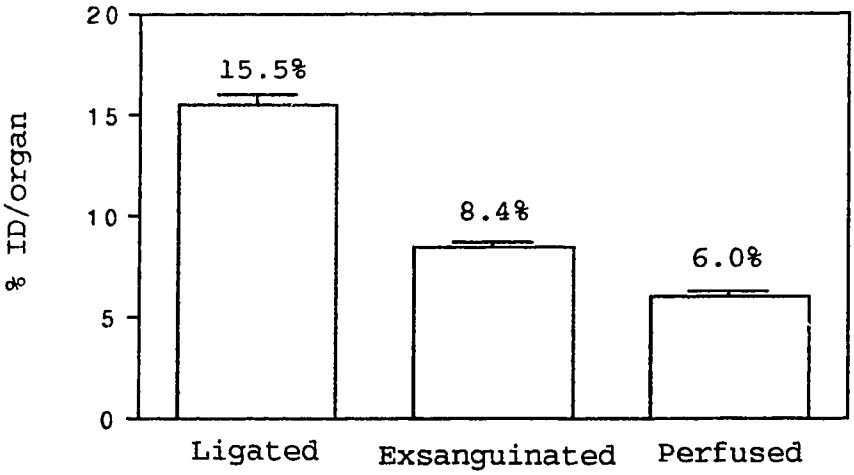

** Uptakes are expressed as mean ± SD, n = 3.

Figure 28. Contributions to ^{99m}Tc activity in mouse liver from the whole blood pool (ligated liver) at 1 h post-administration of ^{99m}Tc-MAb170.*

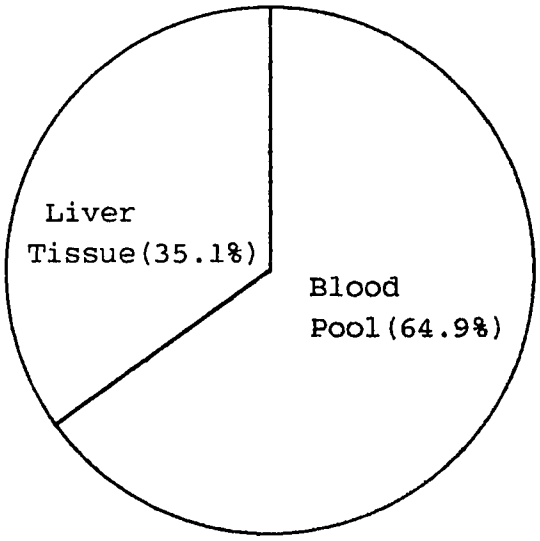

* mean, n = 3.

Figure 29. Contributions to ^{99m}Tc activity in mouse liver from the whole blood pool (ligated liver) at 24 h post-administration of ^{99m}Tc-MAb170.**

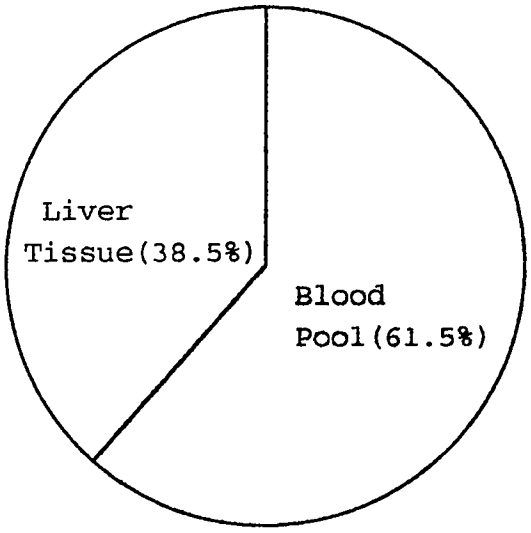

** mean, n = 3.

Figure 30. Contributions to ^{99m}Tc activity in mouse liver from partial blood pool (exsanguinated liver) at 1 h post-administration of ^{99m}Tc-MAb170.*

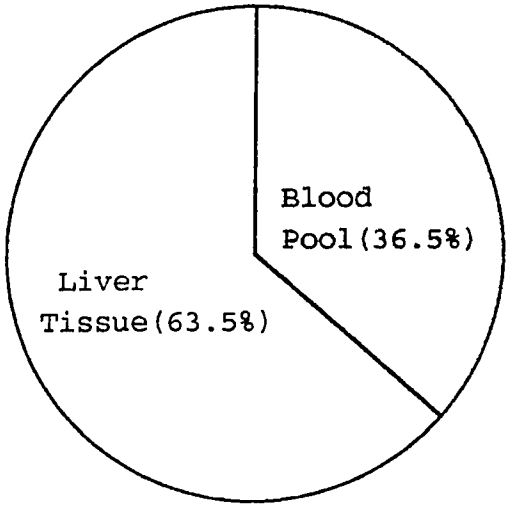

* mean, n = 3.

Figure 31. Contributions to ^{99m}Tc activity in mouse liver from partial blood pool (exsanguinated liver) at 24 h post-administration of ^{99m}Tc-MAb170.**

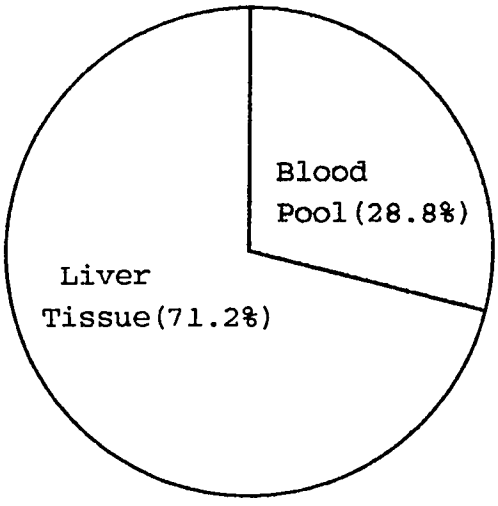

** mean, n = 3.

activity at both 1 h and 24 h. The non-liver-tissue-asssociated radioactivity was probably due to a pooling of both intravascular antibody and that within anatomical spaces such as space of Disse within the liver. The remaining one-third of the activity was probably due to the association of radiolabeled antibody with parenchymal and non-parenchymal cells, bile duct cells and connective tissues. Interestingly, in exsanguinated mice (partial blood pool exists in liver), about one-third of radioactivity was due to the contribution from blood pool. Nevertheless, the radioactivity in liver tissue itself was still significant (11% at 1 h and 6% at 24 h, respectively).

Boyle *et al.*(210) performed experiments on rats with ^{111}In-HMFGI in an attempt to understand the mechanism of hepatic uptake and clearance of radiolabeled antibodies. These authors found that at 24 h and 72 h after injection, 54% and 11%, respectively, of the hepatic radiolabel were due to blood-borne antibody. Ingvar *et al.*(211) calculated the specific tissue uptake that took the blood activity into account. They reported that 80% of radioactivity present in rat liver at 30 h after the administration of ^{125}I-MAb96.5 was due to the radiolabeled antibodies circulating in the blood. Norrgren *et al.*(212) conducted extracorporeal immuno-adsorption (ECIA) after the injection of ^{125}I-labeled biotinylated antibodies in an animal model. In athymic rats, heterotransplanted with human malignant melanoma, 90-95% of the circulating activity was removed with ECIA. The tumor-to-normal tissue ratios at 24 h was increased 4 times (from 1.2

to 5.1) in the liver, 2.5 times (0.7 to 1.8) in the lung, 4 times (1 to 4) in the kidneys and 4 times (1.4 to 5) in the bone marrow. In the case of radioimmunoimaging, the improved ratio increases the possibilities of detecting tumors and metastases in blood-rich organs. For radioimmunotherapeutic purposes, reduction in blood activity may lead to a decreased absorbed dose to critical organs. The observations by the above investigators were congruent to our experimental results concerning the contribution of blood-borne activity to liver radioactivity.

B. Distribution of ^{99m}Tc-MAb170 Activity within the Blood Compartment

Table 9 shows the results of distribution of ^{99m}Tc-MAb170 activity within the blood compartment at various time intervals after the administration of the radiolabeled antibody. The Majority of the radioactivity in blood was due to the ^{99m}Tc-MAb170 in the plasma, which accounted for approximately 98% of the blood activity. Less than 2% of radioactivity was blood-cell associated. Therefore, the measurement of the fate of radiolabeled antibody in serum would be a good indicator of behavior of antibody in blood. As plasma would enter or exit from the space of Disse freely, and thus would facilitate the contact between plasma-borne antibody and the surface of the hepatocyte membrane.

Table 9. Distribution of ^{99m}Tc Radioactivity within Blood at Various Times Post-Administration of ^{99m}Tc-MAb170.

Time	% ^{99m}Tc Radioactivity*	
	Plasma	Blood Cells
0.1 h	98.2 (98.3, 98.1)	1.8 (1.7, 1.9)
1 h	98.5 (98.4, 98.6)	1.5 (1.5, 1.4)
3 h	98.3 (97.9, 98.8)	1.7 (1.2, 2.1)

* Values represent the average of two duplicate samples.

V. ROLE OF TRANSCHELATION IN THE UPTAKE OF ^{99m}Tc-MAb170 IN LIVER AND KIDNEY

A. *In vitro* Transchelation

After the incubation of ^{99m}Tc-MAb170 with cysteine for transchelation studies, the percent bound of ^{99m}Tc-MAb170 decreased with time. Antibody-associated radioactivity decreased from 90% to 64% one hour after transchelation and only 28.2% of the radioactivity was associated with the protein at 24 h. The ^{99m}Tc was removed from MAb to cysteine (Figure 32).

The transchelating capacity of GSH was lower than that of cysteine. When the molar ratio of MAb to GSH was 1:100, the percent bound of ^{99m}Tc-MAb remained unchanged compared with the control. When the molar ratio reached 1:1000, the transchelating effects of GSH became obvious and the ^{99m}Tc binding to the MAb was rapidly transchelated to GSH (Figure 33). When ^{99m}Tc-MAb170 was challenged with 10-fold of MT, no significant difference in percent ^{99m}Tc associated with the MAb was observed between the MT treated and control samples up to 24 h.

The results from these *in vitro* experiments indicate that, in general, when an excess of either cysteine or glutathione exists one would expect a loss of radioactivity from the injected radiolabeled antibody molecule to either of

Figure 32. *In vitro* cysteine transchelation of ^{99m}Tc from MAb170 versus time of incubation with excess cysteine.*

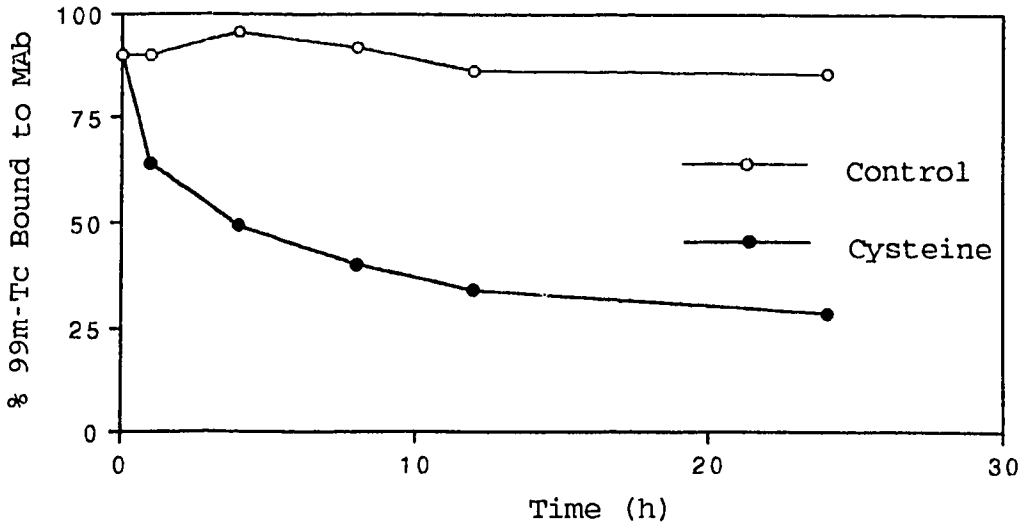

* Molar ratio of MAb to cysteine = 1:50.

Figure 33. *In vitro* glutathione transchelation of ^{99m}Tc from MAb170 versus time of incubation with excess glutathione.**

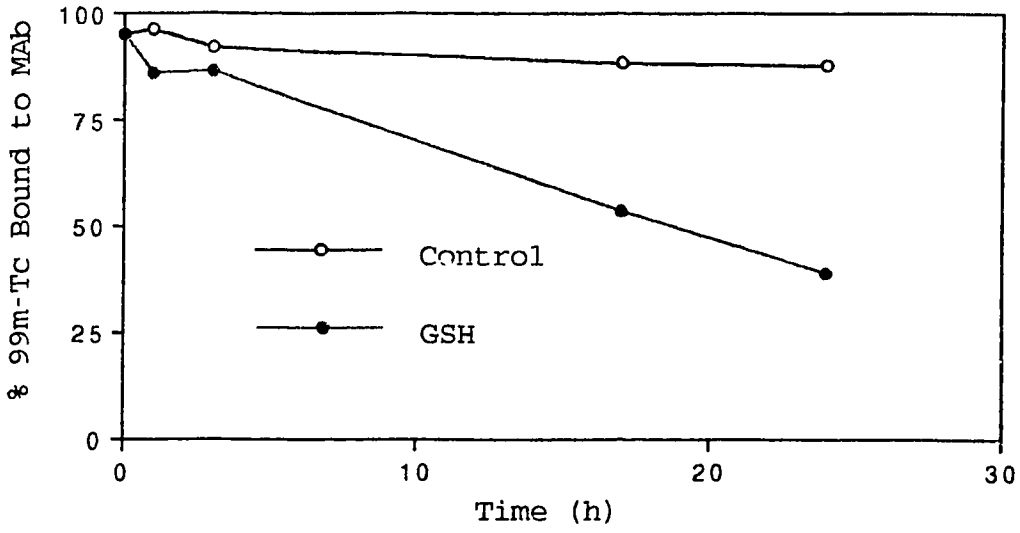

** Molar ratio of MAb to glutathione = 1:1000.

these two biologically important molecules. This also provides an insight as to the roles of the liver and kidney, which are rich in their contents with cysteine and glutathione, hence, the importance of studying the factors that modulate the expression of these molecules *in vivo* and the impact that changes in their concentration on the observed radioactivity in the liver and other organs expressing cysteine and glutathione.

B. Effects of Cysteine Administration on ^{99m}Tc-MAb170 Biodistribution

Administration of different doses of cysteine to mice 1 h after injection of ^{99m}Tc-MAb170 decreased the tissue levels of ^{99m}Tc in blood, liver and kidney. The observed decrease in radioactive levels was dose-dependent, i.e., the higher the dose, the greater the decrease. Correlation analysis indicates that there is a linear association between cysteine dose and the ^{99m}Tc uptake. In the case of the group of aminals where 5 mg cysteine was administered, the tissue levels of ^{99m}Tc decreased by 37%, 40% and 27% for blood, liver and kidney, respectively, compared with the control (Table 10).

Administration of cysteine at 1, 6 and 21 h after injection of ^{99m}Tc-MAb170 (animals sacrificed at 24 h) decreased the radioactivity of ^{99m}Tc in blood, liver and kidney. The decrease in the levels of radioactivity was most noticeable 1 hour after injection. (Table 11).

Table 10. Dose Effect of Administered Cysteine on Tissue Levels of ^{99m}Tc from ^{99m}Tc-MAb170.*

Tissues	Cysteine (mg)					
	0.0	1.0	2.0	3.0	4.0	5.0
Blood #	24.4±2.1	24.2±1.1	21.3±0.2	20.6±1.3	17.0±1.8	15.3±1.4
Liver #	9.0±0.5	9.2±0.6	7.5±0.6	7.0±0.3	6.2±0.4	5.4±0.4
Kidney #	5.1±0.5	5.0±0.2	5.0±0.5	4.4±0.1	3.9±0.3	3.7±0.3

* Values are expressed as %ID/organ (mean ± SD, n = 3). Cysteine was injected 1 h after ^{99m}Tc-MAb injection. Measurement was done 3 h after cysteine injection.

Correlation analysis of cysteine dose vs ^{99m}Tc uptake (n = 6): Blood: $r = -0.98$, $p < 0.005$; Liver: $r = -0.97$, $p < 0.005$; Kidney: $r = -0.95$, $p < 0.005$. Correlation analysis was conducted based on Byrkit (207).

Table 11. Effect of Time of Administration of Cysteine on Tissue Levels of ^{99m}Tc from ^{99m}Tc-MAb170.[a]

Tissues	Time of Cysteine Administration (p.i. ^{99m}Tc-MAb170)			Control
	1 h	6 h	21 h	
Blood [b]	8.1±0.5**	8.9±0.5*	8.8±0.6*	10.3±0.4
Liver [b]	3.1±0.1**	3.9±0.2*	3.8±0.2*	4.6±0.3
Kidney [b]	1.6±0.1**	2.0±0.1*	2.1±0.1	2.3±0.1

[a] Values are expressed as %ID/organ (mean ± SD, n = 3). 4 mg cysteine/mouse was used. Activity measurement was conducted at 24 h post-injection of ^{99m}Tc-MAb170.

[b] t test (treated vs control): ** $p < 0.01$, * $p < 0.05$.

C. Effects of Pretreatment with Thiol-Modulating Agents

After administration of OTC (a cysteine prodrug) the most prominent changes of biodistribution of ^{99m}Tc-MAb170 occurred in the liver. Compared with the control, liver ^{99m}Tc levels of the treated group increased by 40% at 1 h and 123% at 4 h postinjection. Kidney levels of ^{99m}Tc only slightly increased after pretreatment. (Table 12).

Table 12. Effect of OTC Pretreatment on ^{99m}Tc Tissue Levels.[a]

Tissues	1 h		4 h	
	Control	Treated	Control	Treated
Blood [b]	35.5±2.5	36.2±3.2	21.9±1.3	18.1±1.2
Liver [b]	13.1±1.8	18.4±0.1**	7.9±0.6	17.6±0.3**
Kidney [b]	6.5±0.3	7.9±0.6*	5.9±0.5	7.5±0.4*

[a] Values are expressed as %ID/organ (mean ± SD, n = 3). ^{99m}Tc-MAb was injected 2 h after OTC administration (6.5 mmol/kg).

[b] t test (treated vs control): ** $p < 0.01$, * $p < 0.05$.

Pretreatment of mice with BSO (an inhibitor of γ-glutamyl-cysteine synthetase) remarkably changed the distribution pattern of ^{99m}Tc-MAb170 in kidney. Compared with the control group, ^{99m}Tc levels in kidney in BSO treated group increased by 18% at 1 h, 95% at 6 h and 131% at 24 h postinjection of ^{99m}Tc-MAb170. In control group, the radioactivity decreased with time; while for the BSO-treated group of animals, the highest activity was found at 6 h postinjection, being greater than the activity at both 1 h and 24 h. No significant differences of ^{99m}Tc level in both blood and liver have been observed between the BSO treated and control group.

Table 13. Effect of BSO Pretreatment on ^{99m}Tc Tissue Level.[a]

Tissues	Time After ^{99m}Tc-MAb Administration					
	1 h		6 h		24 h	
	Control	BSO	Control	BSO	Control	BSO
Blood [b]	39.7±3.7	40.8±2.3	24.4±0.4	26.2±0.7	13.0±1.6	12.3±0.6
Liver [b]	11.6±0.6	11.2±0.4	8.1±0.3	8.1±0.9	4.8±0.5	5.8±1.3
Kidney [b]	7.6±0.9	9.0±0.2*	5.8±0.2	11.3±0.4**	3.6±0.2	8.3±2.7*

[a] Values are expressed as %ID/organ (mean ± SD, n = 3). ^{99m}Tc-MAb was injected 4 h after BSO administration (4 mmol/kg).

[b] t test (treated vs control): ** $p < 0.01$, * $p < 0.05$.

The biodistribution results of ^{99m}Tc-MAb170 in mice pretreated with $ZnSO_4$ (an MT modulator) is presented in Table 14. MT is a small protein of 6,600 daltons that contains approximately 30% cysteine and no cystine residues (164). The concentration of MT in tissues can be increased by administration of metals such as zinc (164). MT has the ability to bind metals due to its abundance of cysteinyl-free sulfhydryl groups. This MT experiment was designed with the idea that MT might transchelate with ^{99m}Tc from radiolabeled

MAb and hence alter the biodisposition of ^{99m}Tc-labeled antibodies. However, our data indicated that the biodistribution of ^{99m}Tc-MAb170 failed to show any response to the increase in tissue MT after pretreatment with $ZnSO_4$. These results suggest that MT does not directly influence the biodisposition of ^{99m}Tc-labeled antibodies.

Table 14. Effect of Pretreatment with $ZnSO_4$ on Tissue Levels of ^{99m}Tc from ^{99m}Tc-MAb.[a]

Tissues	1 h		24 h	
	Control	Treated	Control	Treated
Blood [b]	48.8±5.0	45.9±9.3	21.1±7.0	17.5±0.9
Liver [b]	17.1±2.6	16.4±1.8	9.3±3.2	8.2±0.7
Kidney [b]	5.6±0.7	5.0±0.8	3.2±1.1	3.9±0.2

[a] Values are expressed as %ID/organ (mean ± SD, n = 3). ^{99m}Tc-MAb was administered 24 h post Zn treatment (50 mg/kg, sc). Radioactivity measurement was done at 1 and 24 h after MAb injection.

[b] t test: No significant difference between the treated and the control at a 0.05 level of significance.

D. Biodistribution of ^{99m}Tc-MAb170 after Challenging with Cysteine

MAb170 was radiolabeled with ^{99m}Tc via direct stannous ion reduction of intra- and inter-disulfides bonds in the antibody molecule. As multiple disulfide bonds and multiple molecules were involved in this process, it is possible that some ^{99m}Tc may be associated to the antibody more strongly than others. If the less strongly bound ^{99m}Tc was removed by challenging the ^{99m}Tc-MAb with cysteine, the *in vivo* behavior of the radiolabeled MAb might be changed.

After a 4 h *in vitro* challenge with 50-fold excess of cysteine, only 46% (average of 45.9% and 46.6%) of ^{99m}Tc was associated with the MAb. A biodistribution study was conducted in mice using the remaining ^{99m}Tc-MAb170 after cysteine challenge. As is shown in Table 15, the *in vivo* behavior of ^{99m}Tc-MAb170 after challenging with cysteine was remarkably similar with that of ^{99m}Tc-MAb170 unchallenged (incubated with PBS). These results suggest that the behavior of radiolabeled antibody is not affected by the actual site of ^{99m}Tc labeling on the antibody molecule.

Table 15. Effect of Cysteine Challenge on the Biodistribution of ^{99m}Tc-MAb170.[a]

		Blood [b]	Liver [b]	Kidney [b]
1 h	Challenge	47.1±2.8	15.0±0.4	5.6±0.2
	Control [c]	44.3±2.1	13.7±1.8	5.9±0.7
3 h	Challenge	39.7±6.2	13.0±1.1	7.1±0.7
	Control	37.9±3.4	12.2±0.4	5.5±0.2
6 h	Challenge	21.7±2.7	8.8±1.1	4.9±0.3
	Control	27.2±5.9	10.1±1.3	4.7±0.4
24 h	Challenge	11.3±1.4	5.4±0.3	2.7±0.1
	Control	13.2±0.4	5.5±0.4	2.1±0.3

[a] Values are expressed as % ID/organ (mean ± SD, n = 3).

[b] t test: No significant difference was observed at 0.05 level of significance.

[c] Uptake was measured using ^{99m}Tc-MAb170 incubated with PBS.

E. Identification of ^{99m}Tc-Labeled Thiols in Bile, Urine and Kidney

Figures 20-22 show the radiochromatograms obtained by analysis on Bio-Gel P2 column of mouse bile, kidney homogenate and urine acquired after administration of ^{99m}Tc-MAb170 in normal mice. The majority of the ^{99m}Tc-containing species in bile and urine and some in kidney homogenate were coeluted with the peaks in the analysis of ^{99m}Tc-GSH and ^{99m}Tc-cysteine. Thus, it is safe to assume that ^{99m}Tc-GSH and ^{99m}Tc-cysteine accounted for the majority of the radioactivity in bile and urine, and part of the activity in kidney after ^{99m}Tc-MAb170 injection.

The object of this investigation was to explore the role of thiols (cysteine and GSH) in the mechanism of localization in normal tissues of tracer from ^{99m}Tc-radiolabeled antibodies. Monoclonal antibodies are radiolabeled with ^{99m}Tc by direct method only after reduction of endogenous intra and inter chain disulfide bonds to sulfhydryl moieties. It is possible that the added ^{99m}Tc may coordinate to both sulfhydryl groups if the original conformation of the protein is not significantly altered or if it can be reestablished (213). *In vitro* transchelation studies have demonstrated that the association of ^{99m}Tc with MAb can be influenced by challenge with cysteine and GSH. Cysteine and glutathione have been found in liver and kidney with high concen-

trations (18, 19). It therefore seems reasonable to assume that the metabolic behavior of the radiolabel after injection of ^{99m}Tc-MAb could involve specific transchelation from the sulfhydryl-^{99m}Tc bond (214, 215).

Cysteine is taken up by cells, usually via the ASC system (216). System ASC activity was trans-stimulated; the external presence of ASC amino acids accelerated the exodus of these amino acids previously accumulated (217). In the cysteine-treated rat, the total thiols (protein + non-protein thiols) in both liver and kidney were decreased compared with the control (218). When cysteine was injected after the administration of ^{99m}Tc-MAb, some would transchelate with ^{99m}Tc-MAb extra-cellularly and in blood to form ^{99m}Tc-cysteine; some might form mixed disulfides with thiols intracellularly and extracellularly, which reduced the ^{99m}Tc-binding ability of the cells. In addition, one would speculate that the external presence of cysteine would accelerate the exodus of ^{99m}Tc-binding cysteine previously accumulated in the cells, and then the ^{99m}Tc-cysteine could be excreted through urine and bile. The total effects one would expect in this case is a decrease of radioactivity in blood, and consequently in the liver and kidney. This is consistent with our observations after the injection of cysteine in the mice.

OTC is a cysteine prodrug (219, 220). When it is administered *in vivo*, 5-oxo-L-prolinase catalyses the conversion of oxothiazolidine to S-carboxyl-L-cysteine, which

decarboxylates spontaneously to L-cysteine (219). By this route, L-cysteine is made available intracellularly. The changing magnitude of tissue cysteine levels after administration of OTC varies. Cysteine content in liver is considerably increased, but only a slight increase has been found in kidney. The pattern of alterations of tissue GSH is similar to that of cysteine after administration of OTC, i.e., notable increases occur in liver and a smaller increase in kidney (220). Administration of ^{99m}Tc-MAb in OTC-treated mice resulted in significant increase in uptake of ^{99m}Tc in liver and small increase in kidney. Increased accumulation of ^{99m}Tc parallelled the reported changes in content of cysteine and GSH in those two organs.

BSO is an inhibitor of gamma-glutamylcysteine synthetase according to this reported pathway (216):

$$\text{Cysteine} \xrightarrow[\text{ATP}]{\text{glutamate}} \text{gamma-glutamylcysteine} \xrightarrow[\text{ATP}]{\text{glycine}} \text{GSH.}$$

This pathway suggests that GSH synthesis will be inhibited by BSO. After administration of BSO, GSH levels in both liver and kidney were considerably decreased (220). On the other hand, hepatic cysteine levels nearly doubled 20 min after BSO treatment, but were not significantly different from control at later time points. In contrast, renal cysteine was significantly depleted from 20 min to 25 h postinjection with a time course closely parallelling that of renal GSH depletion (221).

In normal liver, GSH is found in high concentration (19).

There was still a considerable amount of GSH after BSO pretreatment although significant decrease was observed (220). Our *in vitro* study indicated that GSH had much weaker transchelating capacity compared with that of cysteine which was not affected after BSO treatment. The overall transchelating ability of the thiols from liver did not exhibit much change. This explains the fact that we observed no differences in ^{99m}Tc activity in the liver after injection of ^{99m}Tc-MAb in BSO-treated mice.

In the case of kidney uptake, our data suggested that cysteine and GSH might exert important metabolic and transport functions. The kidney could also process the ^{99m}Tc-containing species reaching it from other organs after injection of ^{99m}Tc-MAb. Both thiol-containing compounds have the capacity to transchelate ^{99m}Tc from ^{99m}Tc-MAb and then the radioactive species could be excreted into the urine. When mice were pretreated with BSO, renal GSH and cysteine were depleted (220, 221) and thus the transchelating capacity decreased correspondingly. Since the excretion of ^{99m}Tc by both thiols also decreased, it is safe to assume that the observed accumulation of ^{99m}Tc species in kidney is due to this phenomenon.

Chromatographic analysis indicated that after injection of ^{99m}Tc-MAb the majority of the ^{99m}Tc-containing species in bile and urine and some in kidney were ^{99m}Tc-labeled cysteine and GSH. This strongly supports the theory that thiols in liver and kidney would transchelate with ^{99m}Tc-MAb *in vivo* and

could thus play an important role in the biodisposition of radioactivity from directly-labeled ^{99m}Tc monoclonal antibodies.

In summary, the data of *in vitro* and *in vivo* thiol transchelation studies, biodistribution alteration of ^{99m}Tc-MAb after specific modulation of endogenous thiol containing compounds, and the finding of ^{99m}Tc-labeled cysteine and GSH in bile, urine and kidney after administration of ^{99m}Tc-MAb demonstrated that transchelation by thiols (cysteine and GSH) played an important role in the localization of radiotracer from ^{99m}Tc-labeled MAb in normal tissues such as liver and kidney.

VI. ROLE OF LIVER RECEPTORS, Fc, F(ab')$_2$, AND INTACT ANTIBODY IN THE UPTAKE OF ^{99m}Tc-LABELED ANTIBODY BY THE LIVER

A. *In Vitro* Binding Studies of ^{99m}Tc-Labeled Antibody to Mouse Hepatocytes

1. Binding Studies of ^{99m}Tc-MAb170 to Mouse Hepatocytes

(1) Kinetics of *In Vitro* Association of ^{99m}Tc-MAb170 by Hepatocytes

The binding kinetics of ^{99m}Tc-MAb170 by hepatocytes was studied using the binding assay with cells in suspension. This method allows the rapid separation of cell-bound from

free ^{99m}Tc-MAb170.

Isolated hepatocytes were incubated with ^{99m}Tc-MAb170 at 37°C for different durations of time up to 1 h (Figure 34). Most of the ^{99m}Tc-MAb170 binding process occurred at a fast rate within the first 15 min. The amount of ^{99m}Tc-MAb bound to hepatocytes increased almost linearly to a maximum at 15 min, and decreased slowly thereafter reaching a plateau after 30 min. In subsequent experiments, a 15 min incubation period was used at 37°C.

The uptake of ^{99m}Tc-MAb170 was dependent on the dose of the radiolabel. As seen in Figure 35, when the number of hepatocytes was held constant and the dose of ^{99m}Tc-MAb170 was varied from 37 kBq/1 µg to 777 kBq/20 µg, there were significant differences in the amount of ^{99m}Tc-MAb170 that was taken up by the hepatocytes. The uptake of the radiolabel increased with the dose escalation. However, no linear relationship was observed between the uptake and dose. This indicated that there was a saturation of binding sites on the surface of the cells.

(2) Effect of Unlabeled Specific MAb on the Uptake of ^{99m}Tc-MAb170 by Hepatocytes

The specificity of ^{99m}Tc-labeled MAb170 binding was investigated by determining the effects of inhibition obtained with unlabeled monomeric MAb170 (Figure 36). The binding of ^{99m}Tc-MAb170 to mouse hepatocytes could be inhibited by unlabeled specific MAb170. The inhibition

Figure 34. Kinetics of *in vitro* ^{99m}Tc-MAb170 uptake by mouse hepatocytes.*

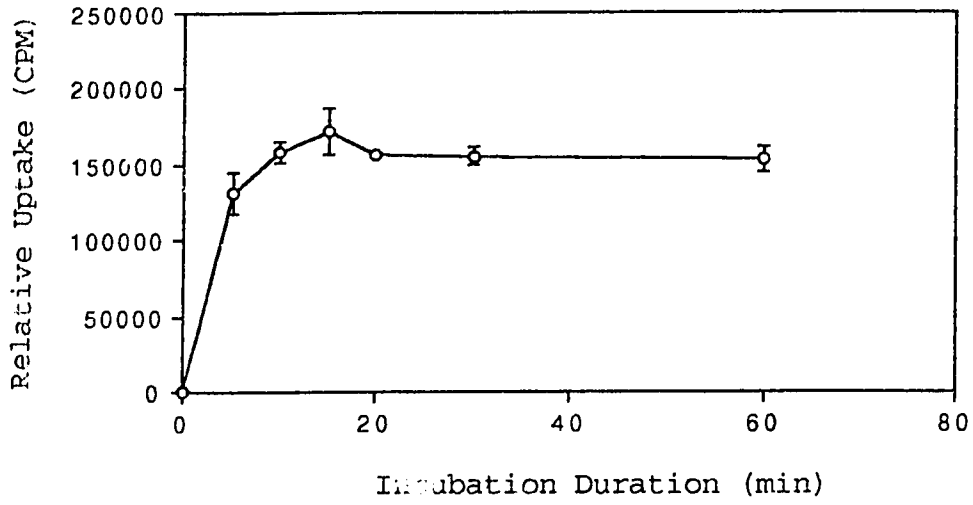

* Uptake is expressed as the radioactivity of cell pellets. Dose of ^{99m}Tc-MAb170 = 37 kBq/µg. (mean ± SD, n = 3).

Figure 35. Uptake of ^{99m}Tc-MAb170 by mouse hepatocytes as a function of the doses of ^{99m}Tc-MAb170.**

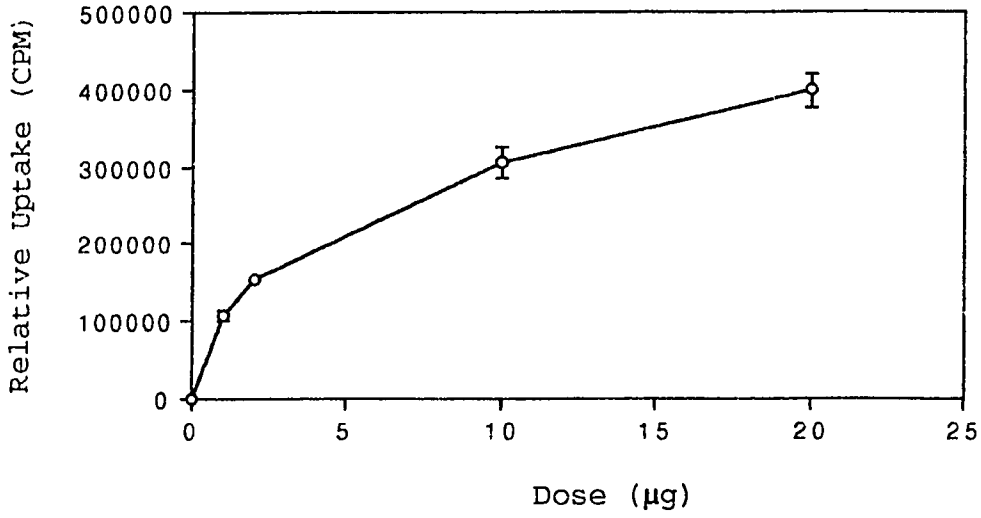

** Uptake is expressed as the radioactivity of cell pellets. (mean ± SD, n = 3). Dose = 37 kBq/µg.

effects increased with the dose of unlabeled MAb. The binding of ^{99m}Tc-MAb170 to hepatocytes was reduced to 2/3 of the control value by a 50-fold excess of unlabeled MAb170, to 1/3 of the control by a 100-fold excess of the unlabeled MAb.

Numerous reports have provided evidence that hepatocytes possess binding sites for the Fc portion of immunoglobulin G and for the third complement component (C3) on their plasma membrane (172, 173, 222-225). In the present study, the uptake of ^{99m}Tc-MAb170 by hepatocytes was probably an Fc receptor-mediated process. Unlabeled MAb170 could compete with ^{99m}Tc-MAb170 for Fc receptor binding. The co-administration of excessive unlabeled MAb170 inhibited the binding of ^{99m}Tc-MAb170 to hepatocytes and decreased the hepatocyte uptake. This kind of uptake could not be completely inhibited by 100-fold excess of unlabeled MAb, which suggested that there might be alternative liver mechanisms for retention of the ^{99m}Tc label, probably the transchelation of ^{99m}Tc by thiols in hepatocytes.

The use of radiolabeled antibody fragments in imaging has been reported (162), following suggestions that hepatic uptake of radiolabeled antibodies is mediated via Fc receptor (205). The liver uptake was reduced when radiolabeled fragments were used, being accompanied by decreased tumor concentrations due to the short biological half life and increased kidney uptake of the fragments (24, 104, 162).

2. Effects of Native HIgG, $F(ab')_2$ and Fc on ^{99m}Tc-HIgG Uptake by Mouse Hepatocytes

As previously reported in the present work, the *in vitro* uptake of ^{99m}Tc-labeled MAb170 by hepatocytes was inhibited by unlabeled specific MAb. To further investigate the roles of various portions of the antibody in the cellular uptake, hepatocytes in suspension were incubated with both ^{99m}Tc-labeled HIgG and various amounts of unlabeled native HIgG, $F(ab')_2$ or Fc fragments. The ^{99m}Tc-HIgG binding data are presented in Figures 37, 38 and 39. Competitive binding between labeled and unlabeled proteins were observed. The patterns of inhibition obtained with either intact native HIgG, $F(ab')_2$ or Fc fragments were similar. ^{99m}Tc-HIgG binding to hepatocytes was reduced to about 40% of the control with a 10-fold excess of unlabeled proteins, and to about 1/3 of the control with a 100-fold excess of unlabeled proteins.

It follows from the fact that both $F(ab')_2$ and Fc fragments inhibit the uptake of ^{99m}Tc-HIgG by hepatocytes that the ability of HIgG to compete for binding sites seems to reside in both Fc and Fab portions of the antibody molecule.

Numerous studies have described antibody binding sites on both parenchymal and non-parenchymal cells of the liver (162, 173, 175, 176). Carbohydrate receptors and Fc receptors which bind immunoglobulin occur on both parenchymal and non-parenchymal cells. Consequently, both may contribute to the

Figure 36. Effect of native MAb170 on *in vitro* uptake of ^{99m}Tc-MAb170 by mouse hepatocytes.*

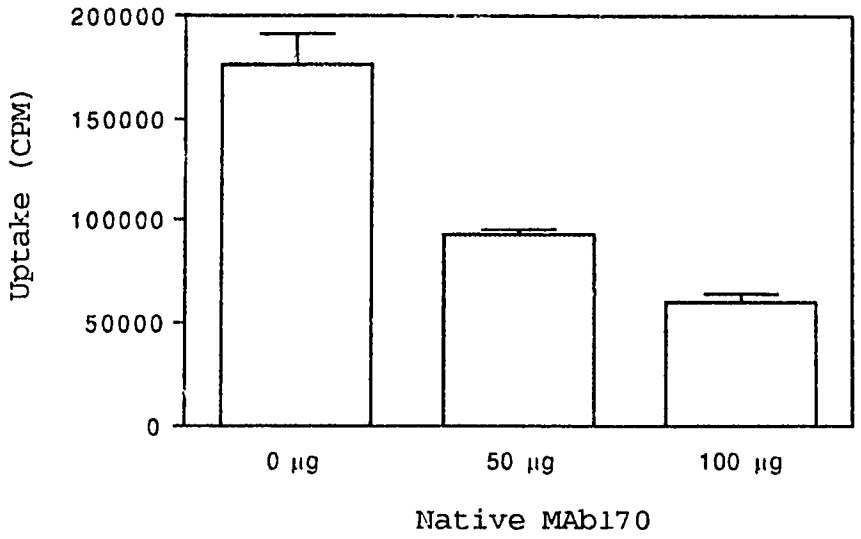

* The molar ratio of unlabeled/labeled MAb was 0, 50 and 100. Dose of labeled MAb = 1 µg. (mean ± SD, n = 3).

Figure 37. Inhibiting effect of HIgG on *in vitro* uptake of ^{99m}Tc-HIgG by mouse hepatocytes.**

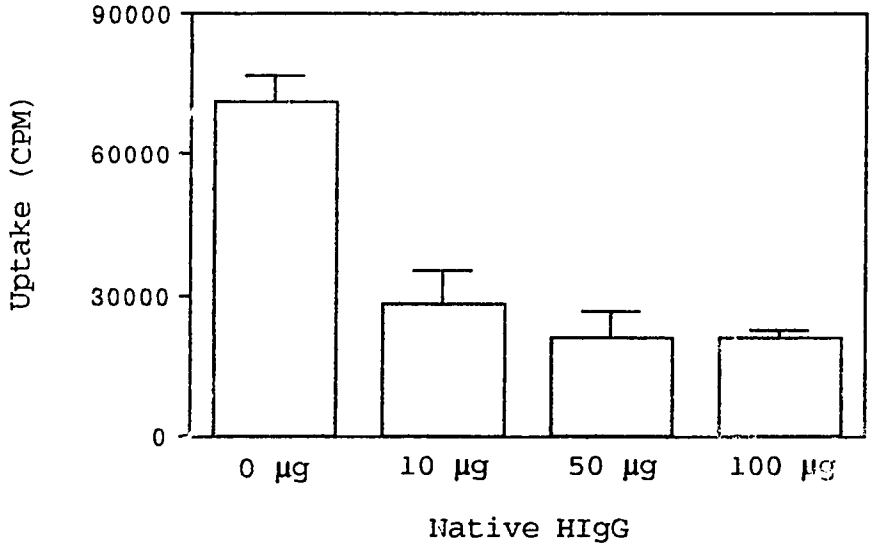

** The molar ratio of unlabeled/labeled HIgG was 0, 10, 50 and 100. Dose of labeled HIgG = 1 µg. (mean ± SD, n = 3).

Figure 38. Effect of native human $F(ab')_2$ on *in vitro* uptake of ^{99m}Tc-HIgG by mouse hepatocytes.*

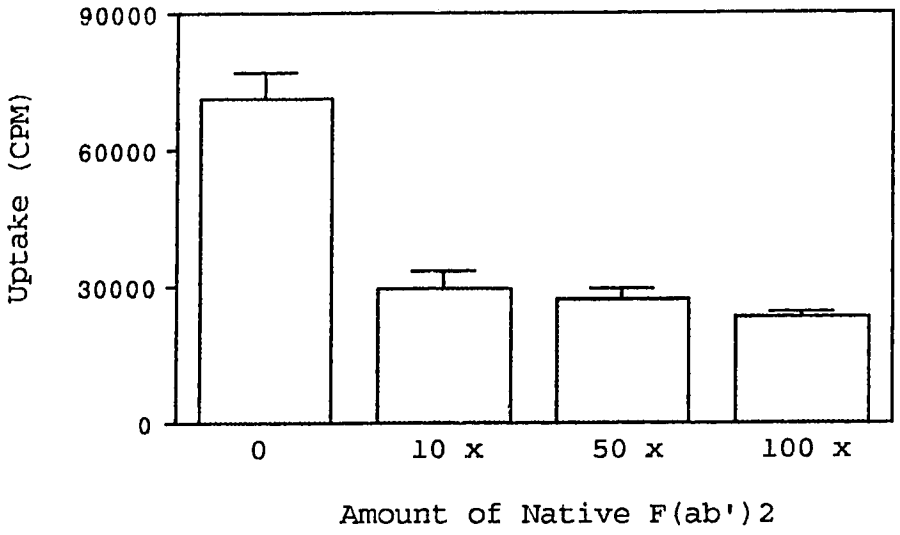

*The molar ratio of unlabeled $F(ab')_2$/labeled HIgG was 0, 10, 50 and 100. Dose of labeled HIgG = 1 µg. (mean ± SD, n = 3).

Figure 39. Inhibiting effect of native human Fc on *in vitro* uptake of ^{99m}Tc-HIgG by mouse hepatocytes.**

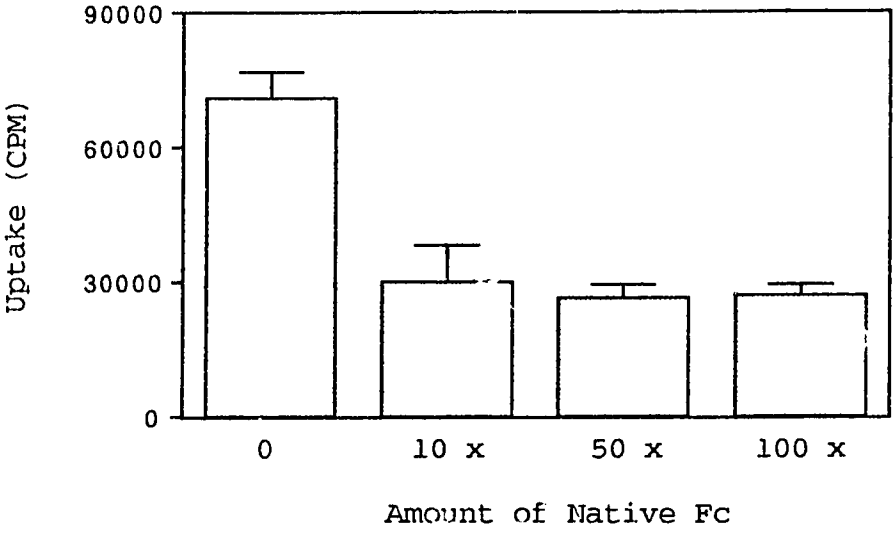

**The molar ratio of unlabeled Fc/labeled HIgG was 0, 10, 50 and 100. Dose of labeled HIgG = 1 µg. (mean ± SD, n = 3).

hepatic uptake of a radioisotope which is attached to an antibody. The biodistribution of radiolabeled $F(ab')_2$ after the removal of Fc portion of the antibody showed that the absolute uptake by liver cells was reduced (162). The predominant cell type responsible for the uptake was identified as the parenchymal cell (hepatocytes), due to its greater number in the liver. This suggests that the uptake by liver cells is dependent on the Fc portion of the molecule. However, the uptake of radiolabeled $F(ab')_2$ by liver is still significant. The ability of HIgG to compete for binding sites suggests that the mechanism does not seem to reside exclusively in the Fc portion of the antibody molecule. The mechanism for the *in vivo* uptake of foreign compounds such as human IgG by mouse hepatocytes is thought to involve binding a receptor followed by macropinocytosis (177). As a part of whole IgG, $F(ab')_2$ possesses similar structure and immunoreactivity as its parent molecule. It is postulated that $F(ab')_2$ might share some transporting and metabolic mechanisms with intact IgG.

B. *In Vivo* Interventional Biodistribution Studies of ^{99m}Tc-MAb170

1. Effects of Native and Aggregated Specific MAb on ^{99m}Tc-MAb170 Biodistribution

Table 16 shows the results of ^{99m}Tc-MAb170 biodistribution in mice after pretreatment with unlabeled monomeric, aggregated specific MAb170 , or saline. No differences were

observed in the uptake of radioactivity by tissues among various treatments. This inability to inhibit the uptake of radiolabeled MAb170 by specific unconjugated MAb suggested the existence of a proportional uptake mechanism in liver, that is to say, the liver incorporated a constant percentage of dose within a certain limit of dose of MAb. This assumption was supported by *in vitro* cell-binding studies with rat liver cells and ^{111}In-HMFG1 (210).

Table 16. Effect of Unconjugated, Aggregated MAb, and Saline on the Biodistribution of ^{99m}Tc-MAb170 in Normal Mice.[a]

Tissues	% ID/organ		
	MAb170	Aggregated MAb	Saline
Blood [b]	47.0±2.2	44.3±4.6	43.7±2.0
Liver [b]	13.8±0.2	13.2±1.1	13.1±0.4
Kidneys [b]	9.6±0.3	8.7±0.4	8.4±0.5

[a] Values are expressed as mean ± SD (n = 3).

[b] No significant difference was observed at 0.05 level of significance.

2. Effect of Cyclophosphamide on ^{99m}Tc-MAb170 Biodistribution

Table 17 presents the results of ^{99m}Tc-MAb170 biodistribution in mice after pretreatment with cyclophosphamide. In the treated mice, the uptake of radiolabel by the liver tissue was decreased.

Table 17. Effect of Cyclophosphamide on ^{99m}Tc-MAb170 Biodistribution.[a]

Tissues	1 h		6 h		24 h	
	Cy	Control	Cy	Control	Cy	Control
Blood [b]	34.9±2.6*	40.0±1.5	18.2±1.2	20.2±1.2	8.4±0.5**	9.9±0.1
Liver [b]	14.6±0.8**	17.1±0.6	8.5±0.3	9.3±0.5	4.6±0.6**	5.6±0.1
Kidneys [b]	5.0±0.9	5.3±0.4	4.1±0.6	4.8±0.2	[illegible]	2.6±0.1

[a] Values are expressed as % ID/organ (mean ± SD, n = 3).

[b] t test (treated vs control): ** $p < 0.025$, * $p < 0.05$.

Cy = cyclophosphamide.

Cyclophosphamide is a potent antineoplastic and immunomodulating drug. It enhances two Fc receptor-mediated functions: antibody-dependent cellular cytotoxicity and phagocytosis. This augmentation has been associated with an increased number of Fc receptors on the effector cells (226, 227). Our results suggest that pretreatment of mice with cyclophosphamide enhanced the processing ability (metabolism and excretion) of liver by Fc receptor modulation. Therefore, it seems reasonable to assume that the administered MAb was metabolized and excreted faster and hence the radioactivity in the organs was decreased. As cyclophosphamide has multiple pharmacological actions, the effect of this drug on antibody disposition should be interpretated carefully.

VII. BINDING STUDIES OF RADIOLABELED MAB WITH KIDNEY SLICES

A. Stability of ^{99m}Tc-MAb170 in an Oxygen Environment

The percentage of ^{99m}Tc attached to MAb170 after different treatments in the presence or absence of oxygen is listed in Table 18. As is shown, about 90% of ^{99m}Tc remained bound to MAb170 after 2 h of O_2 bubbling. This indicates that ^{99m}Tc-MAb170 is quite resistant to O_2 although it is radiolabeled by a reducing technique. Therefore, we concluded that the ^{99m}Tc-labeled MAb can be used in an O_2 environment with limited loss of ^{99m}Tc for at least a period of one hour. The percent of ^{99m}Tc bound to MAb remained unchanged in PBS for 2 hours.

Table 18. The Stability of ^{99m}Tc-MAb170 in O_2 Environment.

Treatments of ^{99m}Tc-MAb170	% ^{99m}Tc Bound to MAb170 [a]		
	5 min	1 h	2 h
Krebs-bicarbonate Buffer + O_2/CO_2 (95/5%)	98.0 (98.3,97.6)	92.3 (91.4,93.2)	88.8 (89.0,88.5)
Krebs-bicarbonate Buffer + N_2	98.5 (98.4,98.5)	95.3 (95.4,95.2)	92.9 (92.9,92.8)
PBS	98.5 (98.4,98.6)	98.6 (98.5,98.6)	98.5 (98.6,98.4)

[a] Values represent the average of two duplicate samples.

B. Comparison of Binding Data Obtained from Two Slice Saver Chambers

The binding results of ^{125}I-MAb170 to kidney slices obtained from two Slice Saver chambers which underwent identical treatment are presented in Table 19. The differences between two sets of binding data at various time points were not significantly different ($p > 0.10$, paired t test). Therefore, the data obtained from the two Saver chambers were considered to be comparable.

Table 19. Comparisons of Binding Data of ^{125}I-MAb170 Obtained from Two Slice Saver Chambers.

Incubation Time (min)	Slices/Chamber	DPM(A)	DPM(B)	% Difference [a] (A-B)/[(A+B)/2]
20	8	441,164	459,751	- 4.1
30	4	202,764	191,385	5.8
60	4	312,756	309,471	1.1

[a] Paired t test: $p > 0.10$.

C. ^{125}I-MAb170 Binding Kinetics to Kidney Slices

Table 20 and Figure 40 show the time-activity course of accumulating ^{125}I-labeled antibody in kidney slices. In the

case of ^{125}I-MAb170, an initial fast accumulation of the radiolabel by kidney slices was observed followed by a continued slow uptake. Dijk *et al.*(228) also observed slow but continued accumulation (up to 16 h) of radiolabeled antibodies by normal kidney tissue using an ex vivo kidney perfusion model. The light-microscopy studies showed that cell morphology after 16-h perfusion was normal, indicating the continued perfusion did not lead to cell damage.

Table 20. Binding Kinetics of ^{125}I-MAb170 to Kidney Slices.

Incubation Duration (min)	% Dose/g	DPM/g	µg MAb/g
5	0.87	550,855	0.05
15	1.22	770,092	0.07
30	1.88	1,193,009	0.11
60	2.84	1,789,334	0.17

Figure 40. *In vitro* binding kinetics of ^{125}I-MAb170 to kidney tissue slices.

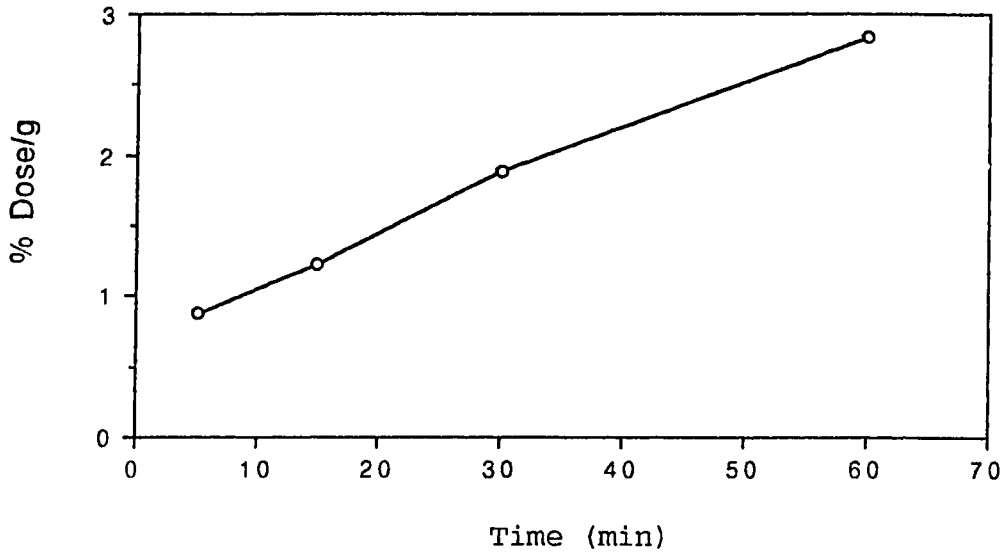

D. Time-Course of ^{125}I-MAb170 Uptake by Kidney Slices

Figure 41 shows the result of ^{125}I-MAb170 binding to kidney slices. With the increase in incubation duration, kidney tissue accumulated more radiolabeled MAb. After 30 min of incubation, the tissue slices were washed and incubated in fresh buffer. The radioactivity was rapidly released from the tissues into the buffer. After 15 min of incubation in fresh buffer, about 2/3 of radioactivity was transferred from the tissues to buffer. More radioactivity was released with the increase in incubation duration. Assay of radioactive species released into the buffer showed that 93% (average of two duplicate samples: 92.9% and 93.4%) of radioactivity was TCA precipitable, indicating that the radioactive species was

Figure 41. Uptake and dissociation of radioactive species by kidney tissue slices while incubated with and without radioiodinated ^{125}I-MAb170.

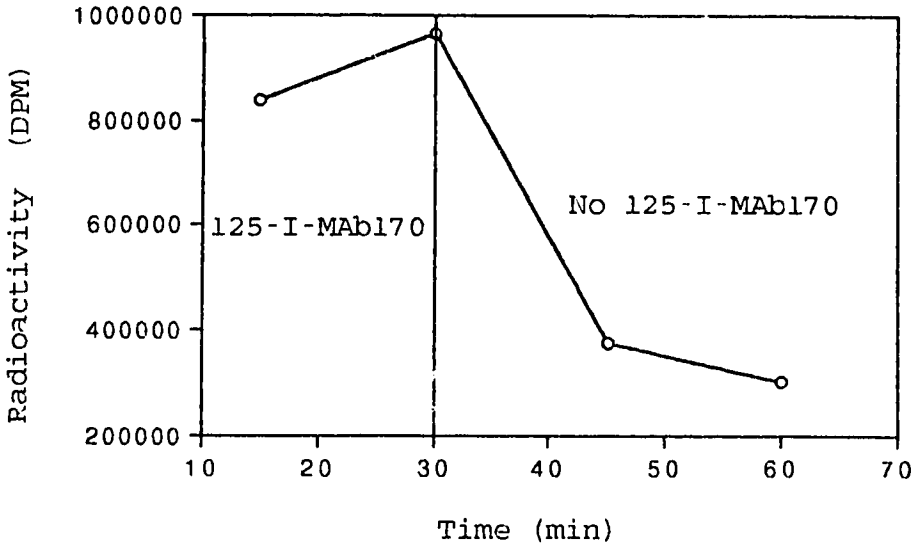

Figure 42. Uptake and dissociation of radioactive species by kidney tissue slices while incubated with and without pertechnetate $Na^{99m}TcO_4$.

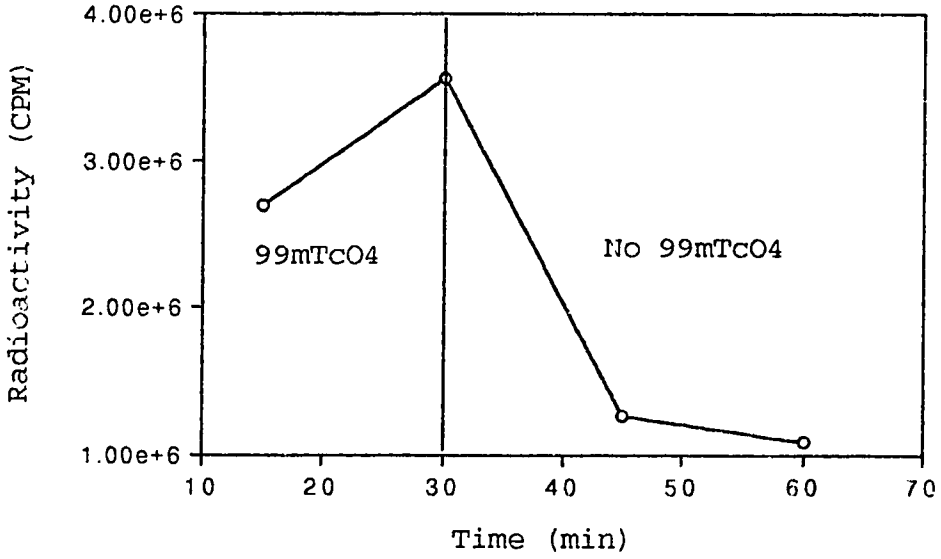

radiolabeled protein. This suggests that the binding of labeled MAb to kidney tissue was not stable, or that the labeled MAb taken up by kidney slices was quickly metabolized and released.

A similar binding pattern was observed during $Na^{99m}TcO_4$ binding studies (Figure 42). However, $Na^{99m}TcO_4$ was released much faster than labeled MAb from the kidney tissue. The similarity implied the nature of non-specific binding of some of the administered labeled MAb to the kidney tissue.

E. Binding of Dual Labeled MAb to Kidney Tissue

When kidney tissues were incubated with dual labeled MAb (^{99m}Tc- and ^{125}I-MAb170), the uptake of both tracers increased with incubation duration and the parallelism of two tracers was obvious (Table 21). At different time intervals, the ratio of $^{99m}Tc/^{125}I$ in kidney tissues showed only a slight difference, which indicated that the protein moiety played a major role while the isotope part played only a minor role in the uptake of labeled MAb by kidney tissues. The slight increase of ratio of $^{99m}Tc/^{125}I$ with incubation duration suggested the existence of possible transchelation of ^{99m}Tc by the thiols in kidney tissues.

Table 21. Binding of Dual Labeled MAb to Kidney Tissues.

Incubation Duration(min)	Total Radioactivity Bound to Tissues(CPM)		Ratio of $^{99m}Tc/^{125}I$
	^{99m}Tc	^{125}I	
5	229,645	314,444	0.73
30	384,561	506,075	0.76
60	626,030	778,941	0.80

F. Effects of Chloroquine and Protein G on the Uptake of ^{99m}Tc-MAb by Kidney Tissues

Figure 44 demonstrated the effects of chloroquine on the uptake of ^{99m}Tc-MAb170 by kidney tissues. The uptake of the radiolabel was reduced by 23% after pretreatment of kidney slices with chloroquine. Chloroquine is a lysosomotropic agent which accumulates in the lysomes (229). The lysosomotropic agent has been demonstrated to interfere with receptor-mediated uptake and degradation of numerous ligands, including asialoglycoproteins (229), mannose-6-phosphate terminated ligands (230), alpha-2-macroglobulin-protease complex (231), mannosylated albumin (232), and low-density lipoproteins (233). The lysosomotropic agent can raise the pH of lysosomes and endosomes which are now known to be acidic and interfere with receptor recycling by sequestering

receptors within intracellular compartment (234, 235). MAb170 is a glycoprotein. The reduced uptake of ^{99m}Tc-labeled MAb170 by chloroquine-treated kidney tissues is probably due to the decrease in binding sites on the cell surface. It is suggested that receptor-mediated process might be involved in the uptake of radiolabeled MAb by kidney tissues.

The role of Fc portion on the antibody molecule has been established in the uptake of ^{99m}Tc-antibody by mouse hepatocyte. As is reported preciously in this thesis, the uptake of ^{99m}Tc-HIgG by hepatocyte is significantly inhibited by excess of unlabeled HIgG and its corresponding Fc fragment. In an attempt to investigate if some sites on Fc fragment might be responsible for its blocking effect, the protein G study was designed.

Protein G is an immunoglobulin-binding molecule produced by some streptococcus species. Protein G was found to bind all human IgG subclasses and also rabbit, mouse, and goat IgG. On the IgG molecule, the Fc part is responsible for the interaction with Protein G (236, 237). In the present study, the effect of protein G on the uptake of ^{99m}Tc-MAb170 by kidney tissues was investigated with the idea to investigate effect of blocking the Fc component of the antibody structure on the kidney tissue uptake. Figure 45 shows the results of tissue uptake of both ^{99m}Tc-MAb bound to protein G and ^{99m}Tc-MAb only. No significant difference in uptake between the two was observed, which implies that the protein G-binding site on the Fc portion was not important in the uptake of radio-

Figure 43. Effect of chloroquine on the *in vitro* uptake of ^{99m}Tc-MAb170 by kidney tissue slices.

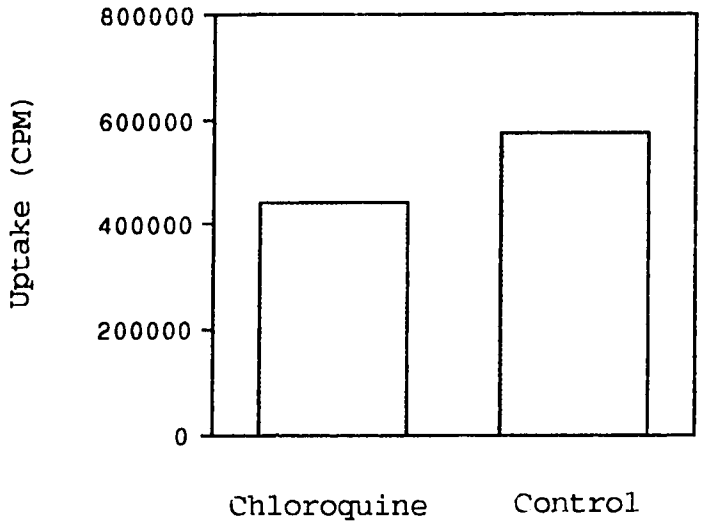

Figure 44. Effect of protein G on the *in vitro* uptake of ^{99m}Tc-MAb170 by kidney tissue slices.

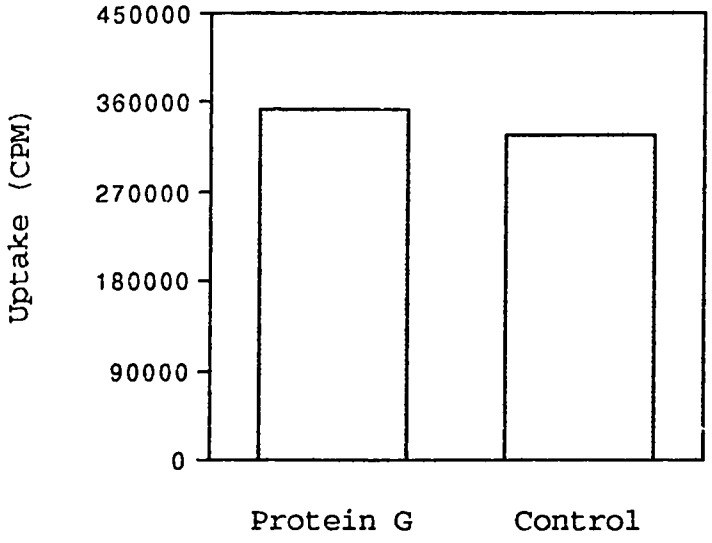

labeled MAb by kidney tissues.

The *in vitro* binding studies of radiolabeled MAb with kidney slices were designed to investigate the binding kinetics and affecting factors in the absence of the interference from the radioactive species from blood and other organs which is encountered during the *in vivo* studies. The uptake of radiolabeled MAb by kidney tissues increased with time. However, a fast washout of radioactivity from the tissues was observed in the fresh buffer. The released radioactive species was assayed as radiolabeled protein. Binding studies of dual labeled MAb (^{99m}Tc- and ^{125}I-MAb170) suggest that the protein moiety played a major role in the uptake of labeled MAb by kidney tissues. A difference, althouth slight, in the disposition of the two radiolabels was also noted. Reduced uptake of the radiolabeled MAb by chloroquine-treated kidney slices suggests that receptor-mediated process might be involved. The protein G-binding site on the Fc portion was found not important in the uptake of radiolabeled MAb by kidney tissues.

SUMMARY AND CONCLUSIONS

The major focus of this thesis was to develop an understanding of the mechanisms involved in the uptake and metabolism of directly-labeled ^{99m}Tc-antibodies by normal tissues.

The metabolism and *in vivo* fate of ^{99m}Tc-MAb were determined by analysis of various biological samples following injection of ^{99m}Tc-MAb into mice. Virtually all of the radioactivity in blood was due to the radiolabel in plasma, which accounted for >98% of the blood radioactivity. Also, 99-100% of the radioactivity in serum was associated with the intact antibody. The radioactivity in the liver homogenates was strictly protein-bound to either intact MAb or low molecular weight species. In kidney extracts, the majority of the radioactivity was protein-bound ^{99m}Tc, including ^{99m}Tc-MAb. Only 5-8% of the activity was from non-protein-bound ^{99m}Tc. Multiple ^{99m}Tc-containing species were observed in urine and bile. Both ^{99m}Tc-cysteine and ^{99m}Tc-glutathione were strongly suggested as present in bile, kidney and urine. No evidence for the *in vivo* formation of ^{99m}Tc pertechnetate was observed.

The mechanisms of tissue uptake of radiolabeled antibodies were investigated by determining the roles of radionuclide (^{99m}Tc), protein moiety and the nature of tissues *in vivo* and *in vitro*.

Data of *in vitro* and *in vivo* thiol transchelation studies, biodistribution alteration of ^{99m}Tc-MAb after specific modulation of endogenous thiol-containing compounds,

and the finding of ^{99m}Tc-labeled cysteine and glutathione in bile, urine and kidney following administration of ^{99m}Tc-MAb indicated that the transchelation of ^{99m}Tc by thiols (cysteine and glutathione) played an important role in the localization of radiotracer from ^{99m}Tc-MAb in normal tissues such as liver and kidney.

In vitro binding studies of radiolabeled antibodies with hepatocytes and kidney slices demonstrated that the uptake of the radiolabel was the function of incubation duration and dose dependent. The uptake of ^{99m}Tc-antibodies could be inhibited by excessive unlabeled $F(ab')_2$ and Fc fragments as well as intact antibody. Alterations of the biodistribution of ^{99m}Tc-antibody was observed in mice pretreated with agents to block the Fc receptor recycling or increase Fc receptor expression. These observations indicated that both Fab and Fc portions on the antibody molecule as well as the intact antibody played important roles in the uptake of the radiolabel by normal tissues.

The influence of blood pooling of the radiolabeled MAb on data interpretation was also assessed. It was observed that liver blood-pooling contributed about two-thirds of the *in vivo* liver radioactivity.

In conclusion, the uptake of ^{99m}Tc radioactivity by normal tissues such as liver and kidneys following administration of directly-labeled ^{99m}Tc-antibodies is a result of a complex interaction between physiological and chemical conditions. This work therefore supports that this

process can be manipulated *in vivo* by pharmacological interventions, which has the potential for improvements in radioimmunoscintigraphy and radioimmunotherapy. Increased clearance of blood radioactivity by these interventions would reduce the radioactivity levels in various tissues, which would enhance the imaging contrast in clinical setting. These studies on disposition of ^{99m}Tc-antibody has also yielded important clues for the proper design of labeled antibodies. Depending upon the particular antibody system and due to the variable retention and excretion characteristics of the radiolabel, certain attachment methodologies may be preferable over others. The established biodisposition pattern for directly-labeled ^{99m}Tc-antibodies suggests the inherent instability can be advantageous to provide an opportunity for further clinical enhancement of these agents for lesion diagnosis.

BIBLIOGRAPHY

1. Kohler G and Milstein C. Continuous cultures of fused cells secreting antibodies of predefined specificity. Nature 256:495-497, 1975

2. Chatal JF, Peltier P, Bardies M, *et al*. Does immunoscintigraphy serve clinical needs effectively? Is there a future for radioimmunotherapy? Eur J Nucl Med 19:205-213, 1992

3. Goldenberg DM. Monoclonal antibodies in cancer detection and therapy. Am J Med 94:297-312, 1993

4. Corstens FHM, Oyen WJG and Becker WS. Radioimmunoconjugates in the detection of infection and inflammation. Semin Nucl Med 23(2):148-164, 1993

5. Manspeaker P, Weisman HF and Schaible TF. Cardiovascular applications: Current status of immunoscintigraphy in the detection of myocardial necrosis using antimyosin (R11D10) and deep venous thrombosis using antifibrin (T2G1s). Semin Nucl Med 23(2):133-147, 1993

6. Hnatowich DJ. Antibody radiolabeling, problems and promises. Int J Radiat Appl Instrum Part B 17(1):49-55, 1990

7. Bradwell AR, Fairweather DS, Dykes PW, *et al*. Limiting factors in the localization of tumors with radiolabeled antibodies. Immunol Today 6:163-170, 1985

8. Epenetos AA, Snook D, Durbin H, *et al*. Limitations of radiolabeled monoclonal antibodies for localization of human neoplasms. Cancer Res 46:3183-3191, 1986

9. Msirikale JS, Klein JL, Schroeder J, *et al*. Radiation enhancement of radiolabeled antibody deposition in tumors. Int J Radiat Oncol Biol Phys 13:1839-1844, 1987

10. Srivastava S, Schlom J, Raubitschek A, *et al*. Studies

concerning the effect of external irradiation on localization of radiolabeled monoclonal antibody B72.3 to human colon carcinoma xenografts. Int J Radiat Oncol Biol Phys 16:721-729, 1989

11. Smyth MJ, Pietersz GA and McKenzie IFC. Use of vasoactive agents to increase tumor perfusion and the antitumor efficacy of drug-monoclonal antibody conjugates. J Natl Cancer Inst 79:1367-1373, 1987

12. Munz DL, Alavi A, Koprowski H, *et al*. Improved radio-immunoimaging of human tumor xenografts by a mixture of monoclonal antibody $F(ab')_2$ fragments. J Nucl Med 27:1739-45, 1984

13. Kemshead JT, Jones DH and Lashford L. ^{131}I-coupled to monoclonal antibodies as therapeutic agents for neuroectodermally derived tumors. Fact or fiction? Cancer Drug Deliv 3:25-43, 1986

14. Gaffar SA, Pant KD, Shochat D, *et al*. Experimental studies of tumor radioimmunodetection using antibody mixtures against carcinoembryonic antigen (CEA) and colon-specific antigen-p (CSAp). Int J Cancer 27:101-105, 1981

15. Greiner JW, Pestka S, Fisher PB, *et al*. Recombinant interferon enhances monoclonal antibody targeting of carcinoma lesions *in vivo*. Science 235:895-898, 1987

16. Guadagni F, Schlom J, Pothen S, *et al*. Parameters involved in the enhancement of monoclonal antibody targeting *in vivo* with recombinant interferon. Cancer Immunol Immunother 26:222-230, 1988

17. Rhodes BA. Direct labeling of proteins with ^{99m}Tc. Int J Radiat Appl Instrum Part B 18(7):667-676, 1991

18. Cooper AJL. Biochemistry of sulfur-containing amino

acids. Ann Rev Biochem 52:187-222, 1983

19. Griffith DW, Meistor A. Glutathione: interorgan translocation, turnover, and metabolism. Proc Natl Acad Sci USA 76:5606-5610, 1979

20. Bogard WC, Dean RT, Deo Y, *et al*. Practical consideration in the production, purification, and formulation of monoclonal antibodies for immunoscintigraphy and immunotherapy. Semin Nucl Med 19(3):202-220, 1989

21. Serafini AN. From monoclonal antibodies to peptides and molecular recognition units: An overview. J Nucl Med 34:533-536, 1993

22. Porter RR. The hydrolysis of rabbit gamma-globulin and antibodies with crystalline papain. Biochem J 73:119-126, 1959

23. Morrison SL and Schlom J. Recombinant chimeric monoclonal antibodies. In: Important Advances in Oncology (Vincent T, Devita Jr, edt). J.B. Lippincott Company, Philadelphia, 1990

24. Zuckier LS, Rodriguez LD, and Scharff MD. Immunologic and pharmacologic concepts of monoclonal antibodies. Semin Nucl Med 19(3):166-186, 1989

25. Jager RD, Abdel-Nabi H, Serafini A, *et al*. Current status of cancer immunodetection with radiolabeled human monoclonal antibodies. Semin Nucl Med 23(2):165-179, 1993

26. James K and Bell GT. Human antibody production. Current status and future prospects. J Immunol Methods 100:5-40, 1982

27. Sikora K, Alderson T, Ellis J, *et al*. Human hybridoma from patients with malignant disease. Br J Cancer 47:135-145, 1983

28. Glassy MC and Dillman RO. Molecular biotherapy with human monoclonal antibodies. Mol Biother 1:7-12, 1988

29. Hanna MG, Haspel MV, McCabe RP, *et al*. Development and application of human monoclonal antibodies. Antibody Immunoconj Radiophar 4:67-75, 1991

30. Morrison SL. Transfectomas provide novel chimeric antibodies. Science 229:1202-1207, 1985

31. Sun LK, Curtis P, Rakowicz-Szulczynska E, *et al*. Chimeric antibody with human constant regions and mouse variable regions directed against carcinoma-associated antigen 17-1A. Proc Natl Acad Sci USA 84:214-218, 1987

32. Fanger MW. Bispecific antibodies. Critical Reviews Immunol 12(3,4):101-124, 1992

33. Brennan M, Davison PE, and Paulus H. Preparation of monoclonal immunoglobulin G1 fragments. Science 229:81-83, 1985

34. Songsivilai S, Clissold P and Lacmann P. A novel strategy for producing chimeric bispecific antibodies by gene transfection. Biochem Biophys Res Comm 164:271-276, 1989

35. Tada H, Toyoda Y, and Iwasa S. Bispecific antibody-producing hybrid hybridoma and its use in one-step immunoassay for human lymphotoxin. Hybridoma 8:73-83, 1989

36. Suresh MR, Cuello AC, and Milstein C. Bispecific monoclonal antibodies from hybrid hybridomas. Methods Enzymol 121:210-228, 1986

37. Takashi M and Fuller SA. Production of murine hybrid-hybridomas secreting bispecific monoclonal antibodies for use in urease-based immunoassays. Clin Chem 34:1693-1696, 1988

38. Urnowitz HB, Chang Y, Scott M, *et al*. IgA:IgM and IgA:IgA hybrid hybridomas secreting heteropolymeric immunoglobulins that are polyvalent and bispecific. J Immunol 140:558-563, 1988

39. Bhargava KK and Acharya SA. Labeling of monoclonal antibodies with radionuclides. Semin Nucl Med 19(3):187-201, 1989

40. Rayudu GVS. Production of radionuclides for medicine. Semin Nucl Med 20(2):100-110, 1990

41. Britton KE, Granowska M, and Mather SJ. Radiolabeled monoclonal antibodies in oncology I. Technical aspects. Nucl Med Commun 12:65-76, 1991

42. Goldenberg DM. Future role of radiolabeled monoclonal antibodies in oncological diagnosis and therapy. Semin Nucl Med 19(4):332-339, 1989

43. Cecil R and Mcphee JR. The sulfur chemistry of proteins. Adv Protein Chem 24:255-389, 1959

44. Anfinsen CB. Principles that govern the folding of protein chains. Science 181:223-230, 1973

45. Anfinsen CB, Haber E, Sela M, and White FH Jr. The kinetics of formation of native ribonuclease during oviation of the reduced polypeptide chain. Proc Natl Acad Sci USA 47:1309-1314, 1961

46. Creighton TE. Disulfide bonds as probes of protein folding pathways. Methods Enzymol 131:83-106, 1986

47. Steigman J, Williams HP, and Solomon NA. The importance of the protein sulphydryl group in HSA labeling with ^{99m}Tc. J Nucl Med 16:573, 1975

48. Paik CH, Phan L, Hong J, *et al*. The labeling of high

affinity sites of antibodies with ^{99m}Tc. Int J Nucl Med Biol 12:3-8, 1986

49. Pettit WA, DeLand FH, Bennett SJ, *et al*. Improved protein labeling by stannous tartrate reduction of pertechnetate. J Nucl Med 21:59-62, 1980

50. Thakur ML, DeFulvio J, and Park CH. Determination of reduced disulfide groups in monoclonal antibodies. Bio Techniques 8:512-516, 1990

51. Rhodes BA, Torvestaad DA, Burchiel SW, and Austin RK. A kit for direct labeling of antibody and antibody fragments with ^{99m}Tc. J Nucl Med 21:54, 1980

52. Eckelman WC and Steigman J. Direct labeling with ^{99m}Tc. Int J Radiat Appl Instrum Part B 18(1):3-7, 1991

53. Schwarz A and Steinstraber A. A novel approach to ^{99m}Tc-labeled monoclonal antibodies. J Nucl Med 28:721, 1987

54. Reno JM and Bottino BJ. Improved radionuclide antibody coupling. European Patent Office Application EP 0237150 A2, 1987

55. Joiris E, Bastin B and Thornback R. A new method for labeling of monoclonal antibodies and their fragments with technetium-99m. Int J Radiat Appl Instrum Part B 18(3):353-356, 1991

56. Thakur ML, DeFulvio J, Richard MD, and Park CH. Technetium-99m labeled monoclonal antibodies: Evaluation of reducing agents. Int J Radiat Appl Instrum Part B 18(2):227-233, 1991

57. Sykes TR, Woo TK, Qi P, *et al*. Direct labeling of monoclonal antibodies with technetium-99m by a novel photoactivation process. J Nucl Med 34:100p, 1993 (abstract)

58. Delmon-Moingeon LI, Mahmood A, Davison A, and Jones AG. Strategies for labeling monoclonal antibodies and antibody-like molecules with technetium-99m. J Nucl Biol Med 35:47-59, 1991

59. Khaw BA, Strauss HW, Carvalho A, *et al*. ^{99m}Tc labeling of antibodies to cardiac myosin Fab and to human fibrinogen. J Nucl Med 23:1011-1019, 1982

60. Paik CH, Murphy PR, Eckelman WC, *et al*. Optimization of the DTPA mixed-anhydride reaction with antibodies at low concentration. J Nucl Med 24:932-936, 1983

61. Brown BA, Drozynski CA, Dearborn CB, *et al*. Conjugation of metallothionein to a murine monoclonal antibody. Anal Biochem 172:22-28, 1988

62. Brown BA, Dearborn CB, Drozynski CA, and Sands H. Pharmacokinetics of ^{99m}Tc metallothionein-B72.3 and its F(ab')$_2$ fragment. Cancer Res 50:835s-839s, 1990

63. Arano Y, Yokoyama A, Furukawa T, *et al*. ^{99m}Tc-labeled monoclonal antibody with preserved immunoreactivity and high *in vivo* stability. J Nucl Med 28:1027-1033, 1987

64. Baidoo KE, Scheffel U, and Lever SZ. ^{99m}Tc labeling of proteins: Initial evaluation of a novel diaminedithiol bifunctional chelating agent. Cancer Res 50:799s-803s, 1990

65. Abrams MJ, Schwart DA, Hauser MM, *et al*. A novel method of labeling proteins with technetium-99m based on bifunctional aromatic hydrazines. J Nucl Med 31:776, 1990 (abstract)

66. Fritzberg AR, Abrams PG, Beaumier PL, *et al*. Specific and stable labeling of antibodies with technetium-99m with a diamide dithiolate chelating agent. Proc Natl Acad Sci

USA 85:4025-4029, 1988

67. Linder KE, Wen MD, Sharkey RM, *et al*. Preparation and characterization of the antibody B72.3 labeled with ^{99m}Tc BATO isothiocyanates. J Nucl Med 31:747, 1990 (abstract)

68. Weber RW, Nedelman M, Lister-James J, and Dean RT. Comparison of ^{99m}Tc labeled antibody Fab' chelator conjugates having mono, di, and triester linkages. Proc Eighth International Symposium on Radiopharmaceutical Chemistry, Princeton, New Jersey, 314, 1990

69. Seevers RH and Counsell RE. Radioiodination techniques for small organic molecules. Chem Rev 82:575, 1982

70. Reogoeczi E. Iodine-Labeled Plasma Proteins. CRC Press, Boca Raton, Fla., 1985

71. Otsuka FL and Welch MJ. Methods to label monoclonal antibodies for use in tumor imaging. Int J Radiat Appl Instrum Part B 14:243, 1987

72. Srivastava SC and Mease RC. Progress in research on ligands, nuclides and techniques for labeling monoclonal antibodies. Int J Radiat Appl Instrum Part B 18(6):589-603, 1991

73. Bolton AE and Hunter WM. The labeling of proteins to high specific radioactivities by conjugation to ^{125}I-containing acylating agent. Biochem J 133:529-539, 1973

74. Wilbur DS, Hadley SW, Hylarides MD, *et al*. Development of a stable radioiodinating reagent to label monoclonal antibodies for radiotherapy of cancer. J Nucl Med 30:216, 1989

75. Vaidyanathan G and Zalutsky MR. Protein radiohalogenation: observations on the design of N-succinimidyl ester acylation agents. Bioconjug Chem 1:269, 1990

76. Hadley SW and Wilbur DS. Evaluation of iodovinyl antibody conjugates: comparison with a *p*-iodobenzoyl conjugate and direct radioiodination. Bioconjug Chem 1:154, 1990

77. Hunter WM and Greenwood FC. Preparation of iodine-131-labeled growth hormone of high specific radioactivity. Nature 194:495-496, 1962

78. Greenwood FC, Hunter WM, and Glover JS. The preparation of ^{131}I labeled human growth hormone of high specific radioactivity. Biochem J 89:114-123, 1963

79. Fraker PJ and Speck JC. Protein and cell membrane iodinations with a sparingly soluble chloramide 1,3,4,6-tetrachloro-3α,6α-diphenylglycouril. Biochem Biophys Res Commun 80:849-857, 1978

80. Marchalonis JJ. An enzymatic method for the trace iodination of immunoglobulin and other proteins. Biochem J 113:299-305, 1969

81. Thorell JI and Johanson BG. Enzymatic iodination of polypeptides with ^{125}I to high specific activity. Biochem Biophys Res Commun 48:464-471, 1972

82. von Schenk H, Larsson I, and Thorell JI. Improved radioiodination of glucagon with the lactoperoxidase method. Clin Chim Acta 69:225-232, 1976

83. Rosa V, Pennise F, Bianchi R, *et al*. Chemical and biological effects of iodination on human albumin. Biocim Biophys Acta 133:486-498, 1967

84. Salvatore M. Immunoscintigraphy with radiolabeled antibodies: an overview of the progress and limitations. J Nucl Biol Med 35:21-23, 1991

85. Goldenberg DM , DeLand FH , Kim E, *et al*. Use of radiolabeled antibodies to carcinoembryonic antigen for

the detection and localization of diverse cancers by external photoscanning. N Engl J Med 298:1384-1386, 1978

86. Belitsky P, Ghose T, Aquino J, *et al*. Radionuclide imaging of metastases from renal cell carcinoma by ^{131}I-labeled antitumor antibody. Radiology 126:515-517, 1978

87. Reisfeld RA and Cheresh DA. Human tumor antigens. Adv Immunol 40:323-377, 1987

88. Old LJ. Cancer immunology. The search for specificity. GHA Clowes Memorial Lecture. Cancer Res 41:361-375, 1981

89. Abdel-Nabi H and Doerr RJ. Clinical applications of indium-111-labeled monoclonal antibody imaging in colorectal cancer patients. Semin Nucl Med 23(2):99-113, 1993

90. Podoloff DA, Patt YZ, Curley SA, *et al*. Imaging of colorectal carcinoma with technetium-99m radiolabeled Fab' fragments. Semin Nucl Med 23(2):89-98, 1993

91. Neal CE, Swenson LC, Fanning J, and Texter JH. Monoclonal antibodies in ovarian and prostate cancer. Semin Nucl Med 23(2):114-126, 1993

92. Breitz HB, Sullivan K, and Nelp WB. Imaging lung cancer with radiolabeled antibodies. Semin Nucl Med 23(2):127-132, 1993

93. Divgi CR and Larson SM. Radiolabeled monoclonal antibodies in the diagnosis and treatment of malignant melanoma. Semin Nucl Med 23(4):252-261, 1989

94. Corstens FHM and Claessens RAMJ. Imaging inflammation with human polyclonal immunoglobulin: Not looked for but discovered. Eur J Nucl Med 19:155-158, 1992

95. Lind P, Langsteger W, Koltringer P, *et al*. Immunoscinti-

graphy of inflammatory processes with a technetium-99m-labeled monoclonal antigranulocyte antibody (MAb BW 250/183). J Nucl Med 31:417-423, 1990

96. Khaw BA, Fallon JT, Beller GA, *et al*. Specificity of localization of myosin specific antibody fragments in experimental myocardial infarction. Circulation 60:1527-1531, 1979

97. Khaw BA, Beller GA, Haber E, *et al*. Localization of cardiac myosin-specific antibody in myocardial infarction. J Clin Invest 58:439-446, 1976

98. Kurdryk B, Rohoza A, Ahadi M, *et al*. Specificity of a monoclonal antibody for the NH_2-terminal region of fibrin. Mol Immunol 21:89-94, 1984

99. Sands H and Gallagher BM. Physiological, pharmacological, and immunological aspects of antibody targeting. In: Zalutsky MR, editor. Antibodies in Radiodiagnosis and Therapy. Boca Raton, Fla, CRC Press. 129-148, 1989

100. Jain RK. Physiological barriers to delivery of monoclonal antibodies and other macromolecules in tumors. Cancer Res 50:814s-819s, 1990

101. Schlom J, Hand PH, Greiner JW, *et al*. Innovations that influence the pharmacology of monoclonal antibody guided tumor targeting. Cancer Res 50:820s-827s, 1990

102. Rosenblum LM, Lamki JL, Murray DJ, *et al*. Interferon-induced changes in pharmacokinetics and tumor uptake of ^{111}I-labeled antimelanoma antibody 96.5 in melanoma patients. J Natl Cancer Inst 80:160-165, 1988

103. Nakamura K, Kubo A, and Hashimoto S. Effect of interleukin 2 on tumor uptake of monoclonal antibody. J Nucl Med 33:934, 1992 (abstract)

104. Fazio F and Giovanni P. Antibody-guided scintigraphy: targeting of the "magic bullet". Eur J Nucl Med 20:1138-1140, 1993

105. Goodwin DA, Mears CF, Diamanti C, *et al*. Use of specific antibody for rapid clearance of circulating blood background from radiolabeled tumor imaging proteins. Eur J Nucl Med 9:209-215, 1984

106. Goodwin DA, Meares CF, McCall MJ, *et al*. Pre-targeted immunoscintigraphy of murine tumors with indium-111-labeled bifunctional haptens. J Nucl Med 29:226-234, 1988

107. Hnatowich DJ, Virzi F, and Rusckowski M. Investigations of avidin and biotin for imaging applications. J Nucl Med 28:1294-1302, 1987

108. Paganelli G, Riva P, Deleide G, *et al*. *In vivo* labelling of biotinylated monoclonal antibodies by radioactive avidin: a strategy to increase tumor radiolocalization. Int J Cancer 2:121-125, 1988

109. Paganelli G, Magnani P, Zito G, *et al*. Three-step monoclonal antibody tumor targeting in carcinoembryonic antigen-positive patients. Cancer Res 51:5960-5966, 1991

110. Lamki LM, Murray JL, Rosenblum MG, *et al*. Effect of unlabeled monoclonal antibody (MoAb) on biodistribution of 111-indium labeled (MoAb). Nucl Med Commun 9:553-564, 1988

111. Haseman MK, Goodwin DA, Meares CF, *et al*. Metabolizable ^{111}In chelate conjugated anti-idiotype monoclonal antibody for radioimmunodetection of lymphoma in mice. Eur J Nucl Med 12:455-460, 1986

112. Sears HF, Atkinson B, Mattis J, *et al*. Phase I clinical trials of monoclonal antibody in treatment of gastro-

intestinal tumors. Lancet 1:762-765, 1982

113. Sears HF, Herlyn D, Steplewski Z, *et al.* Phase II clinical trial of a murine monoclonal antibody cytotoxic for gastrointestinal carcinoma. Cancer Res 45:5910-5913, 1985

114. Schroff RW, Foon KA, Beatty SM, *et al.* Human anti-murine immunoglobulin responses in patients receiving monoclonal antibody therapy. Cancer Res45:879-885, 1985

115. Pimm HV, Perkins AC, Armitage NC, *et al.* The characteristics of blood-borne radiolabels and the effect of anti-murine IgG antibodies on localization of radiolabeled monoclonal antibody in cancer patients. J Nucl Med 26:1011-1023, 1985

116. Hyams D, Reynolds JC, Carrasquillo JA, *et al.* The effect of circulating anti-murine antibody on the pharmacokinetics and biodistribution of injected radiolabeled monoclonal antibody. J Nucl Med 27:922, 1986 (abstract)

117. Herlyn D, Lubeck M, Sears HF, *et al.* Specific detection of anti-idiotypic immune response in cancer patients with murine monoclonal antibody. J Immunol Methods 85:27-28, 1985

118. Traub UC, De Jager RL, Primus J, *et al.* Antiidiotype antibodies in cancer patients receiving monoclonal antibody to carcinoembryonic antigen. Cancer Res 40:4002-4006, 1988

119. Muto MB, Lepisto EM, Van Dem Abbeele AD, *et al.* The influence of human antimurine antibody on CA125 levels in patients with ovarian cancer, undergoing radioimmunotherapy of immunoscintigraphy with murine monoclonal antibody OC125. Am J Obstet Gynecol 161:1206-1212, 1989

120. Miller RA, Oseroff AR, Strotte PT, *et al*. Monoclonal antibody therapeutic trials in seven patients with T-cell lymphoma. Blood 62:988-995, 1983

121. Chatenoud L, Baudrihaye MF, Chkoff N, *et al*. Restriction of the human *in vivo* immune response against the mouse monoclonal antibody OKT3. J Immunol 137:830-838, 1986

122. Zimmer AM, Rosen ST, Spies SM, *et al*. Radioimmunotherapy of patients with cutaneous T-cell lymphoma using an iodine-131-labeled monoclonal antibody: Analysis of retreatment following plasmapheresis. J Nucl Med 29:174-180, 1988

123. Lederman JA, Begent RHJ, Bagshawe RK, *et al*. Repeated antitumor antibody therapy in man with suppression of the host response by cyclosporin A. Br J Cancer 58:654-657, 1988

124. Bjorn M, Weiden P, Wolf S, *et al*. Human anti-mouse antibody (HAMA) suppression with cyclosporin A (CSP). Antibody Immunoconj Radiophar 5:348, 1992 (abstract)

125. Colcher D, Milenic D, Roselli M, *et al*. Characterization and biodistribution of recombinant and recombinant/chimeric constructs of monoclonal antibody B72.3. Cancer Res 49:1738-1745, 1989

126. Hardman N, Gill LL, De Winter RFJ, *et al*. Generation of a recombinant mouse-human chimeric monoclonal antibody directed against human carcinoembryonic antigen. Int J Cancer 44:424-433, 1989

127. LoBuglio AF, Wheeler RH, Trang J, *et al*. Mouse human chimeric monoclonal antibody in man: Kinetics and immune response. Proc Natl Acad Sci USA 86:4220-4224, 1989

128. Dixon FJ, Talmage DW, Maurer PH, *et al*. The half-life of homologous gamma globulin (antibody) in several species.

J Exp Med 96:313-318, 1952

129. Sullivan DC, Silva JS, Cox CE, *et al*. Localization of ^{131}I-labeled goat and primate anti-carcinoembryonic antigen (CEA) antibodies in patients with cancer. Invest Radiol 17:350-355, 1982

130. Weinstein JN, Holton OD III, Black CDV, *et al*. Regional delivery of monoclonal antitumor antibodies: Detection and possible treatment of lymph node metastases. Prog Clin Biol Res 212:1131-1148, 1986

131. Waldman TA and Strober W. Metabolism of immunoglobulins. Prog Allergy 13:1-110, 1969

132. Brambell FWR, Hemmings WA, and Morris IG. A theoretical model of gamma-globulin catabolism. Nature 203:1352-1355, 1964

133. Brambell FWR. The transmission of immunity from mother to young and the catabolism of immunoglobulins. Lancet 2:1087-1093, 1966

134. Larson SM, Carrasquillo JA, McGuffin RW, *et al*. Use of ^{131}I labeled, murine Fab against a high molecular weight antigen of human melanoma: Preliminary experience. Radiology 155:487-492, 1985

135. Rosenblum MG, Murray JL, Hayie TP, *et al*. Pharmacokinetics of ^{111}In-labeled anti-p97 monoclonal antibody in patients with metastatic malignant melanoma. Cancer Res 45:2382-2386, 1985

136. Meredith RF, LoBuglio AF, Plott WE, *et al*. Pharmacokinetics, immune response, and biodistribution of iodine-131-labeled chimeric mouse/human IgG1,K 17-1A monoclonal antibody. J Nucl Med 32:1162-1168, 1991

137. Khazaeli MB, Saleh MN, Liu TP, *et al*. Pharmacokinetics

and immune response of ^{131}I-chimeric mouse/human B72.3 (human gamma4) monoclonal antibody in humans. Cancer Res 51:5461-5466, 1991

138. Gadina M, Canevari S, Ripamonti M, *et al*. Preclinical pharmacokinetics and localization studies of the radio-iodinated anti-ovarian carcinoma MAb MOv18. Int J Radiat Appl Instrum Part B. 18(4):403-408, 1991

139. Pardridge WM, Buciak JL, and Friden PM. Selective transport of an anti-transferrin receptor antibody through the blood-brain barrier *in vivo*. J Pharmacol Exp Ther 259(1):66-70, 1991

140. Benz P, Oberhausen E, and Berberich R. Monoclonal antibody BW431/26 labeled with technetium-99m and indium-111: an investigation of the biodistribution and the dosimetry in patients. Eur J Nucl Med 18:813-816, 1991

141. McQuarrie SA, McEwan AJB, Noujaim AA, *et al*. Pharmacokinetic comparison of the murine and chimeric forms of the ^{99m}Tc-labeled 174H.64 monoclonal antibody. J Nucl Biol Med 37(3):158, 1993 (abstract)

142. Eger RR, Covell DG, Carrasquillo JA, *et al*. Kinetics model for the biodistribution of an ^{111}In-labeled monoclonal antibody in humans. Cancer Res 47:3328-336, 1987

143. Covell DG, Barbet J, Holton OD, *et al*. Pharmacokinetics of monoclonal immunoglobulin G1, F(ab')$_2$, and Fab' in mice. Cancer Res 46:3969-3978, 1986

144. Spiegelberg HL and Weigle WO. The catabolism of homologous and heterologous 7S gamma globulin fragments. J Exp Med 121:323-338, 1965

145. Fahey JL and Robinson AG. Factors controlling serum

gamma-globulin concentration. J Exp Med 118:845-868, 1963

146. Spiegelberg HL and Fishkin BG. The catabolism of human gamma immunoglobulins of different heavy chain subclasses. III. The catabolism of heavy chain disease proteins and of Fc fragments of myeloma proteins. Clin Exp Immunol 10:599-607, 1972

147. Thornburg RW, Day JF, Baynes JW, *et al*. Carbohydrate-mediated clearance of immune complexes from the circulation. A role for galactose residues in the hepatic uptake of IgG-antigen complexes. J Biol Chem 255:6820-6825, 1980

148. Spiegelberg HL and Weigle WO. Studies on the catabolism of γG subunits and chains. J Immunol 95:1034-1040, 1965

149. Lippincott SW, Korman S, Fong C, *et al*. Turnover of labeled normal gamma globulin in multiple myeloma. J Clin Invest 39:565-572, 1960

150. Wells JV and Fudenberg HH. Metabolism of radioiodinated IgG in patients with abnormal serum IgG levels. I. Hypergamma-globulinaemia. Clin Exp Immunol 9:761-774, 1971

151. Birke G, Liljedahl SO, Olhagen B, *et al*. Catabolism and distribution of gammaglobulin. A preliminary study with ^{131}I-labeled gammaglobulin. Acta Med Scand 173:589-603, 1963

152. Wells JV and Fudenberg HH. Metabolism of radioiodinated IgG in patients with abnormal serum IgG levels. II. Hypergamma-globulinaemia. Clin Exp Immunol 9:775-783, 1971

153. Morell A, Terry WD, and Waldmann TA. Metabolic property of IgG subclasses in man. J Clin Invest 49:673-680, 1970

154. Hnatowich DJ, Mardirossian G, Rusckowski M, *et al.* Directly and indirectly technetium-99m-labeled antibodies -- A comparison of *in vitro* and animal *in vivo* properties. J Nucl Med 34:109-119, 1993

155. Colcher D, Milenic DE, Ferroni P, *et al. In vivo* fate of monoclonal antibody B72.3 in patients with colorectal cancer. J Nucl Med 31:1133-1142, 1990

156. DeNardo GL, Young WC, DeNardo SJ, *et al.* Urinary metabolites after injection of monoclonal antibodies (MAb) or fibrinogen (F) radioiodinated with a small and large number of iodine atoms. J Nucl Med 27:958, 1986 (abstract)

157. Carrasquillo JA, Mulshine JL, Bunn PA, *et al.* Indium-111 T101 monoclonal antibody is superior to iodine-131 T101 in imaging of cutaneous T-cell lymphoma. J Nucl Med 28:281-287, 1987

158. Zalutsky MR and Narula AS. A method for the radiohalogenation of proteins resulting in decreased thyroid uptake of radioiodine. Appl Radiat Isot 38:1051-1055, 1987

159. Fukumoto T and Brandon MR. The site of IgG2a catabolism in the rat. Mol Immunol 18(8):741-750, 1981

160. Himmelsbach M and Wahl RL. Studies on the metabolic fate of ^{111}In-labeled antibodies. Int J Radiat Appl Instrum Part B 16(8):839-845, 1989

161. Motta-Hennessy C, Sharkey RM, and Goldenberg DM. Metabolism of indium-111-labeled murine monoclonal antibody in tumor and normal tissue of the athymic mouse. J Nucl Med 31:1510-1519, 1990

162. Jones PL, Brown BA and Sands H. Uptake and metabolism of ^{111}In-labeled monoclonal antibody B6.2 by the rat liver.

Cancer Res 50:852s-856s, 1990

163. Beatty BG, O'Conner-Tressel M, Do T, *et al.* Mechanism of decreasing liver uptake of ^{111}In-labeled anticarcino-embryonic antigen monoclonal antibody by specific antibody pretreatment in tumor bearing mice. Cancer Res 50:846s-851s, 1990

164. Klaassen CD and Watkins III JB. Mechanism of bile formation, hepatic uptake, and biliary excretion. Pharmacol Reviews 36(1):1-67, 1984

165. Jones EA and Summerfield JA. Functional aspects of hepatic sinusoidal cells. Semin Liver Disease 5(2):157-174, 1985

166. Fox SI. Human Physiology, Wm.C.Brown Publishers, Iowa, pp516-563, 1984

167. Jones AL and Burwen SJ. Hepatic receptors and their ligands: Problems of intracellular sorting and vectorial movement. Semin Liver Disease 5(2):136-146, 1985

168. Lentz PE and DiLuzio NR. Biochemical characterization of Kupffer and parenchymal cells isolated from rat liver. Exp Cell Res 67:17-26, 1971

169. Kuhlmann L and Steinstrasser A. Effect of DTPA to antibody ratio on chemical, immunological and biological properties of the ^{111}In-labeled $F(ab')_2$ fragments of the monoclonal antibody 431/31. Int J Radiat Appl Instrum Part B 15:617-627, 1988

170. Hagan PL, Halpern SE, Chen A, *et al. In vivo* kinetics of radiolabeled monoclonal anti-CEA antibodies in animal models. J Nucl Med 26:1418-1423, 1985

171. Beatty JD, Beatty BG, O'Conner-Tressel M, *et al.* Mechanisms of tissue uptake and metabolism of

radiolabeled antibody--role of antigen:antibody complex formation. Cancer Res 50:840s-845s, 1990

172. Frommel D and Rachman F. Receptor for the Fc portion of IgG on the plasma membrane of the hepatocytes. Ann Immunol 130C:553-560, 1979

173. Hopf U, Meyer Zum Buschenfelde KH, and Dierich MP. Demonstration of binding sites for IgG Fc and the third complement component (C3) on isolated hepatocytes. J Immunol 117:639-645, 1976

174. Nashi T, Bhan AK, Collins AB, *et al*. Effect of circulating immune complexes on Fc and C3 receptors of Kupffer cells *in vivo*. Lab Invest 44:442-448, 1981

175. Hubbard AL and Stukenbrok H. An electron microscope autoradiographic study of the carbohydrate recognition system in rat liver. II. Intracellular fates of the ^{125}I-ligands. J Cell Biol 83:65-81, 1979

176. Ashwell G and Morell AG. The role of surface carbohydrates in the hepatic recognition and transport of circulating glycoproteins. Adv Enzymol 41:99-128, 1974

177. Arnold W, Muller O, von Mayersbach H, and Mitrenga D. The fate of injected human IgG in the mouse liver. Uptake, immunological inactivation and lysosomal reaction. Cell Tissue Res 156:359-376, 1975

178. Sands H. Experimental studies of radioimmunodetection of cancer: An overview. Cancer Res 50:809s-813s, 1990

179. Sands H and Jones PL. Methods for the study of the metabolism of radiolabeled monoclonal antibodies by liver and tumor. J Nucl Med 28:390-398, 1987

180. Colcher D and Gansow O. Biodistribution of indium-111-

labeled monoclonal antibodies. J Nucl Med 28:1924-1925, 1987

181. Beatty BG, Beatty JD, Williams LE, *et al*. Effect of specific antibody pretreatment on liver uptake of ^{111}In-labeled anti-carcinoembryonic antigen monoclonal antibody in nude mice bearing human colon cancer xenografts. Cancer Res 49:1587-1594, 1989

182. Brechbiel MW, Gansow OA, Atcher RW, *et al*. Synthesis of 1-(*p*-isothiocyanatobenzyl) derivatives of DTPA and EDTA. Antibody labeling and tumor imaging studies. Inorg Chem 25:2772-2781, 1986

183. Esteban JM, Schlom J, Gansow OA, *et al*. New method for the chelation of indium-111 to monoclonal antibodies: biodistribution and imaging of athymic mice bearing human colon carcinoma xenografts. J Nucl Med 26:861-870, 1987

184. Blend MJ, Greager JA, Atcher RW, *et al*. Improved sarcoma imaging and reduced hepatic activity with indium-111-SCN-Bz-DTPA linked to MoAb 19-24. J Nucl Med 29:1810-1816, 1988

185. Wang TST, Fawwaz RA and Alderson PO. Reduced hepatic accumulation of radiolabeled monoclonal antibodies with indium-111-thioether-poly-L-lysine-DTPA-Monoclonal antibody-TP41.2F(ab')$_2$. J Nucl Med 33:570-574, 1992

186. Noujaim AA, Sykes TR, McEwan AJ, *et al*. A new marker for the detection of adenocarcinomas by radioimmuno-scintigraphy. In: Clinical Use of Antibodies (Baum *et al*. edt), p151-168, Kluwer Academic Publishers, Netherland, 1991

187. Golberg L, McEwan AJB, Brzezinski W, *et al*. Evalution of ^{111}In and ^{99m}Tc labeled monoclonal antibody for pre-operative imaging in primary colorectal cancer. Eur J

Nucl Med 16(suppl):54s, 1990 (abstract)

188. McEwan AJ, MacLean GD, Longenecker BM, *et al*. Initial clinical experience with ^{99m}Tc 170H.82, a novel panadenocarcinoma. Eur J Nucl Med 16(suppl):158s, 1990 (abstract)

189. Samuel J, Noujaim AA, MacLean GD, *et al*. Analysis of human tumor associated Thomsen-Friedenreich antigen. Cancer Res 50:4801-4808, 1990

190. Springer GF and Desai PR. Human blood-group MN and precursor specificities: structural and biological aspects. Carbohydr Res 40:183-192, 1975

191. Springer GF. T and Tn, general carcinoma autoantigens. Science 224:1198-1206, 1984

192. Golberg L, McEwan AJB, Brzezinski W, *et al*. Technetium labeled monoclonal antibody 170H.82 in radioimmunoguided colorectal surgery -- A case study. Eur J Nucl Med 16(suppl):s54, 1990 (abstract)

193. Golberg L, McEwan AJB, Noujaim AA, *et al*. SPECT imaging of ^{99m}Tc 170H.82 monoclonal antibody in patients with primary and metastatic adenocarcinoma. Eur J Nucl Med 16(suppl):s68, 1990 (abstract)

194. Sykes TR, Noujaim AA, Sykes CJ, *et al*. Biological considerations in the evaluation of tumor-directed monoclonal antibodies for radioimmunoimaging. In: Advances in Radio-pharmacology, Proceedings of the Sixth International Symposium on Radiopharmacology (Maddalena et al. edt), p164-172, Australia, 1989

195. McEwan AJB, MacLean GD, Hooper HR, *et al*. MAb170H.82: an evaluation of a novel panadenocarcinoma monoclonal antibody labeled ^{99m}Tc and ^{111}In. Nucl Med Commun 13:11-19, 1992

196. McEwan A, MacLean G, Golberg L, *et al.* ^{99m}Tc 170H.82 (Tru-Scint® AD™): A new monoclonal antibody for imaging breast Cancer -- A preliminary analysis. J Nucl Med 34:213p, 1993 (abstract)

197. Chandre R. Introductory Physics of Nuclear Medicine, Third edition, pp21-22, 1987

198. Horrocks DL and Klein PR. Theoretical considerations for the standardization ^{125}I by the coincidence method. Nucl Instrum Method 124:585, 1975

199. Frizberg AR, Lyster DM, and Dolphin DH. ^{99m}Tc-Glutathione: Role of reducing agent on renal retention. Int J Nucl Med Bio 5:87-92, 1978

200. Johannsen B, Syhrre R, Spies H, *et al.* Chemical and biological characterization of different Tc complex of cysteine and cystine derivatives. J Nucl Med 19:816-824, 1978

201. Mardirossian G, Wu C, Rusckowski M, *et al.* The stability of technetium-99m directly labeled to an Fab' antibody via stannous ion and mercaptoethanol reduction. Nucl Med Commun 13:503-512, 1992

202. Klaunig JE, Goldblatt PJ, Hinton DE, *et al.* Mouse liver cell culture. In Vitro 17(10):913-934, 1981

203. Klaunig JE. Primary culture of mouse hepatocytes: Effects of insulin and dexamethasone. In: Isolation, Characterization, and Use of Hepatocytes (Harris RA and Cornell NW, Eds). Elsevier, pp93-97, 1983

204. Renton KW, Deloria LB, and Mannering GJ. Effects of polyriboinosinic acid polyribocytidylic acid and a mouse interferon preparation on cytochrome p-450-dependent monooxygenase systems in cultures of primary mouse hepatocytes. Mol Pharmacol 14:672-681, 1978

205. Sancho J, Gonzalez E, Escanero JF, and Egido J. Binding kinetics of monomeric and aggregated IgG to Kupffer cells and hepatocytes of mice. Immunology 53:283-289, 1984

206. Sancho J, Rivera F, Sanchez-Crespo M, and Egido J. The effect of injection of synthetic platelet activating factor (PAF-acether) on the fate of IgG aggretates in mice. Immunology 47:643, 1982

207. Byrkit DR. Statistics Today: A Comprehensive Introduction. The Benjamin/Cummings Publishing Company, Inc., 1987

208. Kennewell PD. Comprehensive Medicinal Chemistry, Volume 1, pp149, Pergamon Press, 1990

209. Bradley SE, Ingelfinger FJ and Bradley GP. Hepatic circulation in cirrhosis of the liver. Circulation 5:419-429, 1952

210. Boyle CC, Paine AJ, and Mather SJ. The mechanism of hepatic uptake of a radiolabeled monoclonal antibody. Int J Cancer 50:912-917, 1992

211. Ingvar C, Norrgren K, Strand S, *et al*. Biokinetics of radiolabeled monoclonal antibodies in heterotransplanted nude rats: evaluation of corrected specific tissue uptake. J Nucl Med 30:1224-1234, 1989

212. Norrgren K, Strand S, Nilsson R, *et al*. A general, extracorporeal immunoadsorption method to increase the tumor-to-normal tissue ratio in radioimmunoimaging and radioimmunotherapy. J Nucl Med 34:448-454, 1993

213. Mather SJ and Ellisson D. Reduction-mediated technetium-99m labeling of monoclonal antibodies. J Nucl Med 31:692-697, 1990

214. Xue LY, Sykes TR, Woo TK, and Noujaim AA. Effects of sulfhydryl modulation on ^{99m}Tc monoclonal antibody behavior *in vivo*. International Research Group in Immunoscintigraphy and Immunotherapy, Seventh Annual IRIST Meeting, Nijmegen, The Netherlands, 1992

215. Xue LY, Noujaim AA, Sykes TR, and Woo T. Modulation of ^{99m}Tc uptake in liver and kidney from directly-labeled antibodies. The Fourth Conference on Radioimmunodetection and Radioimmunotherapy of Cancer, Princeton, NJ, 1992

216. Deleve LD and Kaplowitz N. Importance and regulation of hepatic glutathione. Seminars in Liver Disease 10(4):251-266, 1990

217. Bannai S. Transport of cystine and cysteine in mammalian cells. Biochim Biophys Acta 779:289-306, 1984

218. Müller L and Stacey NH. Effects of low-level cadmium in rats: Influence of pretreatment with thiol-modulating agents. Environ Res 45:204-212, 1988

219. Williamson JM and Meister A. Stimulation of hepatic glutathione formation by administration of L-2-oxothiazolidine-4-carboxylate, a 5-oxo-prolinase substrate. Proc Natl Acad Sci USA 78:936-939, 1981

220. Meister A. Metabolism and function of glutathione. In Glutathione, Part A (Editors: Dolphin D, Poulson R and Avramovic O). John Wiley & Sons. P367-474, 1989

221. Standeven AM and Wetterhahn KE. Tissue-specific changes in glutathione and cysteine after buthionine sulfoximine treatment of rats and potential for artifacts in thiol levels resulting from tissue preparation. Toxicol Appl Pharmacol 107:269-284, 1991

222. Hopf U, Schaefer HE, Hess G, and Meyer Zum Buschenfelde

KH. *In vivo* uptake of immune complex by parenchyma and non-parenchymal liver cells in mice. Gastroenterology 80:250-259, 1981

223. Ramadori G and Meyer Zum Buschenfelde KH. *In vivo* uptake of immune complex by mouse hepatocytes. Role of the complement. Mol Immunol 19-1396, 1982

224. Finbloon DS, Magilavy DB, Harford JB, and Rifai A. Influence of antigen on immunie complex behavior in mice. J Clin Invest 68:214-224, 1981

225. Rifai A, Finbloon DS, Magilavy DB, and Plotz PH. Modulation of the circulation and hetatic uptake of immune complex by carbohydrate recognition systems. J Immunol 128:2269-2275, 1982

226. Palerma MS, Giordano M, and Isturiz MA. Effect of cyclophosphamide on the clearance of IgG-sensitized red cells in mice. Clin Immunol Immunopathol 58:343-351, 1991

227. Giordano M and Isturiz MA. Enhancement of erythrophagocytosis by cyclophosphamide. Cellular Immunol 81:187-191, 1983

228. Dijk JV, Oosterwijk E, Kroonenburgh M, *et al*. Perfusion of tumor-bearing kidneys as a model for scintigraphic screening of monoclonal antibodies. J Nucl Med 29:1078-1082, 1988

229. Tolleshaug H and Berg T. Chloroquine reduces the number of asialoglycoprotein receptors in the hepatocyte plasma membrane. Biochem Pharmaacol 28:2919-2922, 1979

230. Gonzalez-Noriega A, Grubb JH, Talkad V, and Sly WS. Chloroquine inhibits lysosomal enzyme pinocytosis and enhances lysomal enzyme secretion by impairing receptor recycling. J Cell Biol 85:839-852, 1980

231. Kaplan J and Keogh EA. Analysis of the effects of amines on inhibition of receptor-mediated and fluid phase pinocytosis in rabbit alveolar macrophages. Cell 24:925-932, 1981

232. Tietze C, Schlesinger P, and Stahl P. Chloroquine and ammonium ion inhibit receptor-mediated endocytosis of mannose-glycoconjugates by macrophage: apparent inhibition of receptor recycling. Biochem Biophys Res Commun 93:1-8, 1980

233. Basu SK, Goldstein JL, Anderson RGW, and Brown MS. Monensin interrupts the recycling of low density lipoprotein receptors in human fibroblasts. Cell 24:493-502, 1981

234. Schwartz AL, Bolognesi A, and Fridovich SE. Recycling of the asialoglycoprotein receptor and the effect of lysosomotropic amines in hepatoma cells. J Cell Biol 98:732-738, 1984

235. Tietze C, Schlesinger P, and Stahl P. Mannose-specific endocytosis receptor of alveolar macrophages: demonstration of two functionly distinct intracellular pools of receptor and their roles in receptor recycling. J Cell Biol 92:417-424, 1982

236. Bjorck L and Kronvall G. Purification and some properties of streptococcal protein G, a novel IgG binding reagent. J Immunol 133(2):969-974, 1984

237. Taatjes DJ, Chen TH, Ackerstrom B, *et al*. Streptococcal protein G-gold complex: comparison with staphyllococcal protein A-gold complex for spot blotting and immunolabeling. Euro J Cell Biol 45:151-159, 1987

238. Hawkin EB, Pant KD, and Rhodes BA. Resistance of direct ^{99m}Tc-protein bond to transchelation. Antibody, Immuno-conjugates, and Radiopharmaceuticals 3:17-25, 1990